Supporting Information for

Solvent-Free Synthesis of Metal-Organic Frameworks Using Low-Melting Metal Salts

Tyler J. Azbell,[a] Tristan A. Pitt,[a] Melissa Bollmeyer,[a] Christina Cong,[a] Kyle M. Lancaster,[a] Phillip J. Milner[a,*]

[a]Department of Chemistry and Chemical Biology, Cornell University, Ithaca, NY, 14850, United States
*pjm347@cornell.edu

Table of Contents:

1. General procedures.

All reagents were purchased from commercial vendors and used without additional purification unless specified otherwise. All solvents were purchased from Fisher Scientific and used without additional purification unless specified otherwise. Dry, degassed solvents were obtained by sparging with Ar for 30 min and then passing the solvent through two columns of activated alumina before use. The metal salts $FeCl_3 \bullet 6H_2O$ (99+%, AESAR), $NiCl_2 \bullet 6H_2O$ (99.95%, Arcos) and $CoCl_2 \bullet 6H_2O$ (98%, Lancaster) were stored in desiccators when not in use. The metal salts NaCl (Sigma, 99%) and KCl (99–100.5%, BDH) were stored on the benchtop and used without additional purification. The metal salt $ZnCl_2$ (98%, Beantown) was stored in a N_2-filled glovebox when not in use. The linker 2,5-dihydroxyterephthalic acid (97%, Alfa Aesar) was purchased from commercial vendors and used without additional purification. Surface area data were collected on either a Micromeritics ASAP 2020, Micromeritics ASAP 2460, or Micromeritics 3-Flex gas sorption analyzer using ultrapure N_2 (99.999%) and a liquid N_2 bath. Brunauer-Emmett-Teller (BET) surface areas were determined by linear least squares regression analysis using the linearized form of the BET equation. Laboratory powder X-Ray diffraction (PXRD) data were collected on a Rigaku Ultima IV diffractometer equipped with a Cu K_α source (λ = 1.5406 Å) and were baseline-corrected using OriginPro. Indexing and Pawley refinements of Ni(bdp) prepared under ionothermal conditions were carried out in the TOPAS V6 software package. All reflections present in the experimental powder pattern were used to index the sample, apart from the peak on the right shoulder of the first sample reflection (7.6 °), which is also present in the solvothermal sample of Ni(bdp) and is therefore attributed to an unknown impurity phase. Pawley refinements incorporating the candidate indexing solutions were used to identify the most likely space group and unit cell parameters, as judged by their R_{wp} values and visual fits to the experimental data. ^{1}H NMR data were collected on a Bruker INOVA 500 MHz spectrometer and are referenced to residual solvent. Infrared (IR) spectra were collected on a Bruker Tensor II IR spectrometer with a diamond Attenuated Total Reflectance (ATR) attachment. Thermogravimetric analysis (TGA) measurements were conducted under flowing N_2 (flow rate of 60 mL/min) using a TA Instruments TGA Q5000 with a ramp rate of 3 °C/min. C/H/N/Cl combustion elemental analysis was performed by Atlantic Microlab Inc.

Scanning electron microscopy (SEM) images were taken at 2.0 kV using a Zeiss Gemini 500 scanning electron microscope. Energy-dispersive X-ray spectroscopy (EDS) elemental maps were collected at 20 kV using an Oxford Instruments Ultima Max detector. The powder samples were immobilized on carbon tape mounted on an aluminum stub. The samples were blown using compressed air to remove excess material not stuck to the tape and then were coated with a carbon or gold/palladium layer.

For X-ray photoelectron spectroscopy (XPS) spectra, monochromatic Al K_α X-rays (1486.6 eV) were generated at 250 W (15 kV; 20 mA) with photoelectrons collected from a 2 mm diameter analysis spot. Photoelectrons were collected at a 0° emission angle with source to analyzer angle of 54.7°. A hemispherical analyzer determined electron kinetic energy, using a pass energy of 200

eV for wide/survey scans, and 50 eV for high resolution scans. A flood gun was used for charge neutralization of non-conductive samples. The data were then processed with CasaXPS. The XPS spectra of porous solids often contain higher-than-expected amounts of N and O due to physisorbed air. Indeed, peaks corresponding to N 1s (~400 eV) and O 1s (~525 eV) were observed in all XPS spectra in this work, even for MOFs that do not contain N (*e.g.*, Co_2(dobdc), Figure S87) or O (*e.g.,* Ni(bdp), Figure S74). As such, XPS spectra in this work are treated as a qualitative means of evaluating the elemental composition of samples.[1]

Mössbauer spectra were collected at 85 K and 0 field using a SEECo Resonant Gamma-Ray spectrometer with a Janis Research Model SVT-400 Cryostat. The velocity scale was calibrated with Fe foil at room temperature. Spectra were fit using the WMOSS software package with Theoretical Model 3. Uncertainties were obtained from the standard deviation of 250 Monte Carlo simulations.

Pressed-pellet conductivities were measured using a two-point probe. The sample powder was placed between two stainless-steel contacts encased in a Teflon tube, such that the entire contact area (A, 0.792 cm^2) was covered by the powder. Small positive and negative potential pulses (±2–20 mV) were applied across the device, and the current response was used to generate a *I*-*V* plot. The slope of the plot corresponded to the resistance, *R*, of the sample, and the following equation was used to calculate the conductivity (σ):

$$\sigma = \frac{t}{R \times A}$$

where *t* is the thickness of the layer of material between the two metal contacts.

Ionothermal Synthesis of MOFs (General Procedure A). To a 23 mL Teflon autoclave, linker (1.00 g, 1.00 equiv.) and the corresponding MCl_x salt were added. The autoclave was sealed and placed in an oven that had been pre-heated to a temperature above the melting point of the metal salt (generally 160 ºC when using $NiCl_2$•$6H_2O$ and $CoCl_2$•$6H_2O$, 200 ºC when using $FeCl_3$•$6H_2O$, 225 ºC when using the eutectic mixture of $ZnCl_2$/NaCl/KCl, and 290 ºC when using $ZnCl_2$). The autoclave was allowed to stand in the oven for 16 h. The autoclave was removed from the oven and allowed to cool to room temperature. The solid was transferred to a Pyrex jar along with fresh *N*,*N*-dimethylformamide (DMF) or acetonitrile (50 mL). The jar was placed in an oven that had been heated to 120 °C (DMF) or 65 °C (acetonitrile) and allowed to stand at this temperature for 24 h. At this time, the solvent was decanted and replaced with fresh solvent (50 mL). This soaking procedure was repeated for a total of three hot DMF soaks. Next, the soaking procedure was repeated with methanol (100 mL) at 65 °C, replacing the solvent every 24 h. This soaking procedure was repeated for a total of three hot methanol soaks. The heterogeneous mixture was filtered. The solid was then activated under dynamic vacuum (<100 mTorr) at 150 °C for 24 h, yielding activated MOF. The material was stored in a N_2-filled glovebox when not in use. Prior to gas adsorption measurements, the samples were further activated under high vacuum (<10 μbar).

2. Synthesis of organic linkers.

2a. Synthesis of H_2btdd.

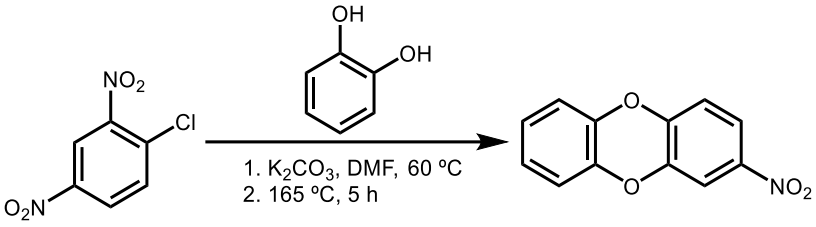

This procedure is adapted from the literature.[2] A 250 mL round-bottom flask equipped with a stir bar was charged with DMF (120 mL), potassium carbonate (30.0 g, 217 mmol, 2.19 equiv.), and catechol (11.9 g, 108 mmol, 1.09 equiv.). The mixture was heated with stirring to 60 °C, at which time 1-chloro-2,4-dinitrobenzene (20.0 g, 98.7 mmol, 1.00 equiv.) was added. A reflux condenser was affixed, and the reaction mixture was stirred at reflux at 165 °C for 5 h. At this time, the mixture was allowed to cool to room temperature, poured onto crushed ice (250 mL), and filtered. The solid was washed with deionized (DI) water, evacuated to dryness, and then dissolved in boiling acetone (1 L). The solution was cooled to room temperature and then to 0 °C using an ice-water bath. Upon the addition of DI water (400 mL), a yellow solid precipitated from solution. The solid was filtered and washed with DI water, a small amount of diethyl ether, and hexanes, yielding 2-nitrodibenzo[*b*,*e*][1,4]dioxine as a yellow solid (20.1 g, 88% yield). ^{1}H NMR (500 MHz, DMSO-d_6): δ 7.89 (dd, *J* = 8.9, 2.7 Hz, 1H), 7.79 (d, *J* = 2.7 Hz, 1H), 7.21 (d, *J* = 8.9 Hz, 1H), 7.10–7.00 (m, 4H) ppm; ^{13}C NMR (126 MHz, DMSO-d_6): δ 147.4, 143.8, 141.9, 140.8, 140.8, 125.9, 125.5, 121.0, 117.5, 117.2, 117.0, 112.4 ppm.

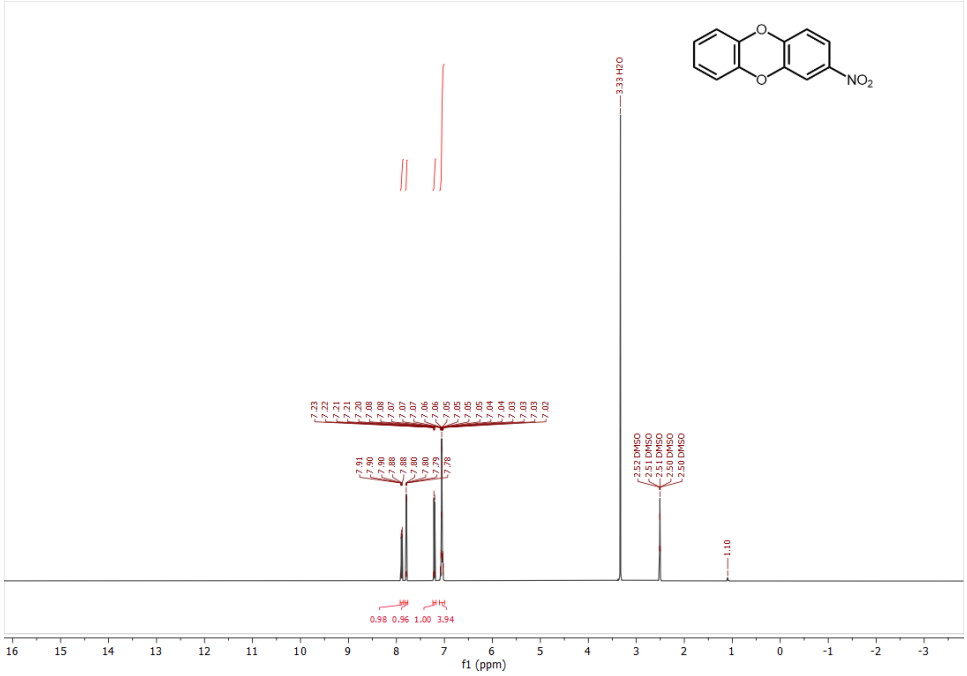

Figure S1. ^{1}H NMR spectrum (500 MHz, DMSO-d_6) of 2-nitrodibenzo[*b*,*e*][1,4]dioxine used in this work.

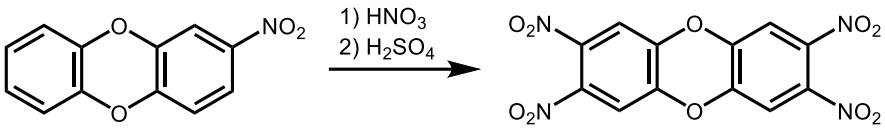

This procedure is adapted from the literature.[3] A 500 mL round-bottom flask equipped with a stir bar was charged with 2-nitrodibenzo[*b*,*e*][1,4]dioxine (19.9 g, 86.8 mmol, 1.00 equiv.) and fuming nitric acid (80 mL). A reflux condenser was equipped and concentrated sulfuric acid (55 mL) was added slowly through the top of the condenser while the reaction mixture was stirred. The reaction mixture was stirred at 70 °C for 14 h. The reaction mixture was cooled to room temperature and filtered. The resulting solid was washed thoroughly with DI water. The aqueous mother liquor was removed and quenched. Using a new filter flask, the solid was further washed thoroughly with methanol and hexanes and allowed to air-dry overnight, yielding 2,3,7,8-tetranitrodibenzo[*b*,*e*][1,4]dioxine as a pale yellow solid (25.8 g, 81% yield). ^{1}H NMR (500 MHz, DMSO-d$_6$): δ 8.03 (s, 4H) ppm; ^{13}C NMR (101 MHz, DMSO-d$_6$): δ 144.1, 139.2, 114.3 ppm. These spectra are consistent with those reported in the literature.[3]

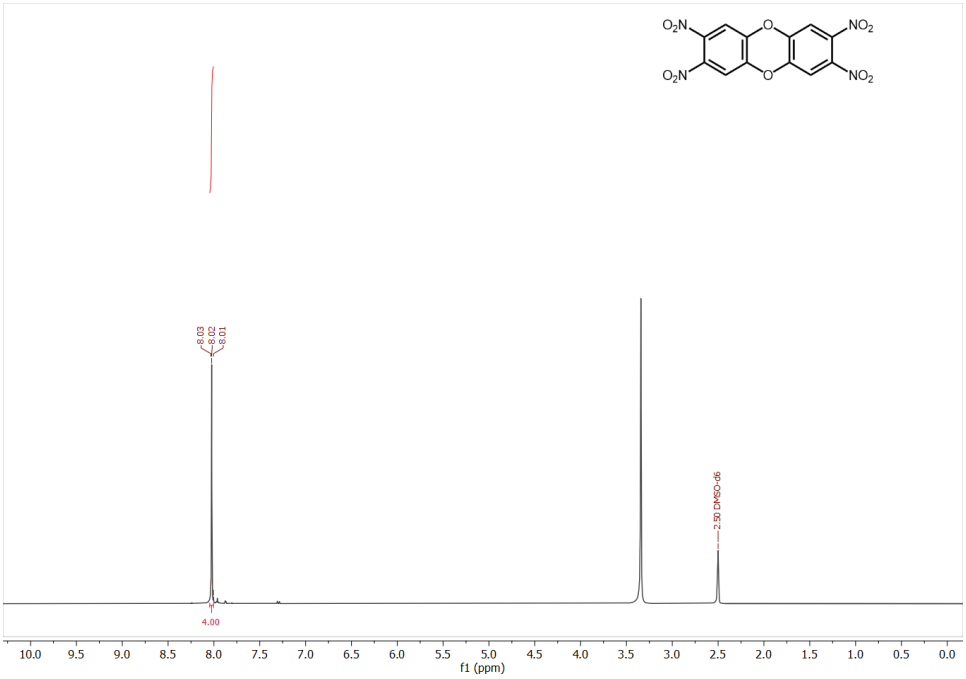

Figure S2. ^{1}H NMR spectrum (500 MHz, DMSO-d$_6$) of 2,3,7,8-tetranitrodibenzo[*b*,*e*][1,4]dioxine used in this work.

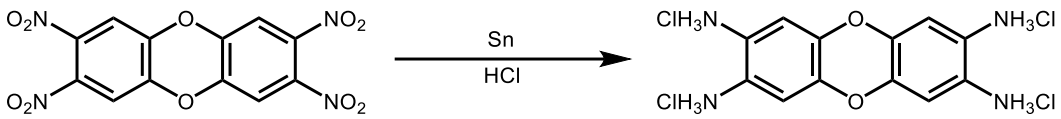

This procedure is adapted from the literature.[2] A 1 L three-neck round-bottom flask equipped with a stir bar was charged with 2,3,7,8-tetranitrodibenzo[*b*,*e*][1,4]dioxine (25.8 g, 70.8 mmol, 1.00 equiv.) and concentrated HCl (532 mL). The flask was affixed with a reflux condenser. Tin powder (134.4 g, 1.13 mol, 16.0 equiv.) was slowly added while the reaction mixture was vigorously stirred. After foaming subsided, the reaction mixture was heated at reflux (90 °C) for 14 h. The reaction mixture was cooled to 0 °C and filtered. The resulting solid was washed with concentrated HCl, ethanol, and diethyl ether, yielding dibenzo[*b*,*e*][1,4]dioxine-2,3,7,8-tetraamonium chloride (29.0 g) as an off-white solid. This solid was dried under vacuum and used in the next step without further purification.

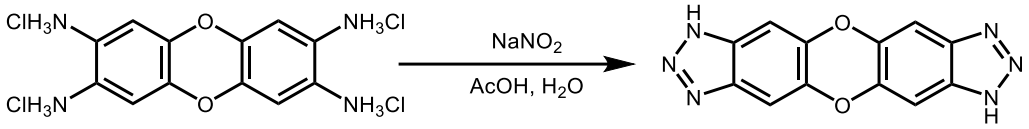

This procedure is adapted from the literature.[2] A 1 L round-bottom flask equipped with a stir bar was charged with dibenzo[*b*,*e*][1,4]dioxine-2,3,7,8-tetraammonium chloride (29.0 g, ~74.0 mmol, 1.00 equiv.), acetic acid (270 mL), and DI water (90 mL). The flask was cooled to below 0 °C using a salted ice-water bath. A solution of $NaNO_2$ (12.5 g, 181 mmol, ~2.45 equiv.) in DI water (90 mL) was added slowly to the reaction mixture. During the process of addition, the reaction mixture changed from light orange to green to orange-brown in color. The reaction was stirred at below 0 °C in the salted ice-water bath for 30 min. The bath was removed, allowing the reaction mixture to warm slowly to room temperature, and the reaction mixture was allowed to stir at room temperature for 14 h. The mixture was diluted with DI water (230 mL) and filtered. The resulting solid was washed thoroughly with DI water. The aqueous mother liquor was removed and quenched. Using a new filter flask, the solid was further washed with ethanol and diethyl ether and air-dried, yielding bis(1*H*-1,2,3-triazolo[4,5-b],[4',5'-i])dibenzo[1,4]dioxin) (H_2btdd, 17.8 g, ~90% yield) as a brown solid. ^{1}H NMR (500 MHz, DMSO-d6): δ 7.64 (bs, 4H) ppm. This spectrum is consistent with that reported in the literature.[2]

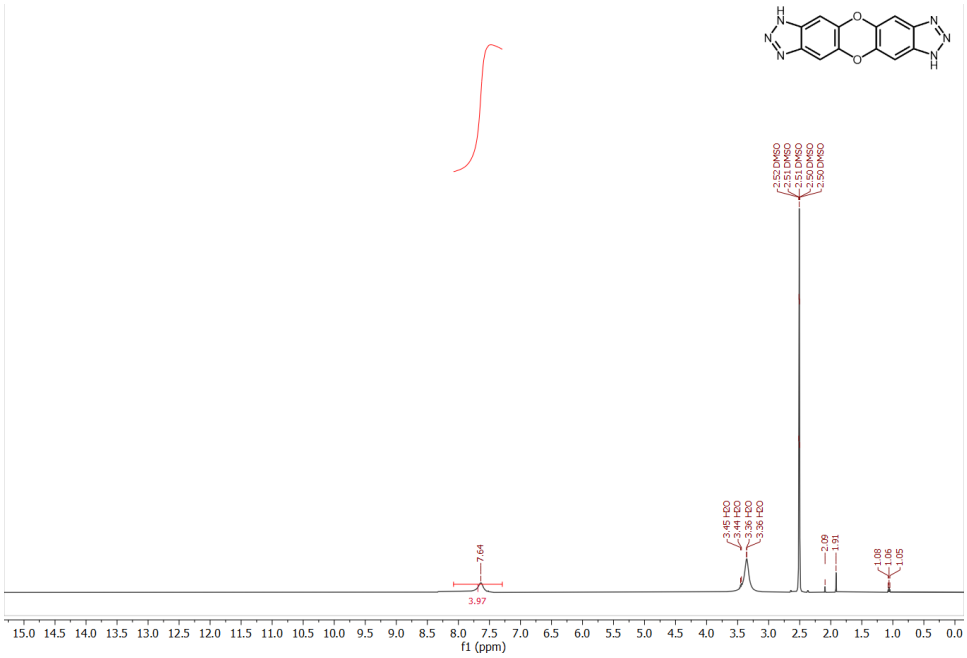

Figure S3. ^{1}H NMR spectrum (500 MHz, DMSO-d_6) of H_2btdd used in this work.

2b. Synthesis of H_3btp.

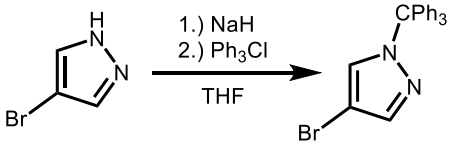

This procedure is adapted from the literature.[4] An oven-dried 500 mL round-bottom flask equipped with a stir bar was charged with 4-bromo-1*H*-pyrazole (10.0 g, 68.0 mmol, 1.00 equiv.). The flask was placed under high vacuum and backfilled with N_2. This procedure was repeated a total of three times. Anhydrous THF (250 mL) was added, and the flask was cooled to 0 °C using an ice-water bath. Under high N_2 flow, NaH (60% dispersion in mineral oil, 3.30 g, ~81.6 mmol, ~1.20 equiv.) was added portion-wise. The reaction mixture was allowed to stir at 0 °C for 90 min. At this time, trityl chloride (20.9 g, 74.8 mmol, 1.10 equiv.) was added under strong N_2 flow, upon which the reaction mixture turned orange and then dark gray. The reaction mixture was stirred under N_2 for 36 h, during which time the mixture turned dark yellow-green. DI water (500 mL) was added and the reaction mixture was filtered. The resulting solid was washed with DI water (200 mL) and MeOH (200 mL), yielding 4-bromo-1-trityl-1*H*-pyrazole (27.3 g) as a light-yellow solid. ^{1}H NMR (500 MHz, $CDCl_3$): δ 7.62 (d, *J* = 0.7 Hz, 1H), 7.39 (d, *J* = 0.7 Hz, 1H), 7.35–7.29 (m, 9H), 7.18–7.08 (m, 6H) ppm; ^{13}C NMR (126 MHz, $CDCl_3$): δ 142.6, 140.2, 132.3, 130.1, 128.0, 127.9, 92.4, 79.4 ppm.

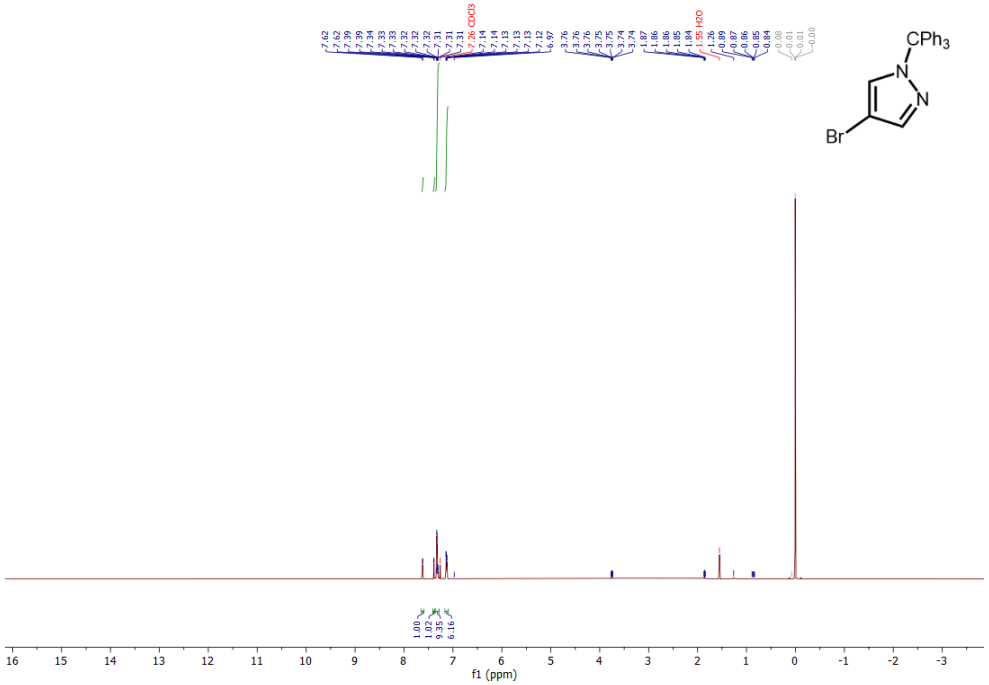

Figure S4. ^{1}H NMR spectrum (500 MHz, $CDCl_3$) of 4-bromo-1-trityl-1*H*-pyrazole used in this work.

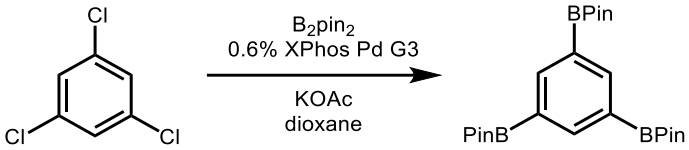

This procedure is adapted from the literature.[5] A 500 mL three-neck round-bottom flask equipped with a stir bar was charged with 1,3,5-trichlorobenzene (4.45 g, 24.5 mmol, 1.00 equiv.), bis(pinacolato)diboron (25.1 g, 98.8 mmol, 4.03 equiv.), KOAc (26.5 g, 270 mmol, 11.0 equiv.), XPhos Pd G3 (0.127 g, 0.15 mmol, 0.61%), and XPhos (0.072 g, 0.15 mmol, 0.61%). A reflux condenser was affixed to the flask. The flask was placed under high vacuum and backfilled with N_2. This procedure was repeated a total of three times. Freshly degassed dioxane (80 mL) was added to the reaction flask. The reaction mixture was then heated under N_2 at reflux for 12 h. The reaction mixture was cooled to room temperature and poured into DI water (400 mL), resulting in the precipitation of a gray solid from solution. This solid was isolated by filtration, washed with DI water (200 mL), and dissolved in chloroform (300 mL). The solution was filtered through celite, eluting with chloroform (300 mL), and dried over $MgSO_4$. After solvent removal under reduced pressure, the resulting light-yellow solid was triturated with cold MeOH and filtered, yielding 1,3,5-tris(pinacalboryl)benzene (5.85 g, 52% yield) as a white solid. ^{1}H NMR (500 MHz, $CDCl_3$): δ 8.36 (s, 3H), 1.33 (s, 36H) ppm; ^{13}C NMR (126 MHz, $CDCl_3$): δ 144.1, 83.7, 24.9 ppm. These spectra are consistent with those reported in the literature.[5]

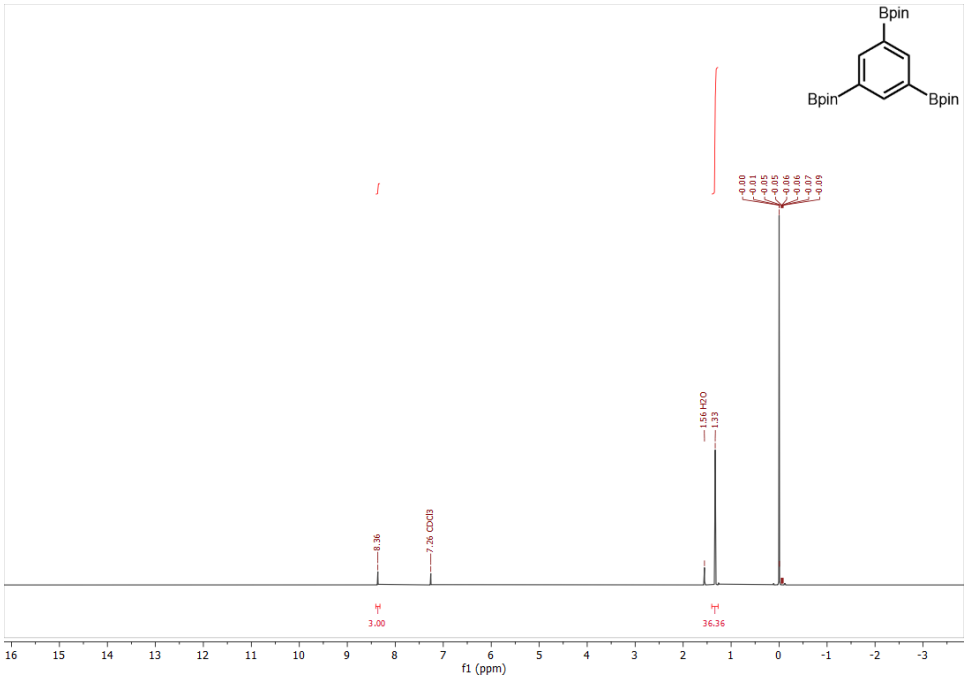

Figure S5. ^{1}H NMR spectrum (500 MHz, $CDCl_3$) of 1,3,5-tris(pinacalboryl)benzene used in this work.

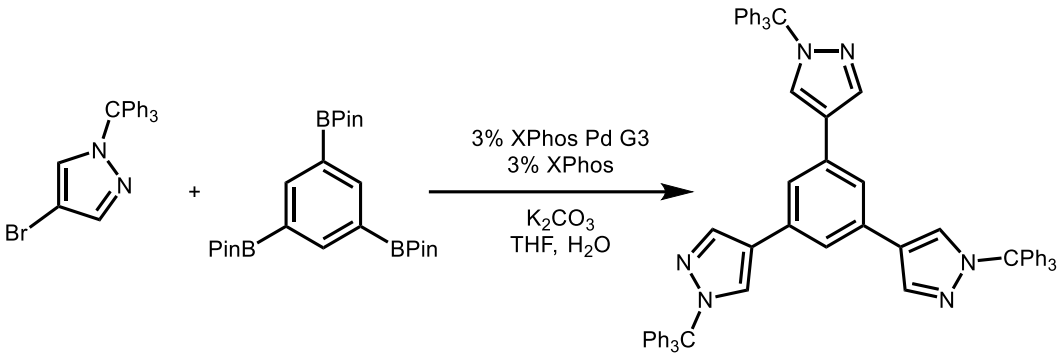

This procedure is adapted from the literature.[3] A 500 mL three-neck round-bottom flask equipped with a reflux condenser and a stir bar was charged with 1,3,5-tris(pinacalboryl)benzene (5.85 g, 12.8 mmol, 1.00 equiv.), 4-bromo-1-trityl-1*H*-pyrazole (15.1 g, 38.7 mmol, 3.02 equiv.), XPhos Pd G3 (0.32 g, 0.38 mmol, 3.00%), XPhos (0.18 g, 0.38 mmol, 3.00%), and K_2CO_3 (10.6 g, 76.5 mmol, 5.98 equiv.). The flask was placed under high vacuum and backfilled with N_2. This procedure was repeated a total of three times. Anhydrous, degassed THF (38 mL) and freshly degassed DI water (77 mL) were added. The reaction was heated under N_2 at reflux (80 °C) for 16 h. The reaction mixture was allowed to cool to room temperature, diluted with ethyl acetate (160 mL), and transferred to a separatory funnel. The aqueous and organic layers were separated. The aqueous phase was further extracted with ethyl acetate (2 × 100 mL). The combined organic layers were washed with brine (2 × 100 mL). Dichloromethane was added to the combined organic layers until the mixture became homogeneous. The resulting clear dark brown solution was dried over Na_2SO_4 and filtered through celite, eluting with dichloromethane. After removal of the solvent under reduced pressure, the resulting brown solid was triturated with MeOH. The resulting heterogeneous mixture was allowed to stand at 5 °C for 12 h and filtered. The resulting off-white solid was washed with cold MeOH, yielding 1,3,5-tris(1-trityl-1*H*-pyrazol-4-yl)benzene as an off-white solid (12.23 g, 95%). This solid was used directly in the next step without further purification.

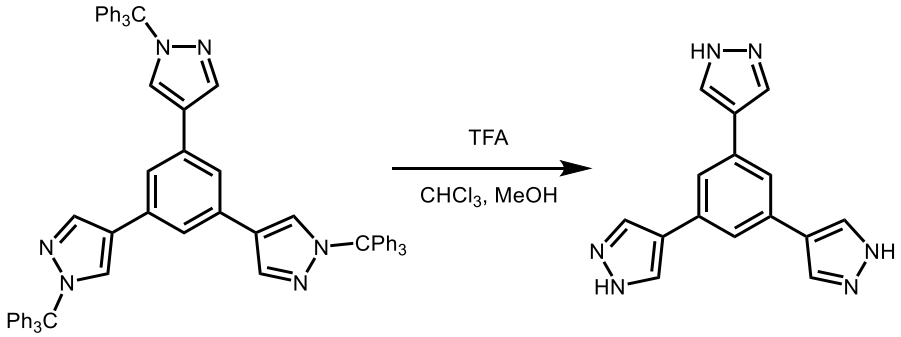

This procedure is adapted from the literature.[3] A 500 mL round bottom flask equipped with a stir bar and reflux condenser was charged with 1,3,5-tris(1-trityl-1*H*-pyrazol-4-yl)benzene (12.2 g, 17.7 mmol, 1.00 equiv.), trifluoroacetic acid (100 mL), chloroform (100 mL), and methanol (25 mL). The reaction mixture was allowed to stir at reflux for 24 h. At this time, the reaction mixture was allowed to cool to room temperature. The solvent was removed under reduced pressure. Toluene (50 mL) was added, and the mixture was filtered. The resulting solid was washed

thoroughly with toluene (50 mL), chloroform (50 mL), methanol (50 mL), and diethyl ether (50 mL). The solid was suspended in water (50 mL) and aqueous 2 M NaOH was added until the pH of the solution was greater than 5. The mixture was filtered, and the resulting solid was washed thoroughly with water (250 mL). The solid was then triturated with a hot 1:1 mixture of acetone and ethyl acetate (100 mL) and filtered. The resulting solid was washed with acetone (100 mL) and ethyl acetate (100 mL), yielding 1,3,5-tri(1*H*-pyrazol-4-yl)benzene (H_3btp, 3.16 g, 93% yield) as an off-white solid. ^{1}H NMR (500 MHz, DMSO-d_6): δ 12.92 (s, 3H), 8.18 (s, 6H), 7.68 (s, 3H) ppm. This spectrum is consistent with that reported in the literature.[3]

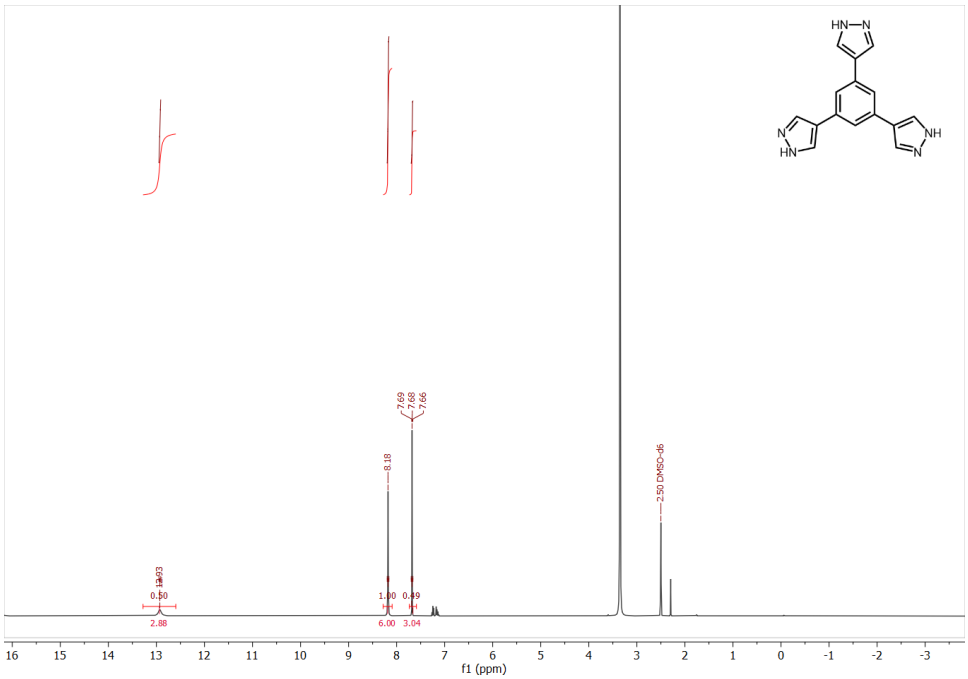

Figure S6. ^{1}H NMR spectrum (500 MHz, DMSO-d_6) of H_3btp used in this work.

2c. Synthesis of H_2bdp.

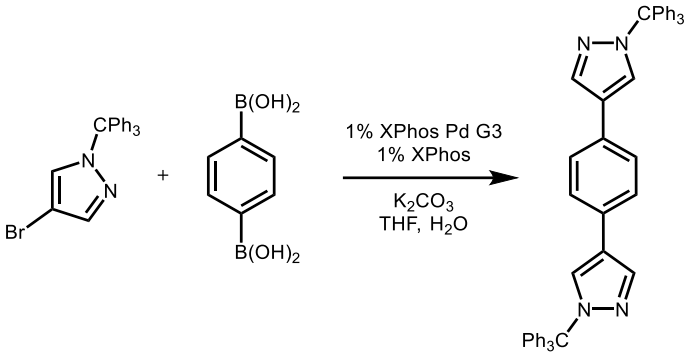

This procedure is adapted from the literature.[4] A 500 mL 3-neck round bottom flask equipped with a stir bar and reflux condenser was charged with benzene-1,4-diboronic acid (4.34 g, 26.2 mmol, 1.00 equiv.), 4-bromo-1-trityl-1*H*-pyrazole (20.4 g, 52.4 mmol, 2.00 equiv.), XPhos Pd G3 (0.22 g, 0.26 mmol, 1.00%), XPhos (0.12 g, 0.26 mmol, 1.00%), and K_2CO_3 (14.4 g, 104 mmol, 4.00 equiv.). The flask was placed under high vacuum and back-filled with N_2. This process was repeated a total of three times. Next, degassed water (120 mL) and THF (80 mL) were added under positive N_2 pressure, and the reaction mixture was stirred at reflux under N_2 for 36 h. The reaction mixture was allowed to cool to room temperature, poured into water (500 mL), and filtered. The resulting pale yellow solid was washed thoroughly with water (200 mL), ethyl acetate (200 mL), and hexanes (50 mL), yielding 1,4-bis(1-trityl-1*H*-pyrazol-4-yl)benzene (14.6 g, 80%) as an off-white solid. ^{1}H NMR (500 MHz, $CDCl_3$): δ 7.92 (s, 2H), 7.60 (s, 2H), 7.37 (s, 4H), 7.31–7.34 (m, 18H), 7.18–7.22 (m, 12H) ppm. This spectrum is consistent with that reported in the literature.[4]

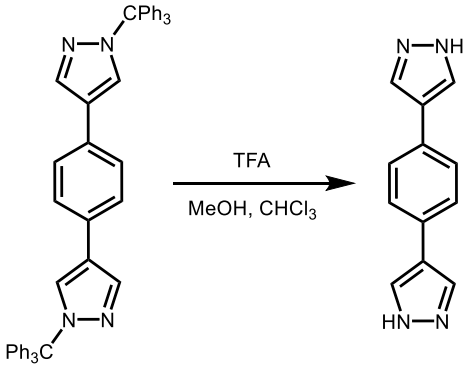

A 2 L round bottom flask equipped with a stir bar and reflux condenser was charged with 1,4-bis(1-trityl-1*H*-pyrazol-4-yl)benzene (14.6 g, 21.0 mmol, 1.00 equiv.), methanol (300 mL), dichloromethane (200 mL), and trifluoroacetic acid (200 mL). The reaction mixture was allowed to stir at reflux for 48 h. The reaction mixture was allowed to cool to room temperature and then to 0 °C, resulting in precipitation of a white solid from solution. The mixture was filtered, and the resulting white solid was washed with toluene (200 mL) and THF (200 mL). The resulting solid was suspended in water (200 mL), and aqueous 2 M NaOH was added slowly until the pH of the solution was greater than 5. The heterogeneous mixture was filtered, and the resulting off-white

solid was washed thoroughly with water (200 mL), THF (100 mL), and hexanes (100 mL). Drying under vacuum for 12 h yielded 1,4-di(1*H*-pyrazol-4-yl)benzene (H_2bdp, 4.00 g, 91%) as a white solid. ^{1}H NMR (500 MHz, DMSO-d_6): δ 8.05 (bs, 4H), 7.58 (s, 4H) ppm. This spectrum is consistent with that reported in the literature.[4]

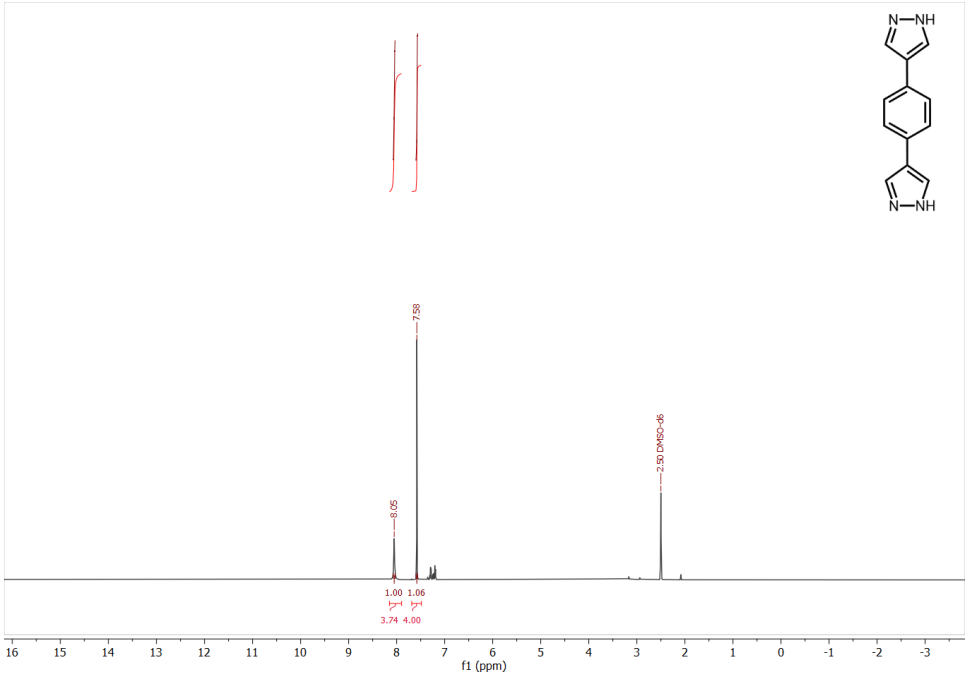

Figure S7. ^{1}H NMR spectrum (500 MHz, DMSO-d_6) of H_2bdp used in this work.

2d. Synthesis of H$_4$*m*-dobdc.

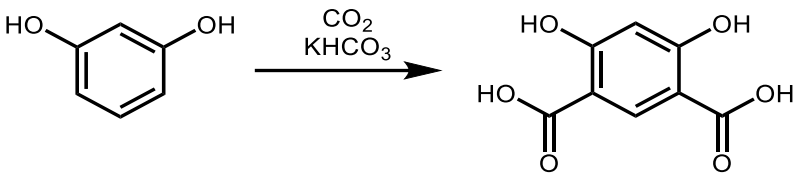

This procedure is adapted from the literature.[3] Resorcinol (5.00 g, 45.2 mmol, 1.00 equiv.) and $KHCO_3$ (10.5 g, 105 mmol, 2.32 equiv.) were pulverized separately using a mortar and pestle and then thoroughly mixed together. The combined solids were sealed in a Parr reactor equipped with a pressure gauge. The Parr reactor was pressurized with CO_2 to 25 bar at room temperature and then vented to the atmosphere. This process was repeated a total of three times. The Parr reactor was pressurized with CO_2 to 25 bar at room temperature and sealed. The Parr reactor was then heated to 230 °C (as measured by an external thermocouple) in a sand bath for 18 h. At this time, the Parr reactor was allowed to slowly cool to room temperature. The pressure was vented and 1 L of water was added to the solid. The solid was broken up mechanically and then by sonication. The resulting suspension was filtered, and the filtrate was acidified with concentrated HCl until the pH of the solution was less than 1, resulting in the precipitation of a white solid from solution. The product was then collected by filtration, and the resulting solid was recrystallized from hot water. The mixture was filtered, yielding 2,4-dihydroxybenzene-1,5-dicarboxylic acid (H$_4$*m*-dobdc, 4.19 g, 47%) as a pale yellow solid. ^{1}H NMR (500 MHz, DMSO-d6): δ 13.7 ppm (br s, 2H), 12.0 (br s, 2H), 8.30 ppm (s, 1H), 6.41 ppm (s, 1H). This spectrum is consistent with that reported in the literature.[4]

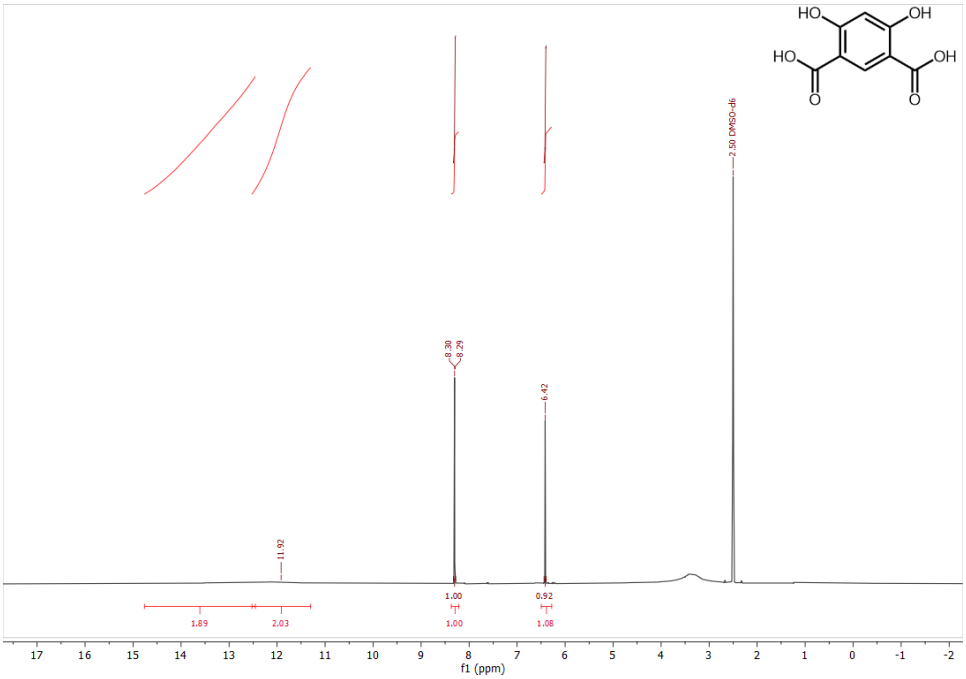

Figure S8. ^{1}H NMR spectrum (500 MHz, DMSO-d$_6$) of H$_4$*m*-dobdc used in this work.

3. Synthesis and characterization of $Co_2Cl_2(btdd)$.

Solvothermal synthesis of $Co_2Cl_2(btdd)$-ST.

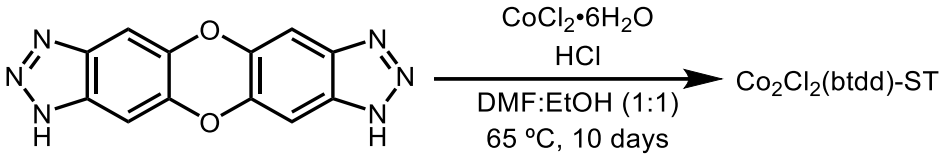

This procedure is adapted from the literature.[6] To a 500 mL round bottom flask, H_2btdd (200 mg, 0.75 mmol, 1.00 equiv.) and DMF (200 mL) were added. The solution was heated to 130 °C for 1 h and then allowed to cool to room temperature. To a separate 1 L Pyrex jar, $CoCl_2•6H_2O$ (356 mg, 1.50 mmol, 2.00 equiv.), EtOH (200 mL), and concentrated HCl (4 mL) were added. The solution of H_2btdd in DMF was added to the 1 L jar, which was then capped and placed in an oven that had been pre-heated to 65 ºC. The jar was allowed to stand at 65 °C for 10 days. At this time, the jar was removed from the oven and allowed to cool to room temperature. The heterogeneous mixture was filtered, and the solid was returned to the Pyrex jar along with fresh DMF (200 mL). The jar was placed in an oven that had been heated to 120 °C. After 24 h, the DMF was decanted and replaced with fresh DMF (200 mL). This soaking procedure was repeated for a total of three hot DMF soaks. Next, the soaking procedure was repeated with methanol (200 mL) at 65 °C, replacing the solvent every 24 h. This soaking procedure was repeated for a total of three hot methanol soaks. The heterogeneous mixture was filtered. The solid was then activated under dynamic vacuum (<100 mTorr) at 150 °C for 24 h, yielding activated $Co_2Cl_2(btdd)$ as a dark green powder.

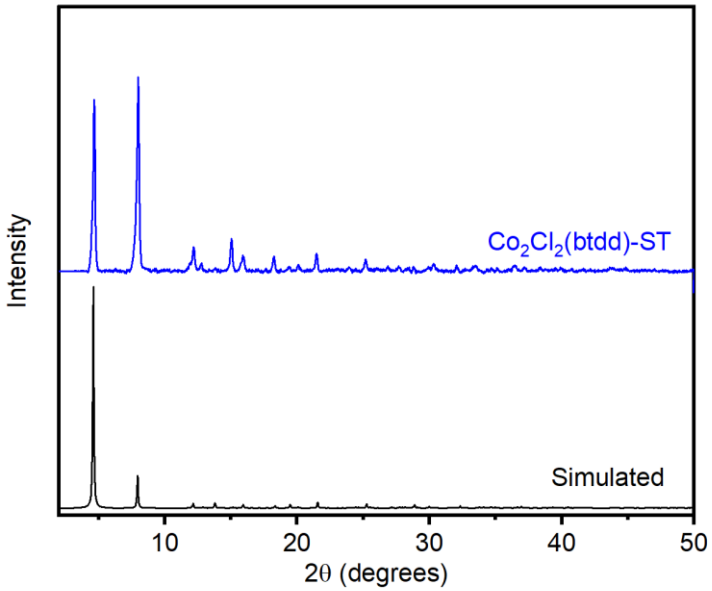

Figure S9. PXRD pattern (λ = 1.5406 Å) of $Co_2Cl_2(btdd)$ prepared under solvothermal conditions. The simulated pattern corresponding to the single-crystal X-ray diffraction structure of $Mn_2Cl_2(btdd)$ is included for reference.[6] The experimental PXRD pattern was baseline corrected.

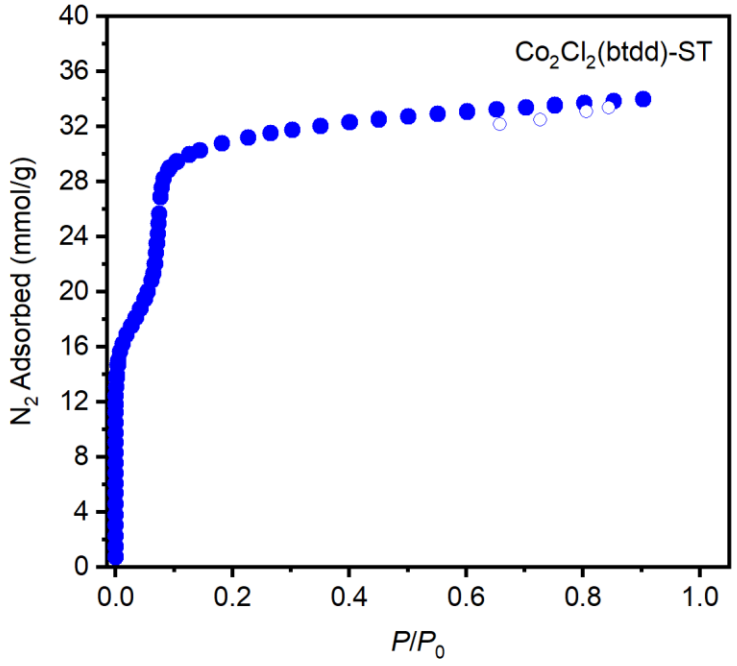

Figure S10. 77 K N_2 adsorption (closed circles) and desorption (open circles) isotherms of Co_2Cl_2(btdd) prepared under solvothermal conditions. Fitting these data yielded a Brunauer–Emmett–Teller (BET) surface area of 2438 ± 14 m^2/g (Lit: 1912 m^2/g).[6]

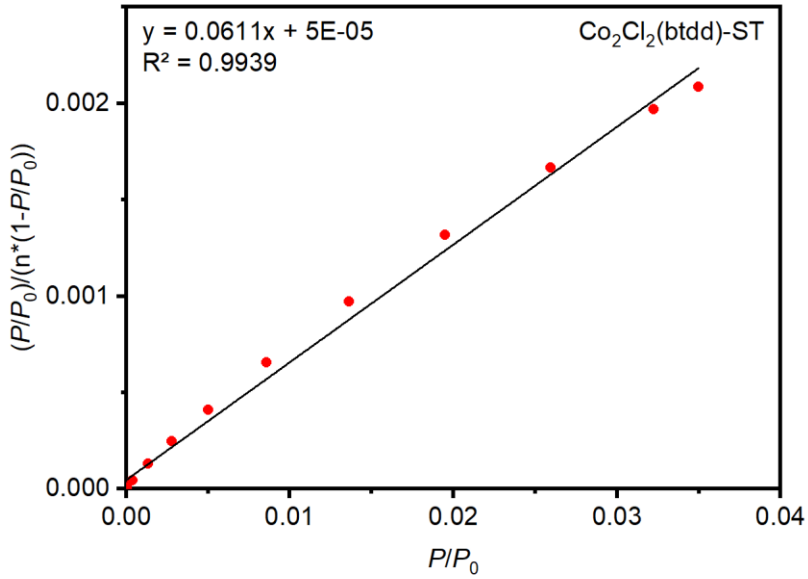

Figure S11. Linearized Brunauer–Emmett–Teller (BET) plot for the adsorption data of Co_2Cl_2(btdd) prepared under solvothermal conditions.

Ionothermal synthesis of Co_2Cl_2(btdd)-IT.

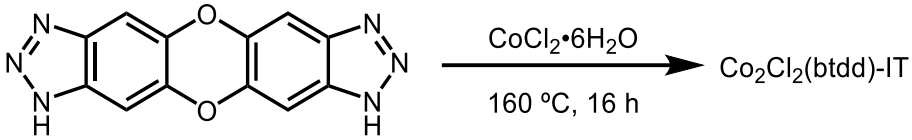

Following General Procedure A, H_2btdd (1.00 g, 3.75 mmol, 1.00 equiv.) and $CoCl_2$•$6H_2O$ (1.78 g, 7.50 mmol, 2.00 equiv.) were combined at 160 °C to yield Co_2Cl_2(btdd) (1.36 g, 80% yield) as a dark green solid after activation under dynamic vacuum (<100 mTorr) at 150 °C for 24 h.

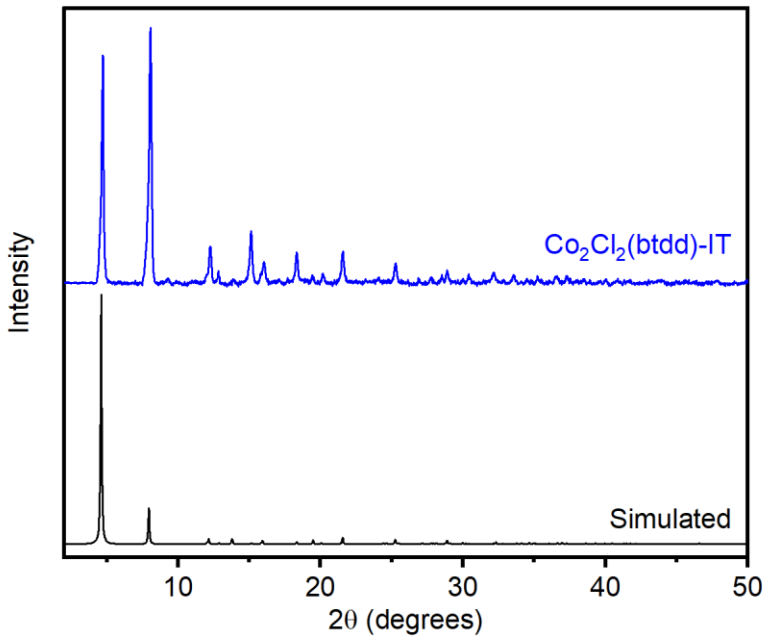

Figure S12. PXRD pattern (λ = 1.5406 Å) of Co_2Cl_2(btdd) prepared under ionothermal conditions. The simulated pattern corresponding to the single-crystal X-ray diffraction structure of Mn_2Cl_2(btdd) is included for reference.[6] The experimental PXRD pattern was baseline corrected.

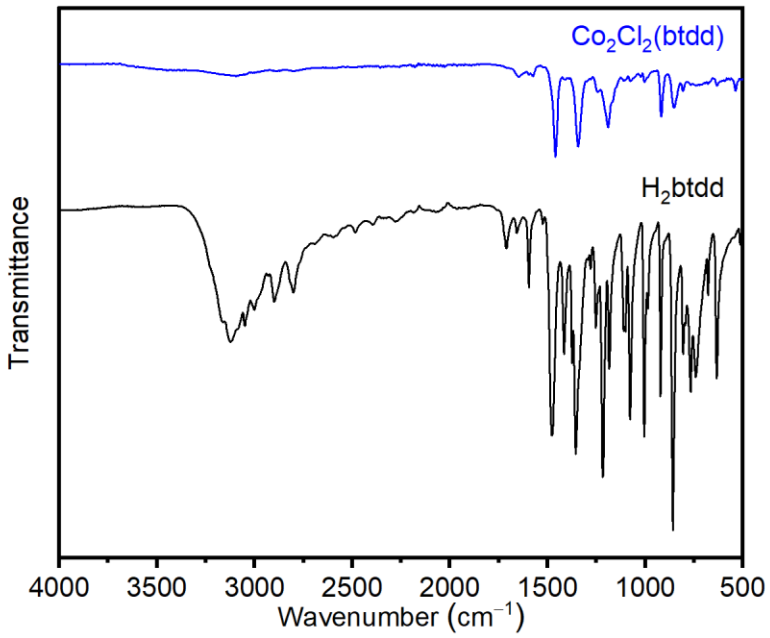

Figure S13. ATR IR spectrum of Co_2Cl_2(btdd) prepared under ionothermal conditions.

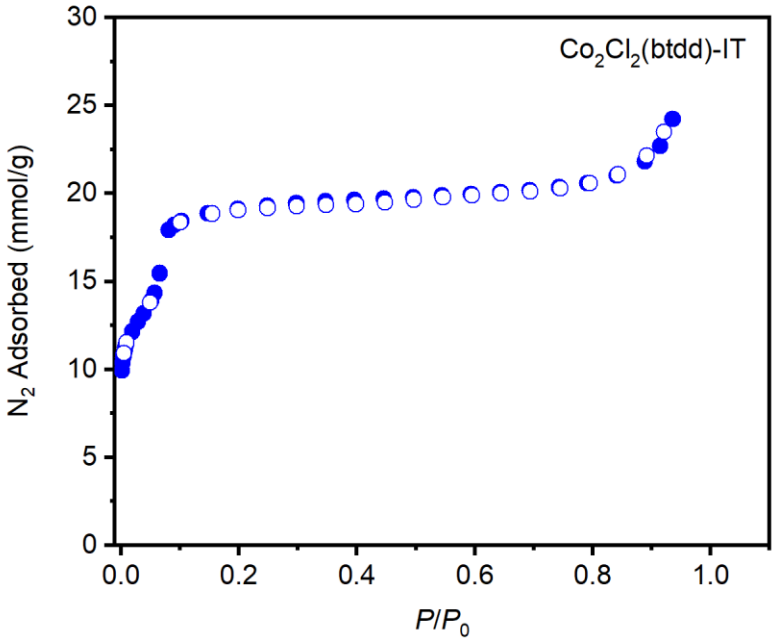

Figure S14. 77 K N_2 adsorption (closed circles) and desorption (open circles) isotherms of Co_2Cl_2(btdd) prepared under ionothermal conditions. Fitting these data yielded a Brunauer–Emmett–Teller (BET) surface area of 2322 ± 8 m^2/g (Lit: 1912 m^2/g).[6]

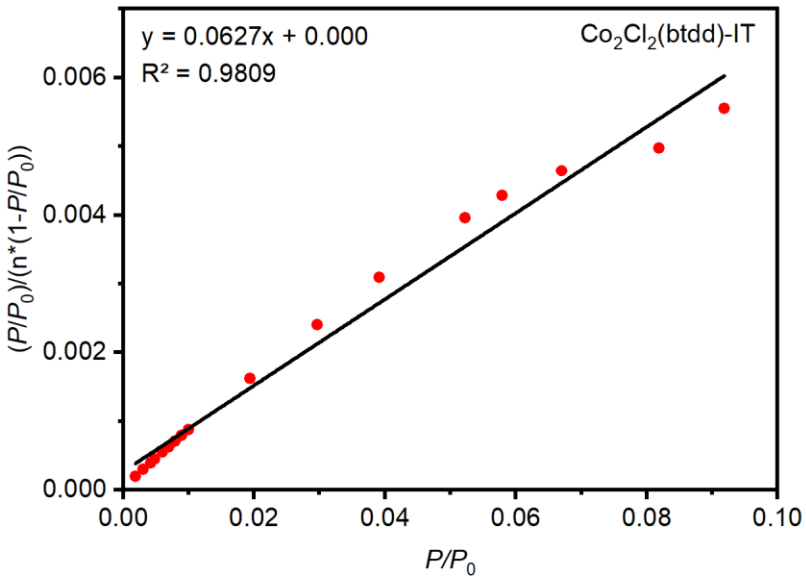

Figure S15. Linearized Brunauer–Emmett–Teller (BET) plot for the adsorption data of Co_2Cl_2(btdd) prepared under ionothermal conditions.

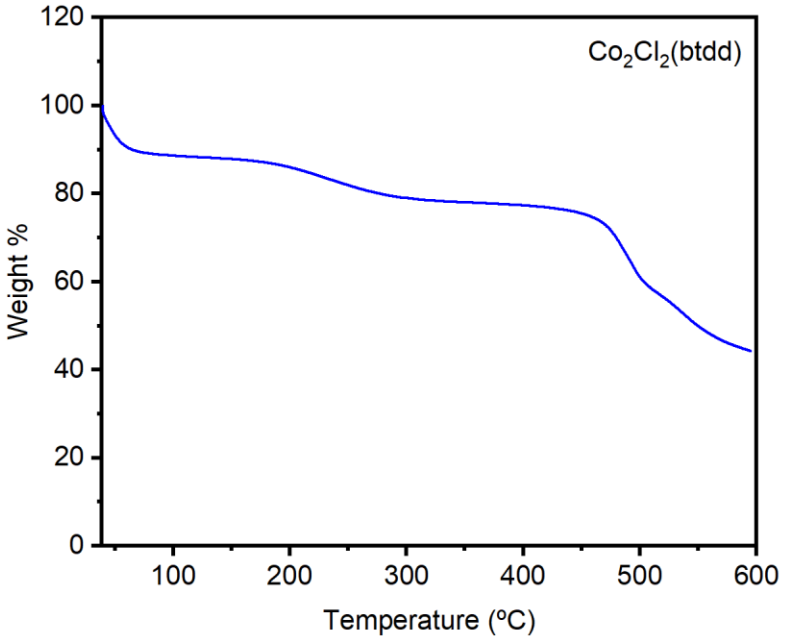

Figure S16. TGA decomposition profile of Co_2Cl_2(btdd) prepared under ionothermal conditions.

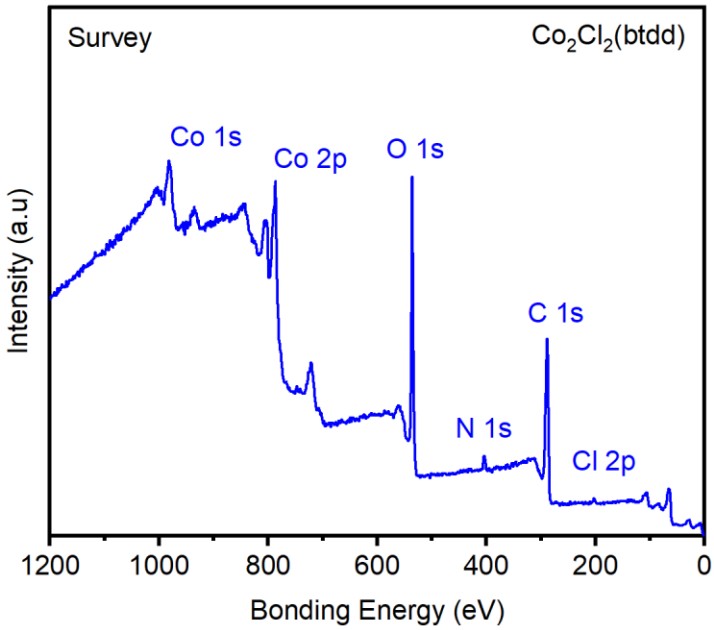

Figure S17. XPS spectral scan of an activated sample of Co_2Cl_2(btdd) prepared under ionothermal conditions.

Table S1. Tabulated survey XPS data for Co_2Cl_2(btdd) prepared under ionothermal conditions.

Element	Peak Label	Position	Area	Atomic %
Co	Co 2p	782.8	1640.72	6.95
Cl	Cl 2p	199.8	5.49	0.20
O	O 1s	531.8	1036.90	28.73
C	C 1s	284.8	763.78	62.02
N	N 1s	399.8	46.66	2.1
Total:				100

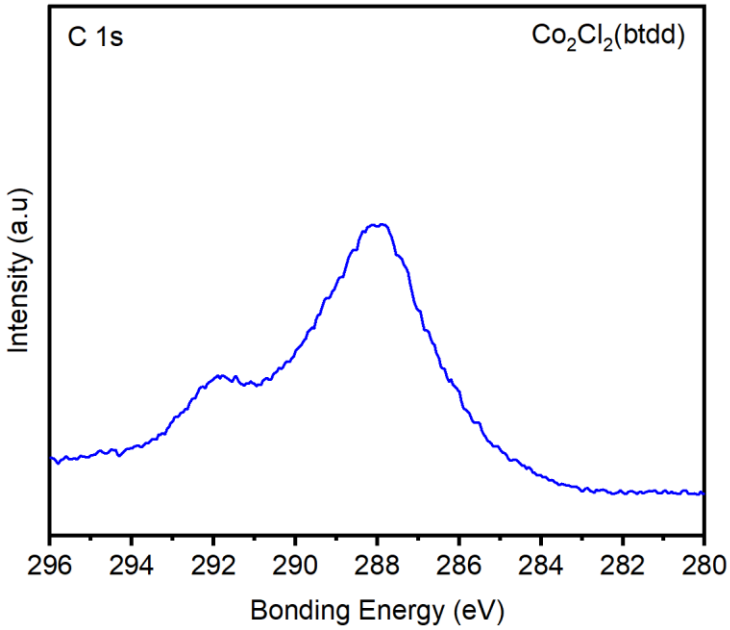

Figure S18. High resolution C 1s XPS spectrum of Co_2Cl_2(btdd) prepared under ionothermal conditions.

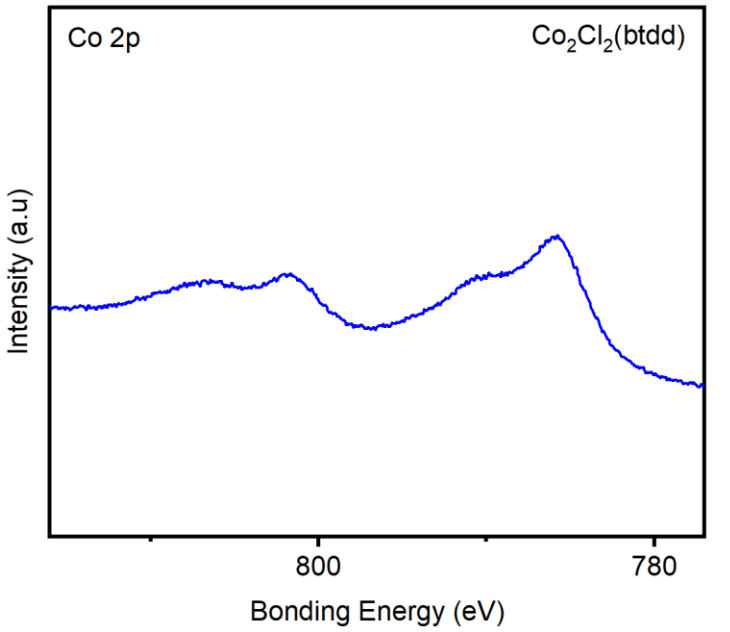

Figure S19. High resolution Co 2p XPS spectrum of Co_2Cl_2(btdd) prepared under ionothermal conditions.

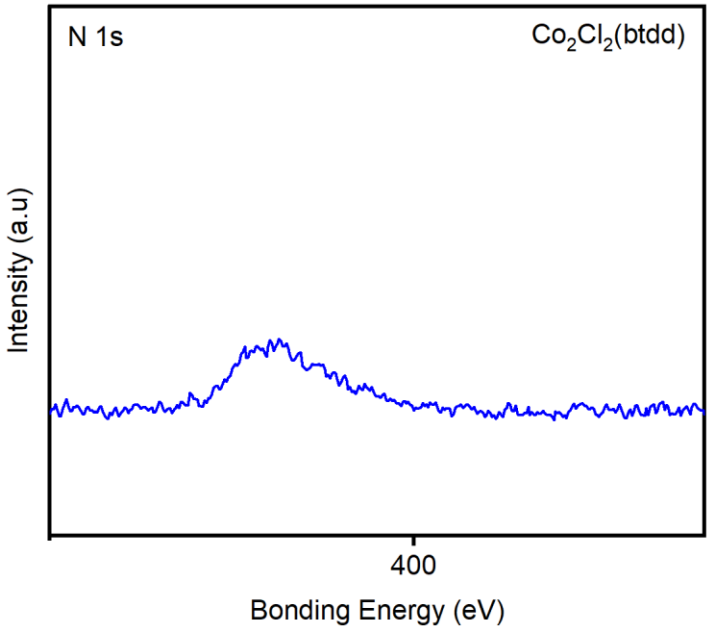

Figure S20. High resolution N 1s XPS spectrum of Co_2Cl_2(btdd) prepared under ionothermal conditions.

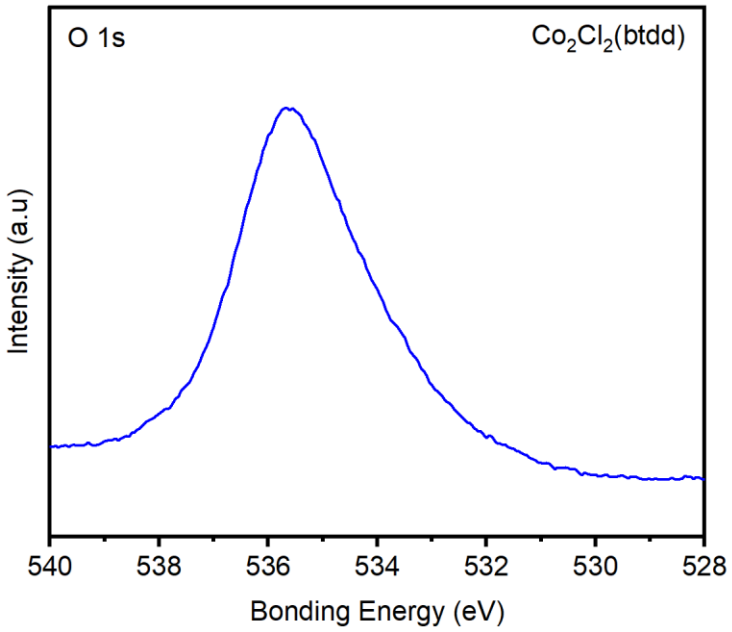

Figure S21. High resolution O 1s XPS spectrum of Co_2Cl_2(btdd) prepared under ionothermal conditions.

Table S2. Combustion elemental analysis data for Co_2Cl_2(btdd) prepared under ionothermal conditions.

Element	Theory for $C_{12}H_4Cl_2Co_2N_6O_2$ (wt %)	Found (wt %)
C	31.82	28.2
H	0.89	1.81
Cl	15.65	13.83
N	18.55	16.36

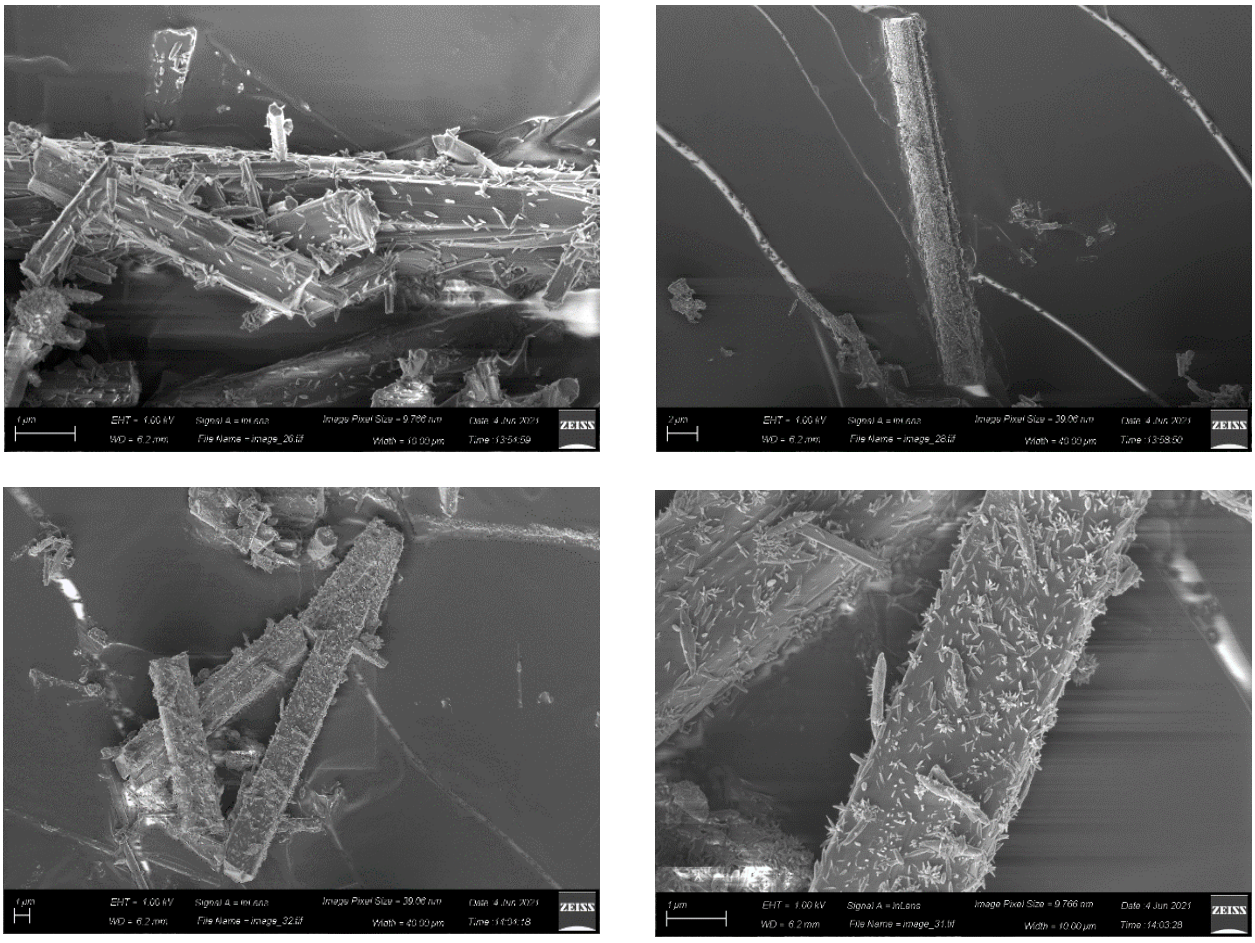

Figure S22. SEM images of Co_2Cl_2(btdd) prepared under ionothermal conditions.

4. Synthesis and characterization of Ni_2Cl_2(btdd).

Solvothermal Synthesis of Ni_2Cl_2(btdd)-ST.

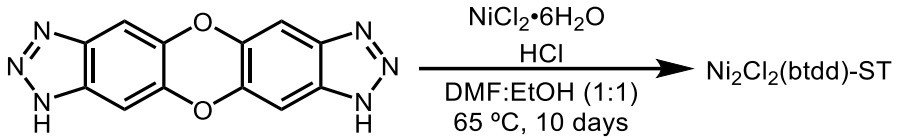

This procedure is adapted from the literature.[6] To a 500 mL round bottom flask, H_2btdd (200 mg, 0.75 mmol, 1.00 eq) and DMF (200 mL) were added. The solution was heated to 130 ºC for 1 h and then allowed to cool to room temperature. To a 1 L Pyrex jar, $NiCl_2$•$6H_2O$ (357 mg, 1.50 mmol, 2.00 eq), EtOH (200 mL), and concentrated HCl (4 mL) were added. The solution of H_2btdd in DMF was added to the 1 L jar, which was then capped and placed in an oven that had been pre-heated at 65 ºC. The jar was allowed to stand at 65 °C for 10 days. After this time, the jar was removed from the oven and allowed to cool to room temperature. The heterogeneous mixture was filtered, and the solid was returned to the Pyrex jar along with fresh DMF (200 mL). The jar was placed in an oven that had been heated to 120 °C. After 24 h, the DMF was decanted and replaced with fresh DMF (200 mL). This soaking procedure was repeated for a total of three hot DMF soaks. Next, the soaking procedure was repeated with methanol (200 mL) at 65 °C, replacing the solvent every 24 h. This soaking procedure was repeated for a total of three hot methanol soaks. The heterogeneous mixture was filtered. The solid was then activated under dynamic vacuum (<100 mTorr) at 150 °C for 24 h, yielding activated Ni_2Cl_2(btdd) as a light green powder.

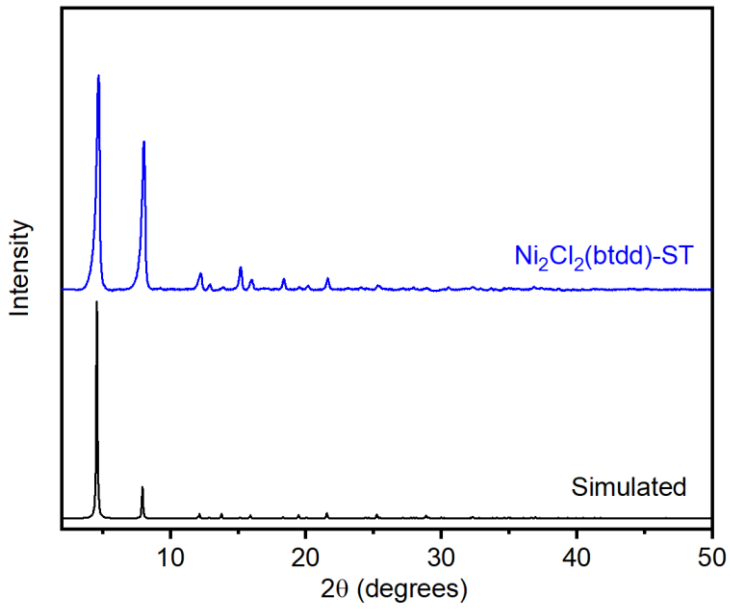

Figure S23. PXRD pattern (λ = 1.5406 Å) of Ni_2Cl_2(btdd) prepared under solvothermal conditions. The simulated pattern corresponding to the single-crystal X-ray diffraction structure of Mn_2Cl_2(btdd) is included for reference.[6] The experimental PXRD pattern was baseline corrected.

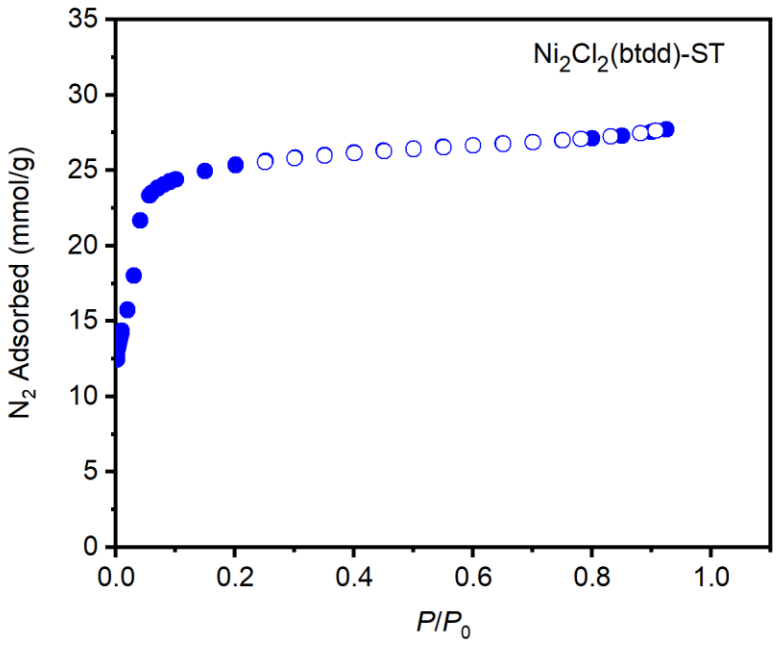

Figure S24. 77 K N_2 adsorption (closed circles) and desorption (open circles) isotherms of Ni_2Cl_2(btdd) prepared under solvothermal conditions. Fitting these data yielded a Brunauer–Emmett–Teller (BET) surface area of 1973 ± 19 m^2/g (Lit: 1763 m^2/g).[6]

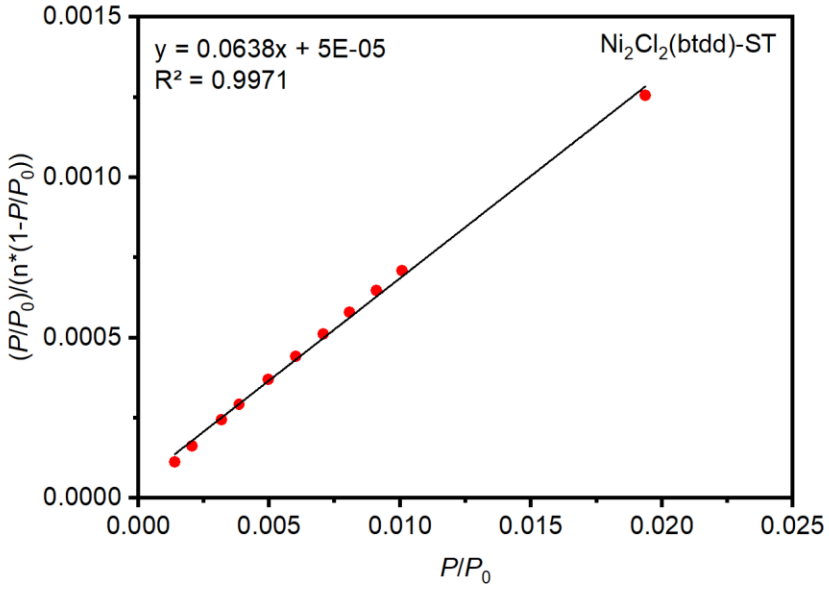

Figure S25. Linearized Brunauer–Emmett–Teller (BET) plot for the adsorption data of Ni_2Cl_2(btdd) prepared under solvothermal conditions.

Ionothermal Synthesis of Ni_2Cl_2(btdd)-IT.

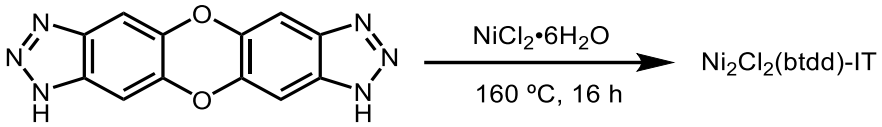

Following General Procedure A, H_2btdd (1.00 g, 3.75 mmol, 1.00 equiv.) and $NiCl_2$•$6H_2O$ (1.80 g, 7.50 mmol, 2.00 equiv.) were combined at 160 °C to yield Ni_2Cl_2(btdd) (1.08 g, 65% yield) as a light green solid after activation under dynamic vacuum (<100 mTorr) at 150 °C for 24 h.

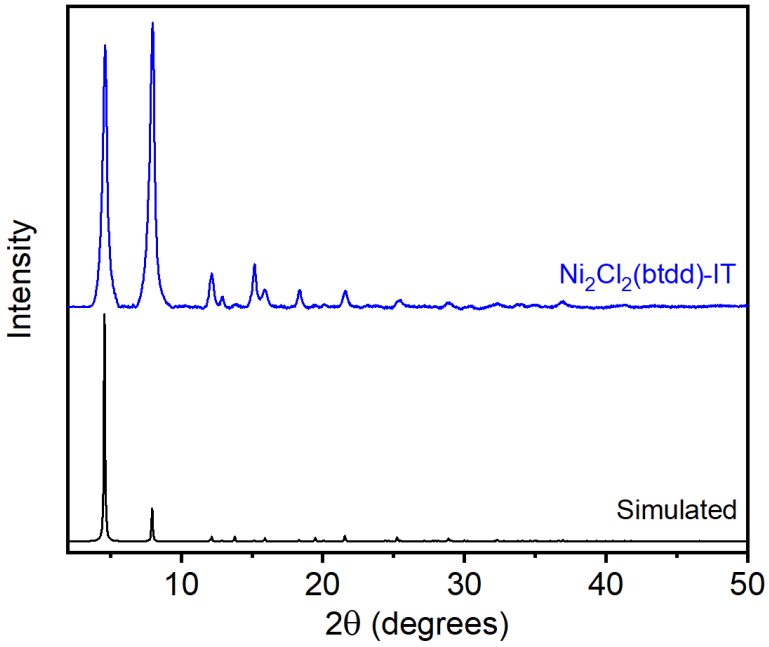

Figure S26. PXRD pattern (λ = 1.5406 Å) of Ni_2Cl_2(btdd) prepared under ionothermal conditions. The simulated pattern corresponding to the single-crystal X-ray diffraction structure of Mn_2Cl_2(btdd) is included for reference. [6] The experimental PXRD pattern was baseline corrected.

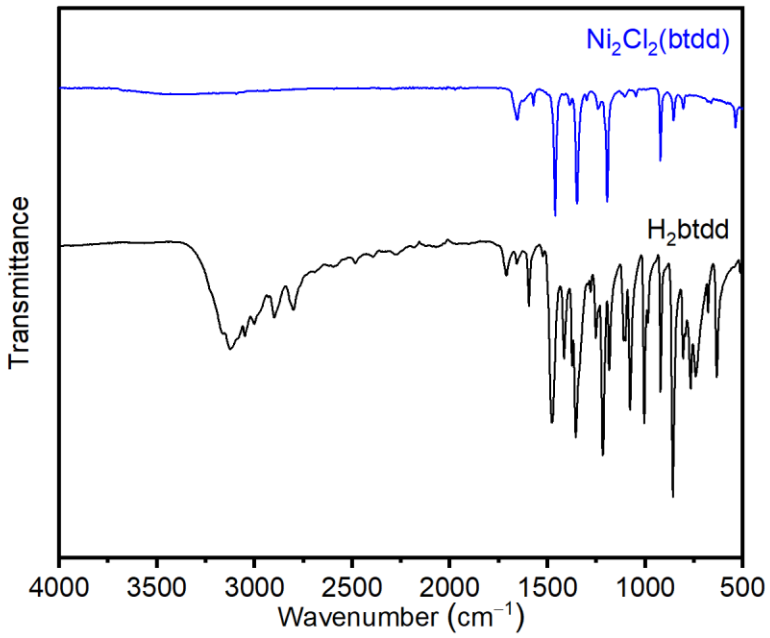

Figure S27. ATR IR spectrum of Ni_2Cl_2(btdd) prepared under ionothermal conditions.

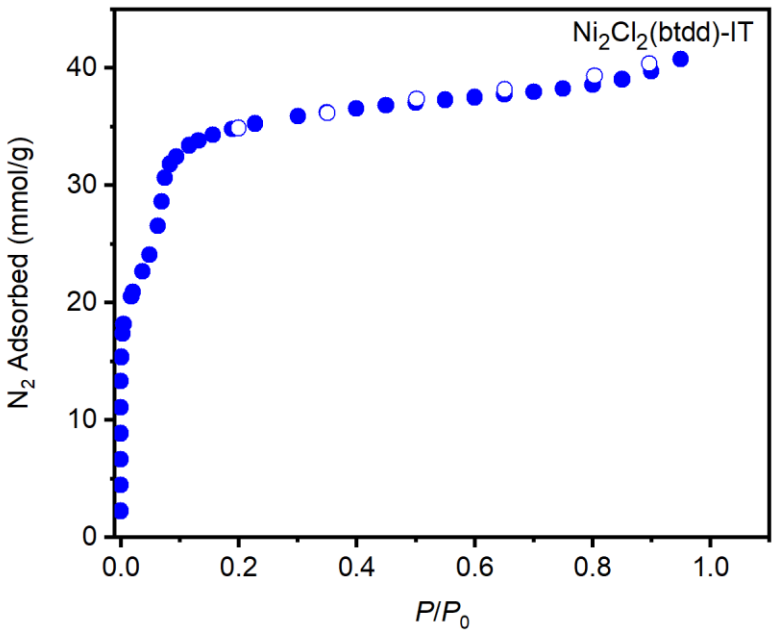

Figure S28. 77 K N_2 adsorption (closed circles) and desorption (open circles) isotherms of Ni_2Cl_2(btdd) prepared under ionothermal conditions. Fitting these data yielded a Brunauer–Emmett–Teller (BET) surface area of 2438 ± 82 m^2/g (Lit: 1763 m^2/g).[6]

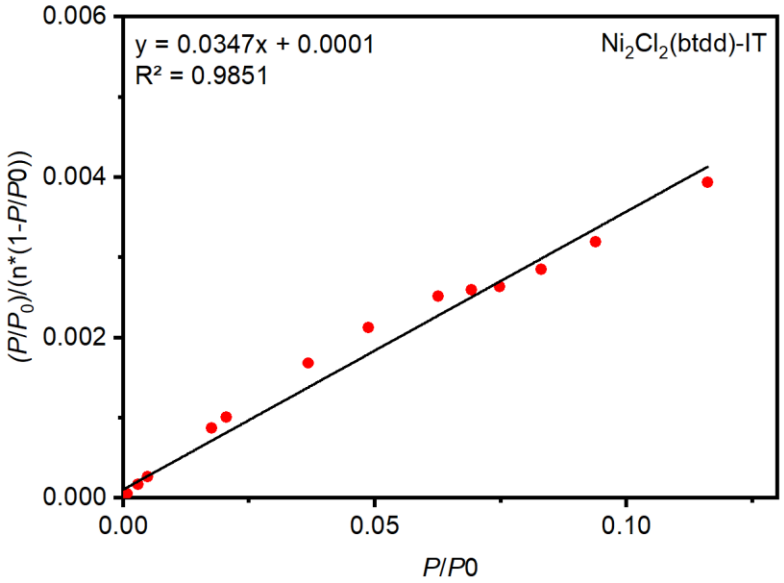

Figure S29. Linearized Brunauer–Emmett–Teller (BET) plot for the adsorption data of Ni_2Cl_2(btdd) prepared under ionothermal conditions.

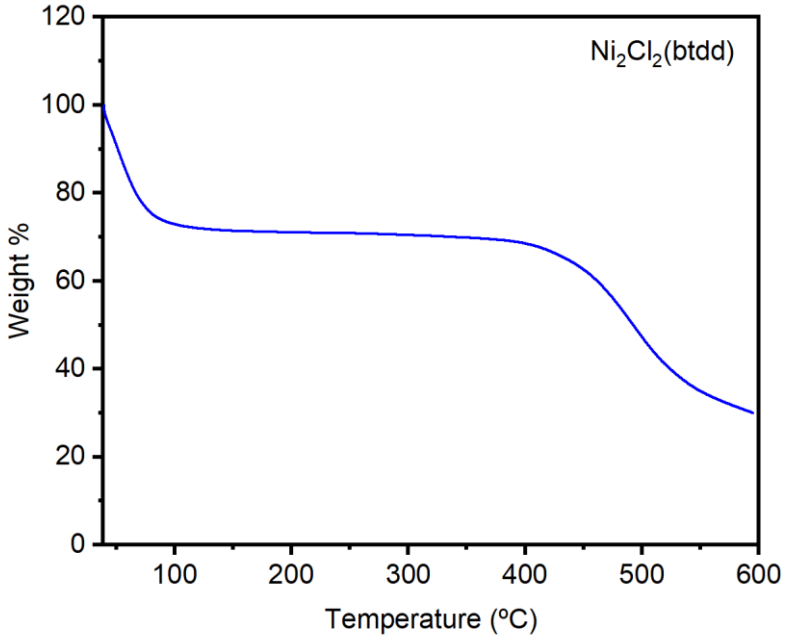

Figure S30. TGA decomposition profile of Ni_2Cl_2(btdd) prepared under ionothermal conditions.

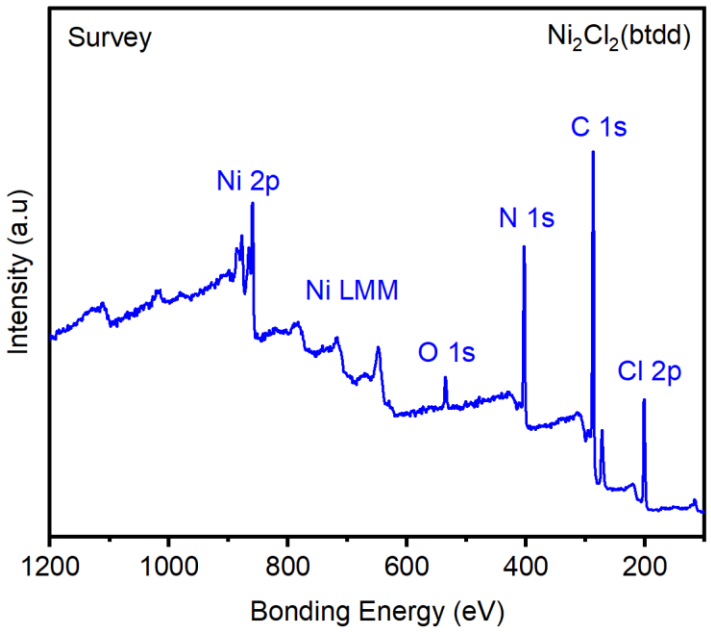

Figure S31. XPS spectral scan of an activated sample of Ni_2Cl_2(btdd) prepared under ionothermal conditions.

Table S3. Tabulated survey XPS data for Ni_2Cl_2(btdd) prepared under ionothermal conditions.

Element	Peak Label	Position	Area	Atomic %
O	O 1s	532.8	104.5	2.28
C	C 1s	284.4	988.61	63.22
N	N 1s	400.8	585.95	20.82
Ni	Ni 2p	856.8	1130.43	3.26
Cl	Cl 2p	197.8	372.58	10.42
Total:				100

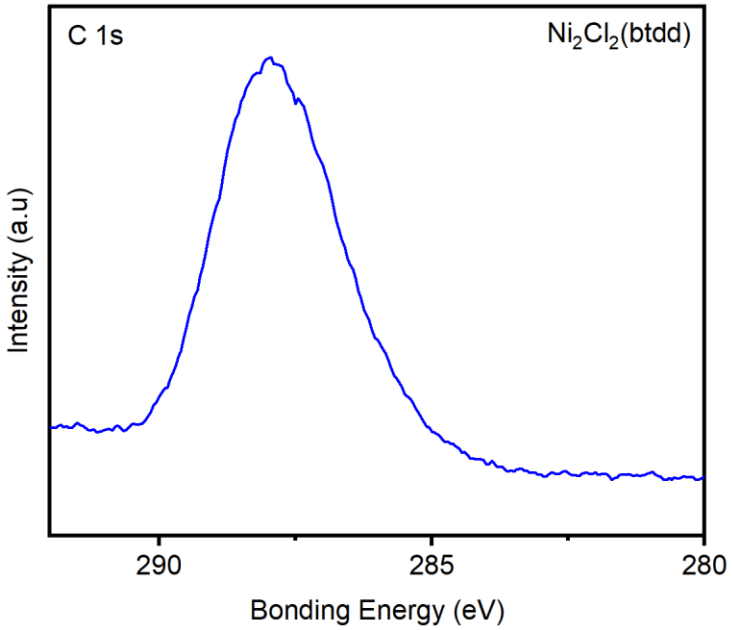

Figure S32. High resolution C 1s XPS spectrum of Ni_2Cl_2(btdd) prepared under ionothermal conditions.

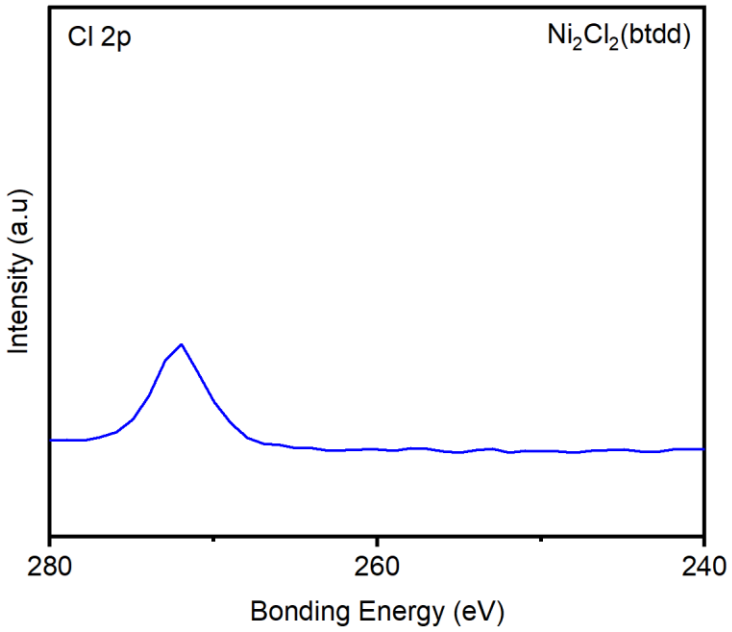

Figure S33. High resolution Cl 2p XPS spectrum of Ni_2Cl_2(btdd) prepared under ionothermal conditions.

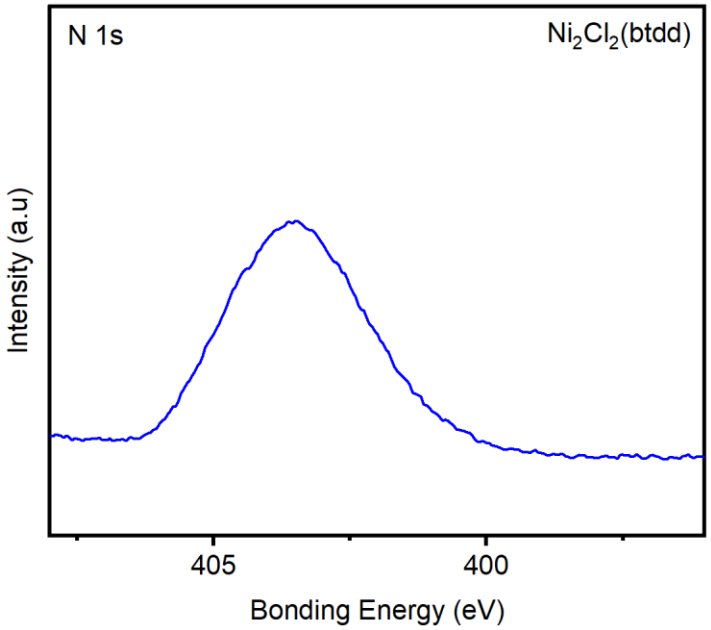

Figure S34. High resolution N 1s XPS spectrum of Ni_2Cl_2(btdd) prepared under ionothermal conditions.

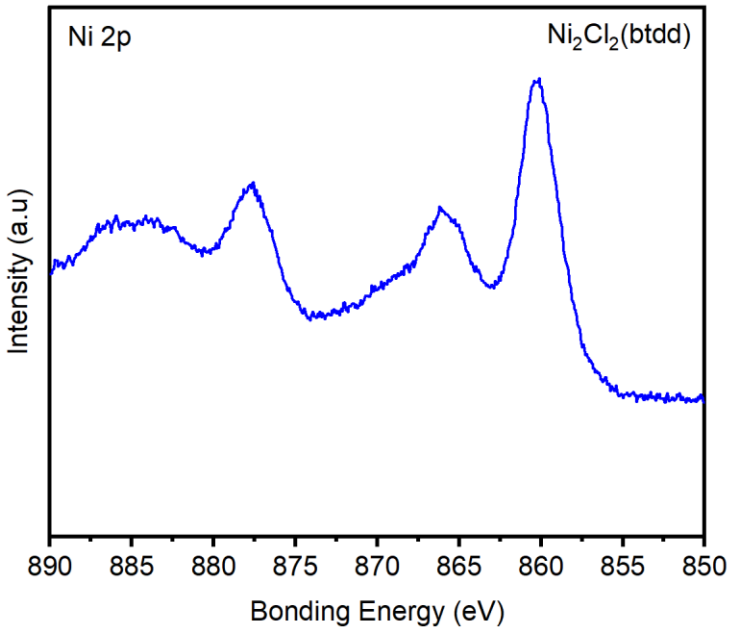

Figure S35. High resolution Ni 2p XPS spectrum of Ni_2Cl_2(btdd) prepared under ionothermal conditions.

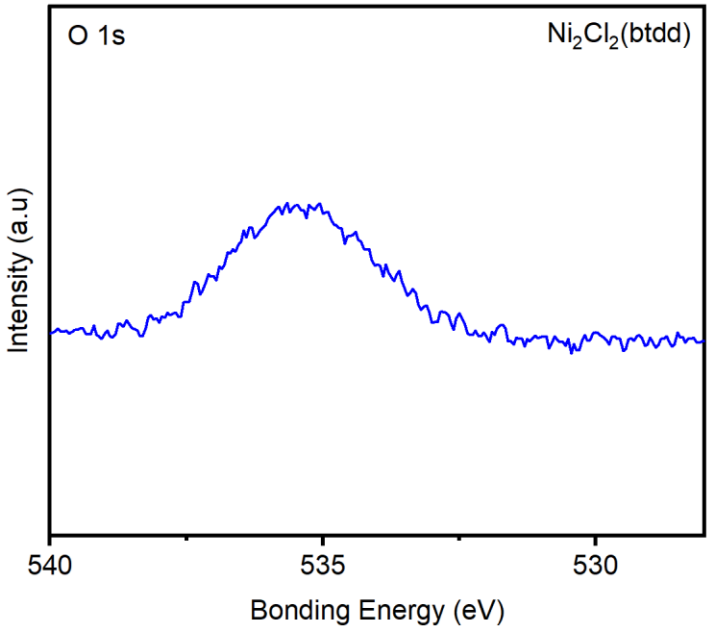

Figure S36. High resolution O 1s XPS spectrum of $Ni_2Cl_2(btdd)$ prepared under ionothermal conditions.

Table S4. Combustion elemental analysis data for $Ni_2Cl_2(btdd)$ prepared under ionothermal conditions.

Element	Theory for $C_{12}H_4Cl_2Ni_2N_6O_2$ (wt %)	Found (wt %)
C	31.85	32.61
H	0.89	2.18
Cl	15.67	12.96
N	18.57	17.88

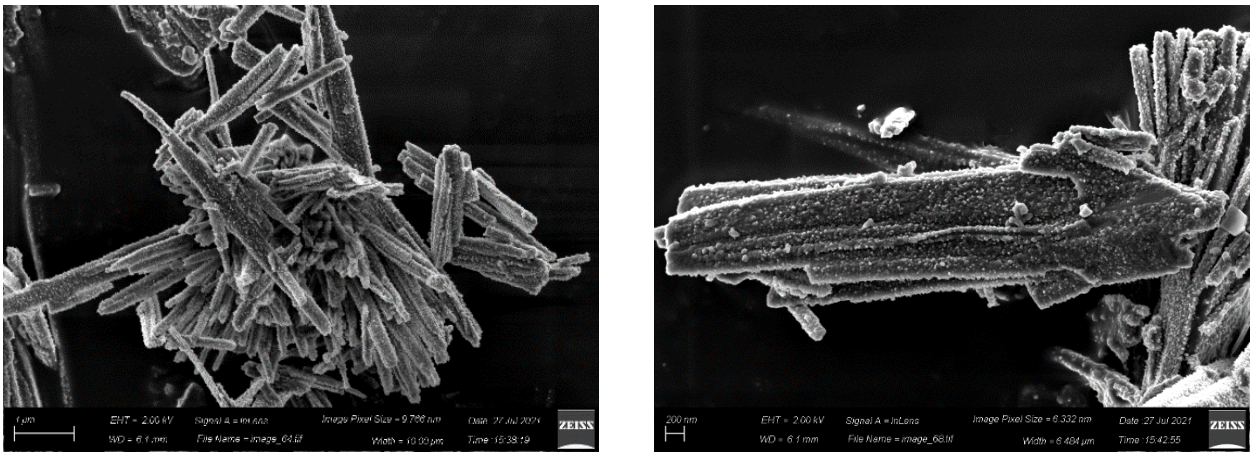

Figure S37. SEM images of Ni_2Cl_2(btdd) prepared under ionothermal conditions.

5. Synthesis and characterization of $Zn_5Cl_4(btdd)_3$.

Solvothermal Synthesis of $Zn_5Cl_4(btdd)_3$-ST.

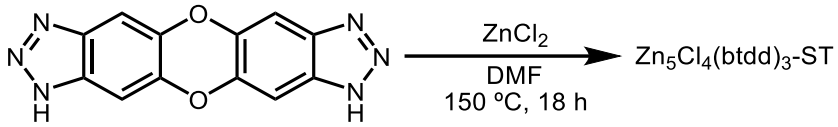

This procedure is adapted from the literature.[3] H_2btdd (760 mg, 2.77 mmol, 1.00 eq) and DMF (760 mL) were added to a 1 L round bottom flask. The mixture was vigorously stirred at 150 ºC for 30 min. At this time, anhydrous $ZnCl_2$ (7.78 g, 57.2 mmol, 20.0 eq) was added in one portion. A reflux condenser was fitted to the flask, and the mixture was stirred at 150 ºC for 18 h. At this time, the reaction mixture was allowed to cool to room temperature. The heterogeneous mixture was filtered, and the solid was returned to the Pyrex jar along with fresh DMF (50 mL). The jar was placed in an oven that had been heated to 120 °C. After 24 h, the DMF was decanted and replaced with fresh DMF (50 mL). This soaking procedure was repeated for a total of three hot DMF soaks. Next, the soaking procedure was repeated with dichloromethane (50 mL) at room temperature, replacing the solvent every 24 h. This soaking procedure was repeated for a total of three dichloromethane soaks. The heterogeneous mixture was filtered. The solid was then activated under dynamic vacuum (<100 mTorr) at 150 °C for 24 h, yielding activated $Zn_5Cl_4(btdd)_3$ as a white powder.

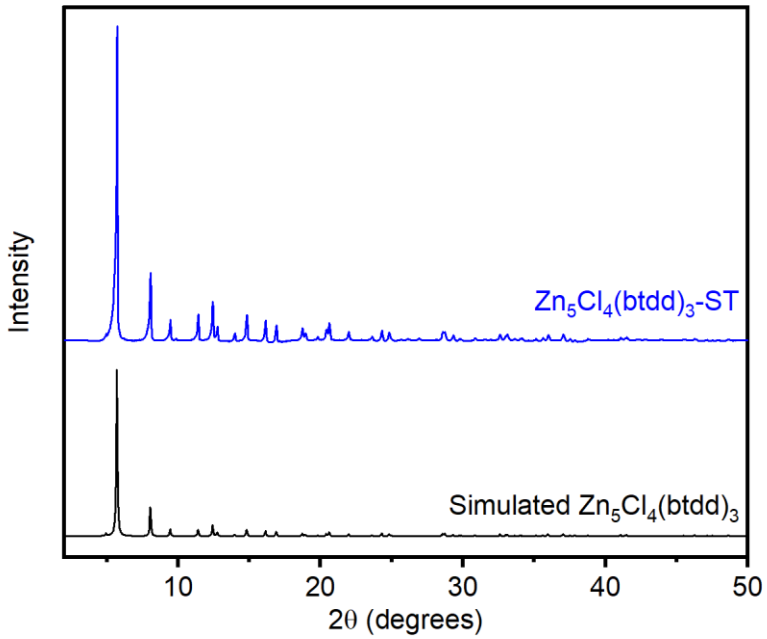

Figure S38. PXRD pattern (λ = 1.5406 Å) of $Zn_5Cl_4(btdd)_3$ prepared under solvothermal conditions. The simulated pattern corresponding to the single-crystal X-ray diffraction structure of $Zn_5Cl_4(btdd)_3$ is included for reference.[3] The experimental PXRD pattern was baseline corrected.

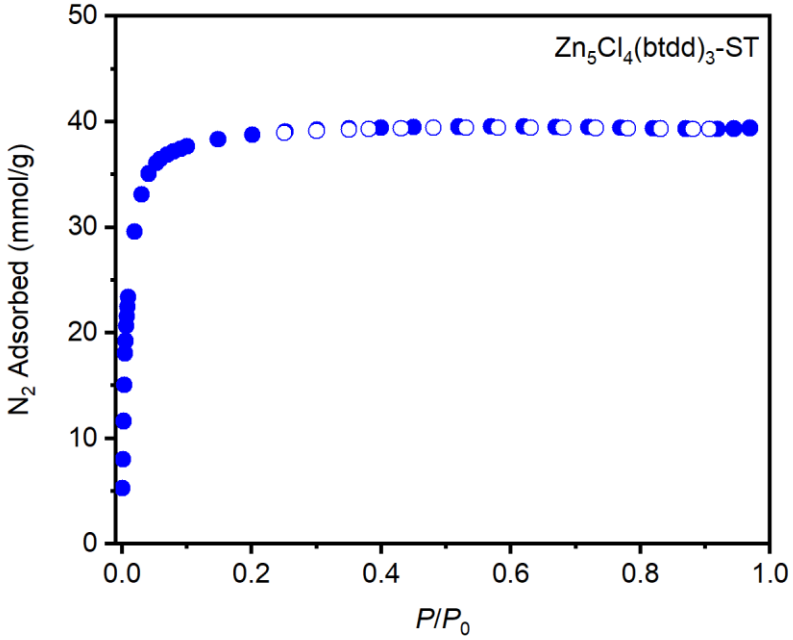

Figure S39. 77 K N_2 adsorption (closed circles) and desorption (open circles) isotherms of $Zn_5Cl_4(btdd)_3$ prepared under solvothermal conditions. Fitting these data yielded a Brunauer–Emmett–Teller (BET) surface area of 2750 ± 4 m^2/g (Lit: 2750 m^2/g).[3]

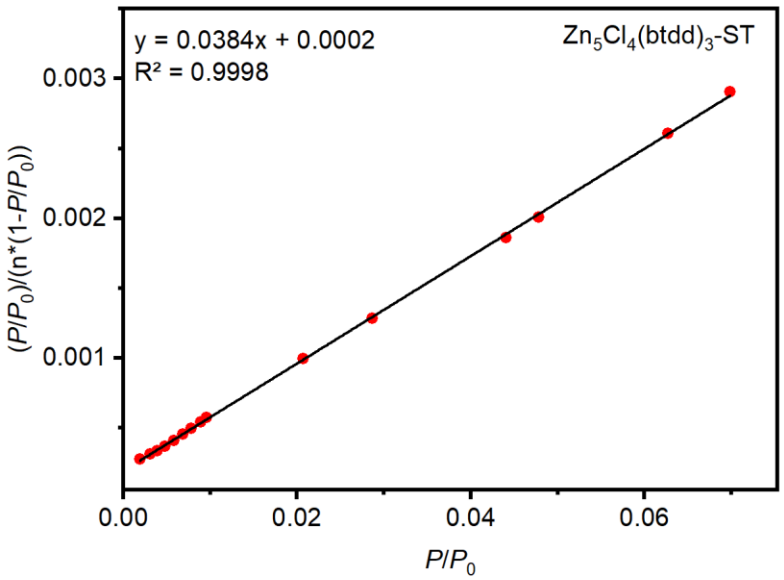

Figure S40. Linearized Brunauer–Emmett–Teller (BET) plot for the adsorption data of $Zn_5Cl_4(btdd)_3$ prepared under solvothermal conditions.

Ionothermal Synthesis of $Zn_5Cl_4(btdd)_3$-IT.

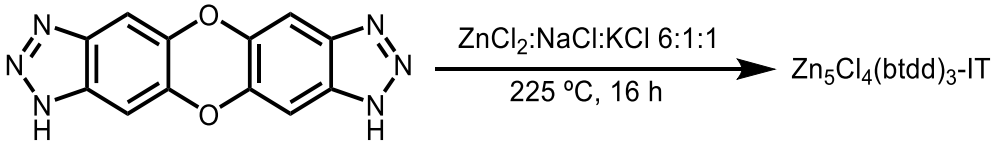

Following a modified General Procedure A, H_2btdd (1.00 g, 3.75 mmol, 1.00 equiv.), $ZnCl_2$ (10.0 g, 73.4 mmol, 19.6 equiv.), NaCl (0.70 g, 12.4 mmol, 3.30 equiv.), and KCl (0.94 g, 12.4 mmol, 3.30 equiv.) were combined in a Teflon autoclave in a N_2-filled glovebox. The vessel was removed from the box and heated in an oven at 225 °C for 16 h. After the washes outlined in General Procedure A, the solid was further washed with DI water (50 mL) to remove residual salts. After activation under dynamic vacuum (<100 mTorr) at 150 °C for 24 h, $Zn_5Cl_4(btdd)_3$ (1.88 g, 75% yield) was obtained as a gray solid. The gray color of this material is likely due to partial graphitization of the sample.

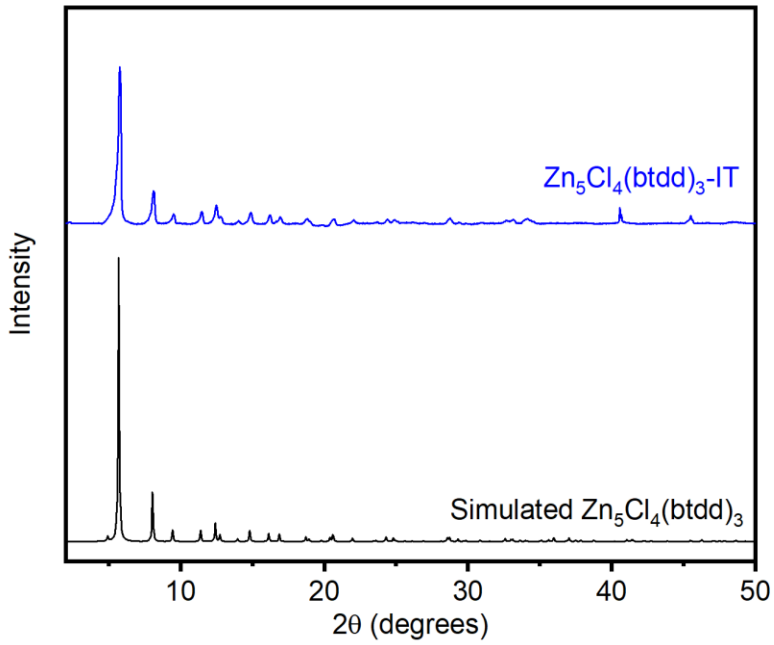

Figure S41. PXRD pattern (λ = 1.5406 Å) of $Zn_5Cl_4(btdd)_3$ prepared under ionothermal conditions. The simulated pattern corresponding to the single-crystal X-ray diffraction structure of $Zn_5Cl_4(btdd)_3$ is included for reference.[2] The experimental PXRD pattern was baseline corrected.

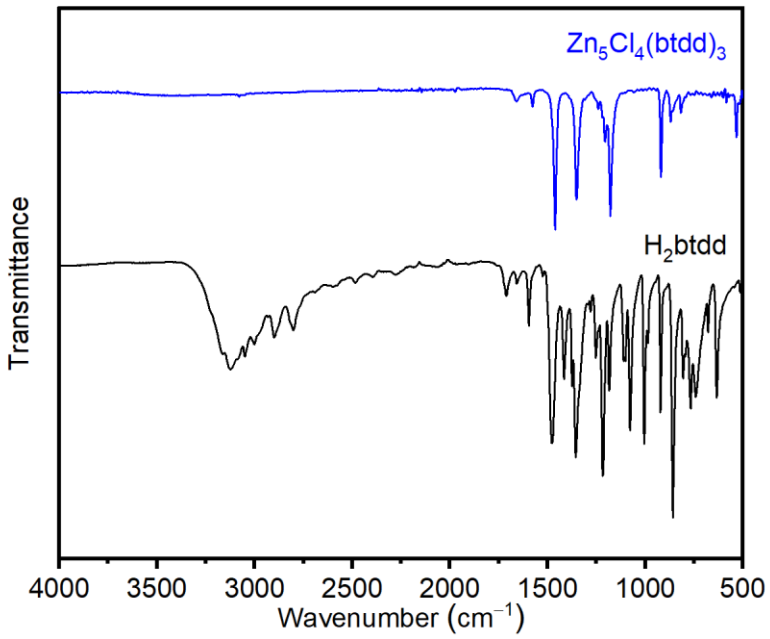

Figure S42. ATR IR spectrum of $Zn_5Cl_4(btdd)_3$ prepared under ionothermal conditions.

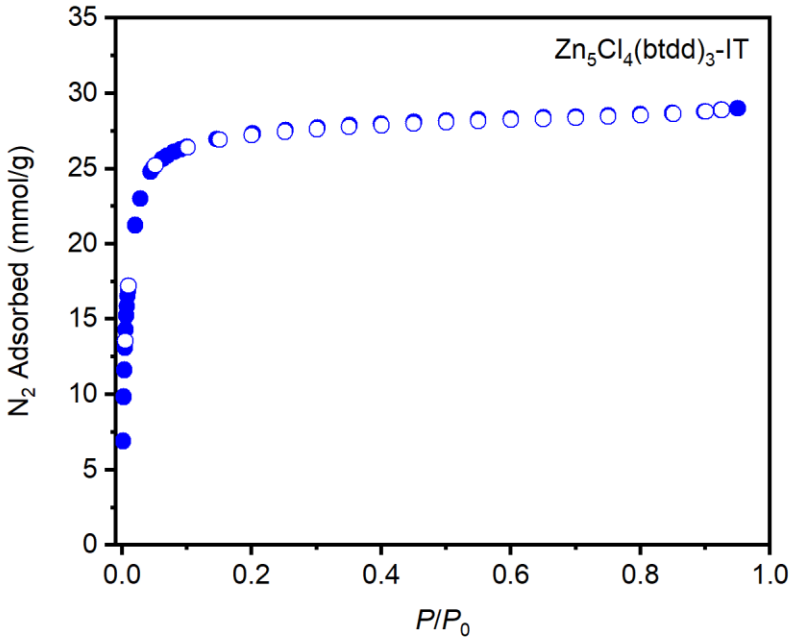

Figure S43. 77 K N_2 adsorption (closed circles) and desorption (open circles) isotherms of $Zn_5Cl_4(btdd)_3$ prepared under ionothermal conditions. Fitting these data yielded a Brunauer–Emmett–Teller (BET) surface area of 2524 ± 10 m^2/g (Lit: 2750 m^2/g).[3] The lower than expected uptake of N_2 at higher pressures (>0.2 P/P_0) is likely due to partial graphitization of the sample.

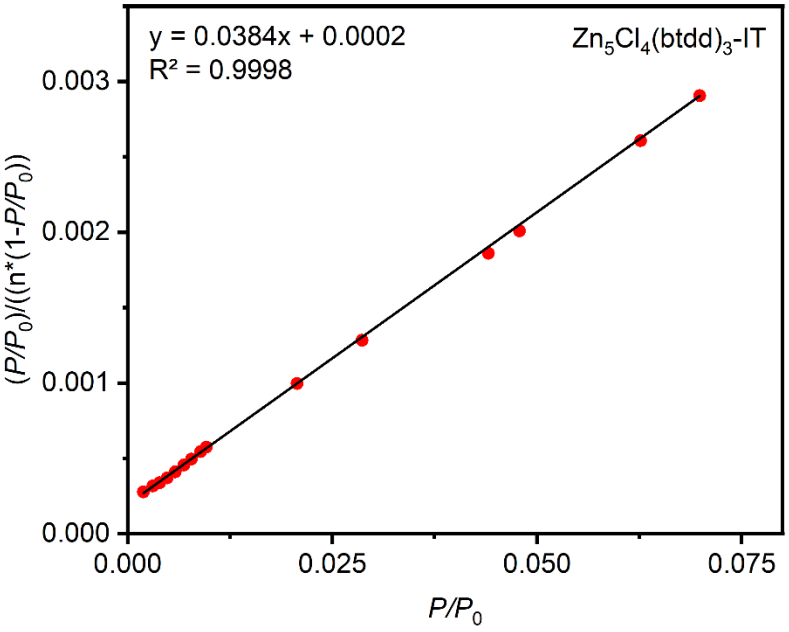

Figure S44. Linearized Brunauer–Emmett–Teller (BET) plot for the adsorption data of $Zn_5Cl_4(btdd)_3$ prepared under ionothermal conditions.

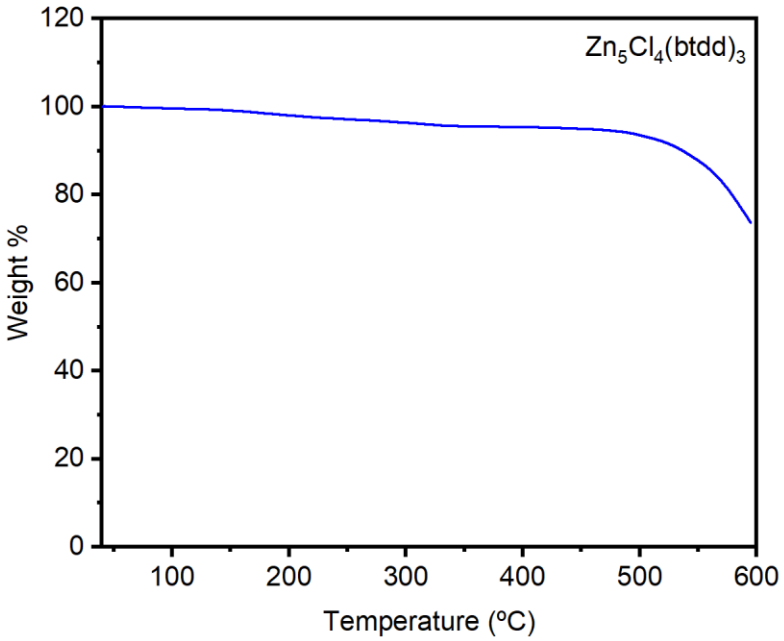

Figure S45. TGA decomposition profile of $Zn_5Cl_4(btdd)_3$ prepared under ionothermal conditions.

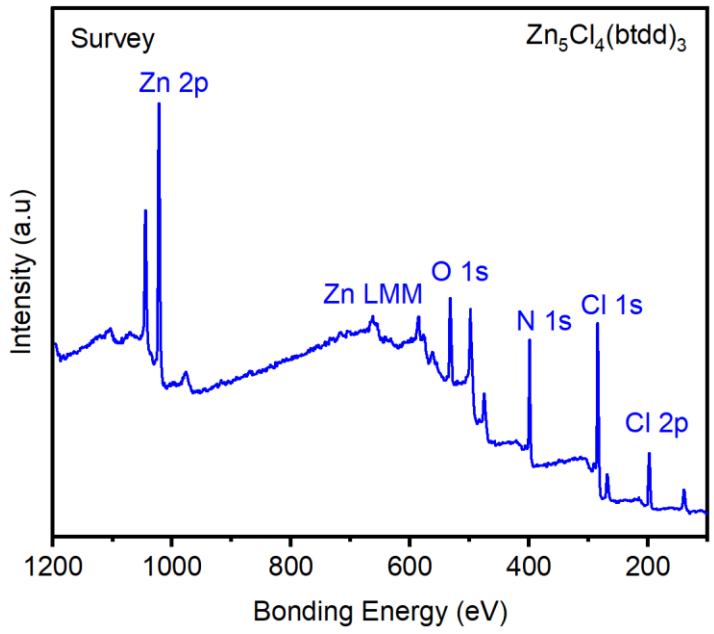

Figure S46. XPS spectral scan of an activated sample of $Zn_5Cl_4(btdd)_3$ prepared under ionothermal conditions.

Table S5. Tabulated survey XPS data for $Zn_5Cl_4(btdd)_3$ prepared under ionothermal conditions.

Element	Peak Label	Position	Area	Atomic %
Zn	Zn 2p	1021.8	1125.8	33.53
C	C 1s	284.8	1081.4	32.21
N	N 1s	399.8	457.9	13.64
O	O 1s	532.8	410.47	12.23
Cl	Cl 2p	197.8	281.9	8.4
Total:				100

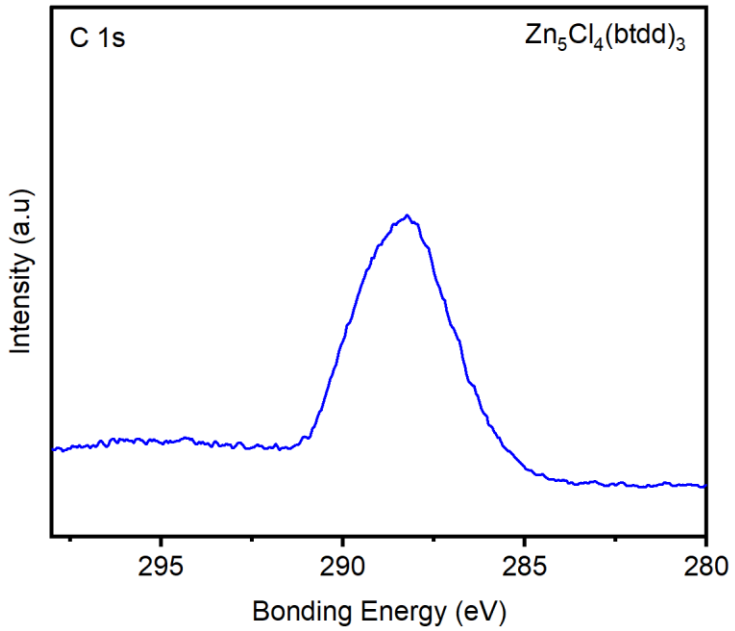

Figure S47. High resolution C 1s XPS spectrum of $Zn_5Cl_4(btdd)_3$ prepared under ionothermal conditions.

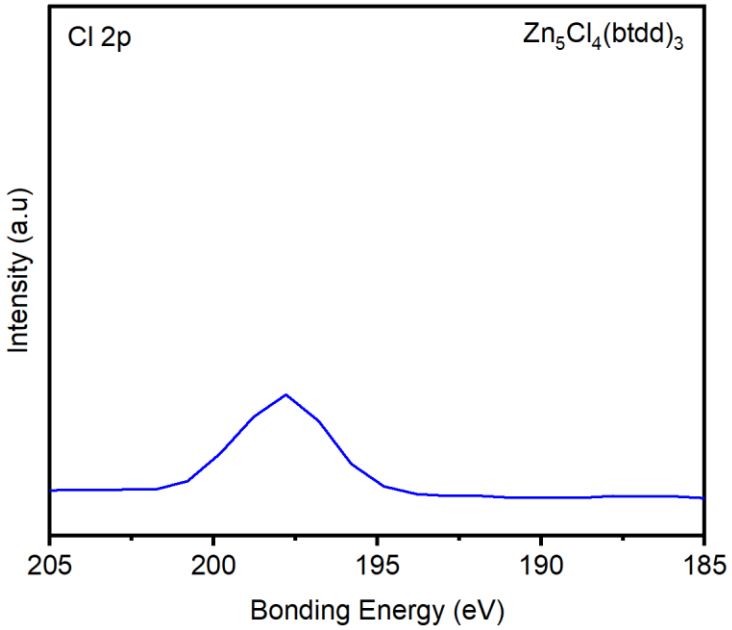

Figure S48. High resolution Cl 2p XPS spectrum of $Zn_5Cl_4(btdd)_3$ prepared under ionothermal conditions.

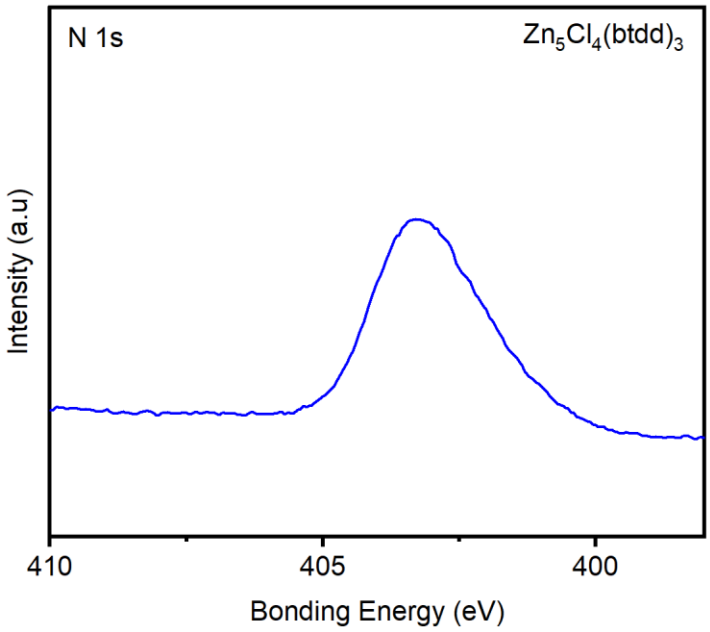

Figure S49. High resolution N 1s XPS spectrum of $Zn_5Cl_4(btdd)_3$ prepared under ionothermal conditions.

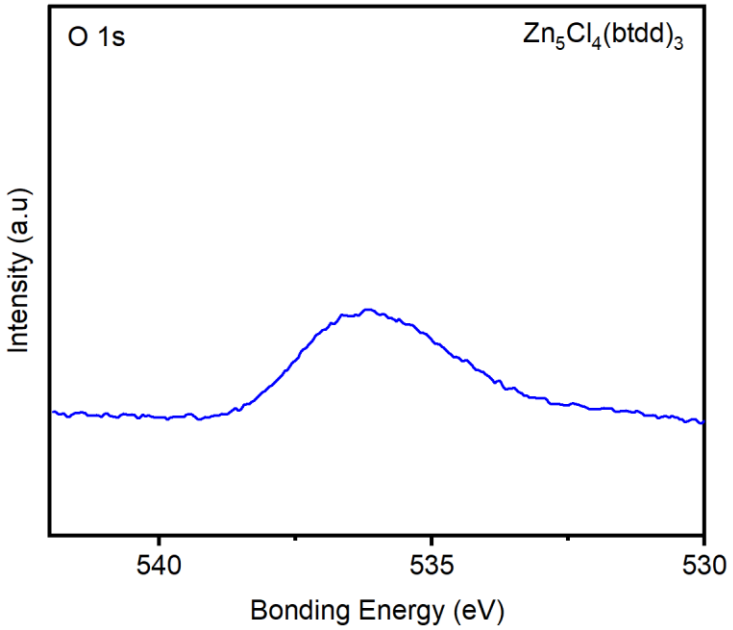

Figure S50. High resolution O 1s XPS spectrum of $Zn_5Cl_4(btdd)_3$ prepared under ionothermal conditions.

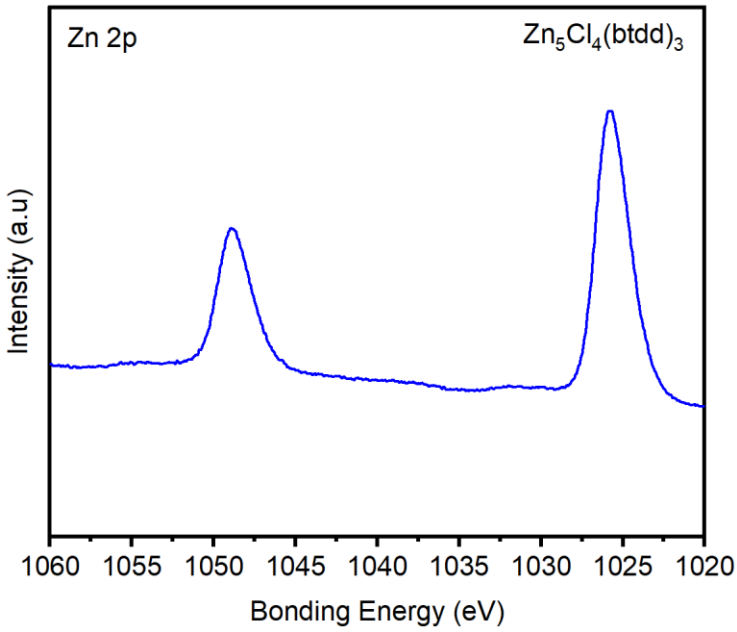

Figure S51. High resolution Zn 2p XPS spectrum of $Zn_5Cl_4(btdd)_3$ prepared under ionothermal conditions.

Table S6. Combustion elemental analysis data for $Zn_5Cl_4(btdd)_3$ prepared under ionothermal conditions.

Element	Theory for $C_{36}H_{12}Cl_4Zn_5N_{18}O_6$ (wt %)	Found (wt %)
C	34.27	34.21
H	0.96	1.19
Cl	11.24	13.83
N	19.99	19.04

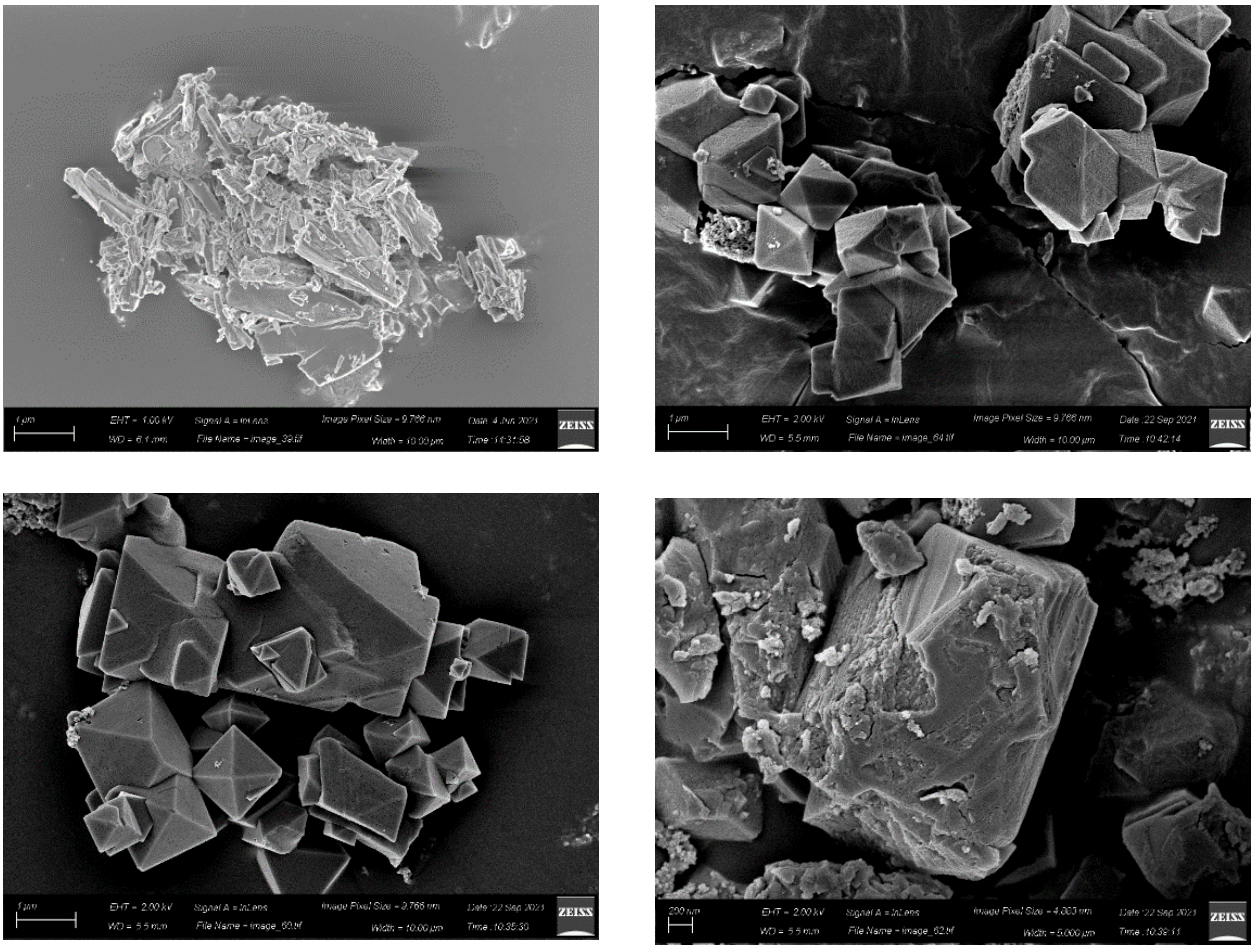

Figure S52. SEM images of $Zn_5Cl_4(btdd)_3$ prepared under ionothermal conditions.

6. Synthesis and characterization of $Ni_3(btp)_2$.

Solvothermal synthesis of $Ni_3(btp)_2$-ST.

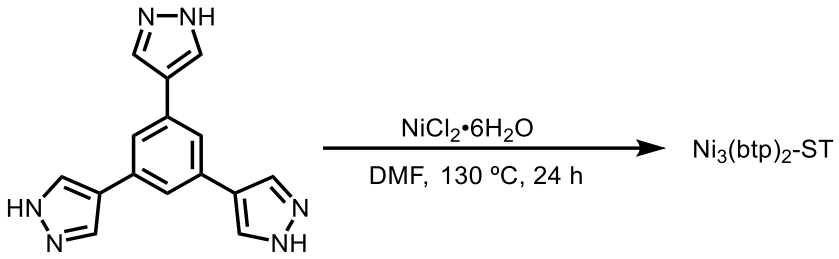

This procedure is adapted from the literature.[7] A 350 mL screwcap high-pressure reaction flask equipped with a stir bar was charged with H_3btp (500 mg, 1.81 mmol, 1.00 equiv.) and DMF (50 mL). The flask was transferred to a silicone oil bath that had been pre-heated to 60 °C, and the reaction mixture was allowed to stir vigorously (700 rpm) at this temperature for 5 min. At this time, $Ni(OAc)_2$•$4H_2O$ (676 mg, 2.72 mmol, 1.50 equiv.) was added in one portion, and the flask was rinsed with additional DMF (5 mL). The reaction vessel was sealed, and the silicone oil bath was heated to 130 °C. The reaction mixture was allowed to vigorously stir (700 rpm) at 130 °C for 24 h, after which the reaction mixture was allowed to cool to room temperature and filtered. The resulting green solid was transferred to a 500 mL Pyrex jar with *N*,*N*-dimethylformamide (250 mL). The jar was placed in an oven that had been heated to 120 °C. After 24 h, the DMF was decanted and replaced with fresh DMF (250 mL). This soaking procedure was repeated for a total of three hot DMF soaks. Next, the soaking procedure was repeated with methanol (100 mL) at 65 °C, replacing the solvent every 24 h. This soaking procedure was repeated for a total of three hot methanol soaks. During the soaking procedure, the solid changed from green to yellow in color. The heterogeneous mixture was filtered. The solid was then activated under dynamic vacuum (<100 mTorr) at 150 °C for 24 h, yielding activated $Ni_3(btp)_2$ as a yellow powder.

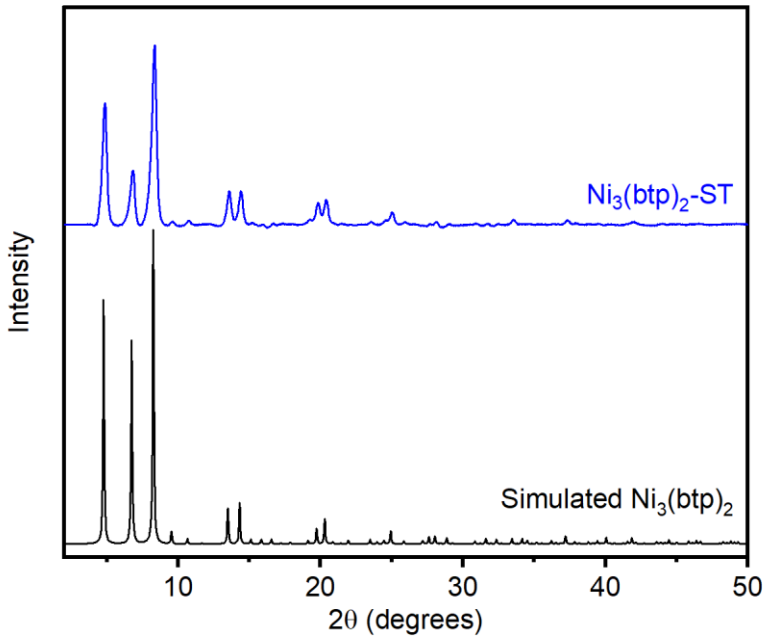

Figure S53. PXRD pattern (λ = 1.5406 Å) of $Ni_3(btp)_2$ prepared under solvothermal conditions. The simulated pattern corresponding to the powder X-ray diffraction structure of $Ni_3(btp)_2$ is included for reference.[7] The experimental PXRD pattern was baseline corrected.

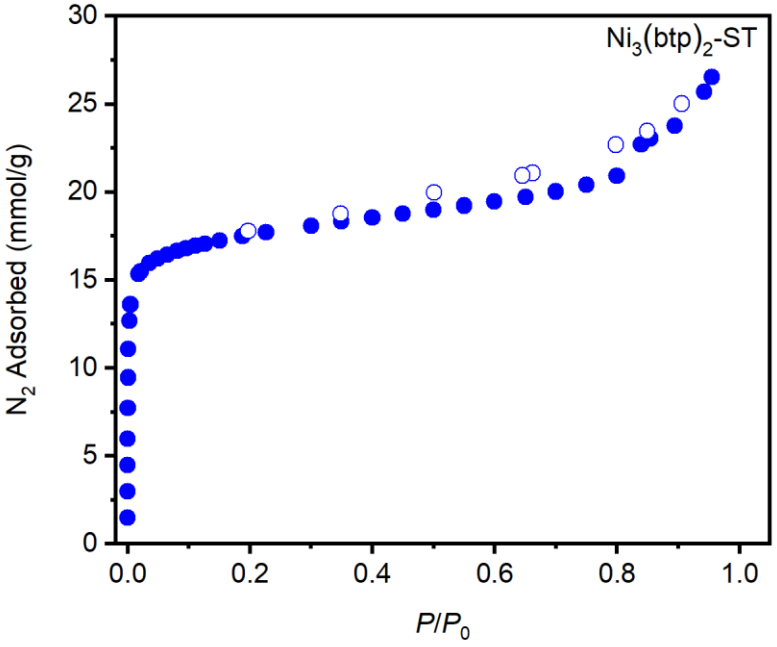

Figure S54. 77 K N_2 adsorption (closed circles) and desorption (open circles) isotherms of $Ni_3(btp)_2$ prepared under solvothermal conditions. Fitting these data yielded a Brunauer–Emmett–Teller (BET) surface area of 2100 ± 11 m^2/g (Lit: 1650 m^2/g).[7]

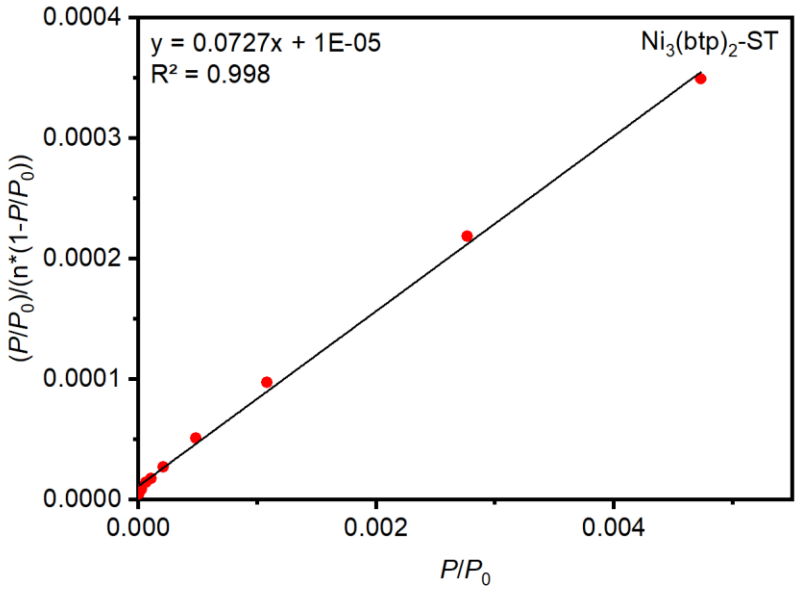

Figure S55. Linearized Brunauer–Emmett–Teller (BET) plot for the adsorption data of $Ni_3(btp)_2$.

Ionothermal synthesis of $Ni_3(btp)_2$-IT.

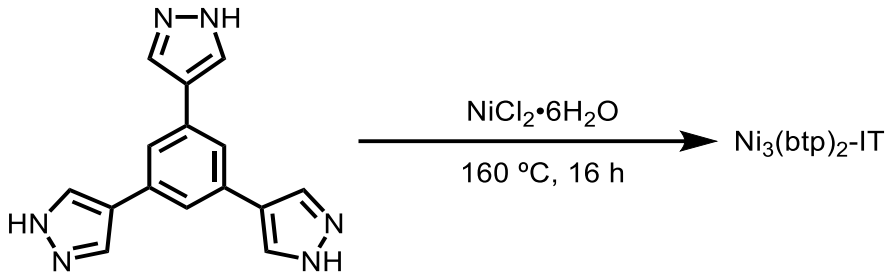

Following General Procedure A, H_3btp (1.00 g, 3.61 mmol, 1.00 equiv.) and $NiCl_2•6H_2O$ (1.52 g, 5.43 mmol, 1.50 equiv.) were combined at 160 °C to yield $Ni_3(btp)_2$ (0.81 g, 29% yield) as a light green solid after activation under vacuum at 150 °C for 24 h.

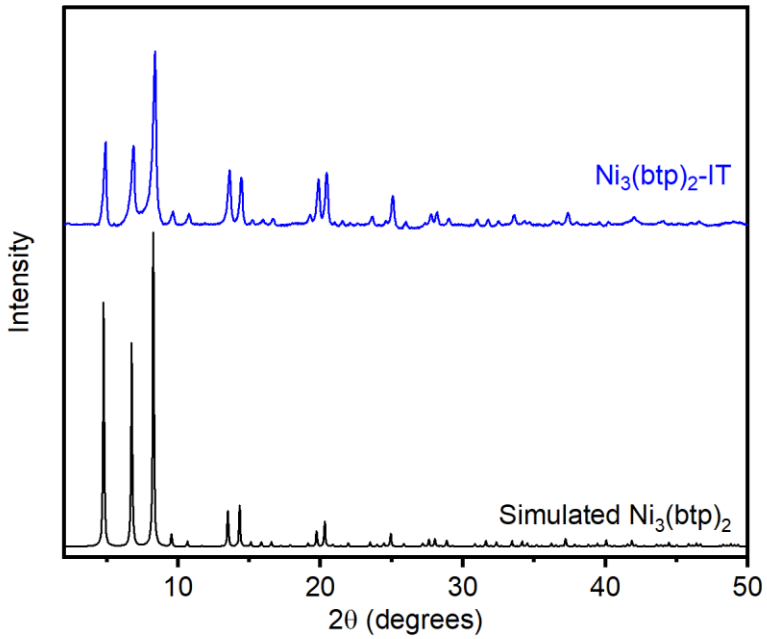

Figure S56. PXRD pattern (λ = 1.5406 Å) of $Ni_3(btp)_2$ prepared under ionothermal conditions. The simulated pattern corresponding to the single-crystal X-ray diffraction structure of $Ni_3(btp)_2$ is included for reference.[7] The experimental PXRD pattern was baseline corrected.

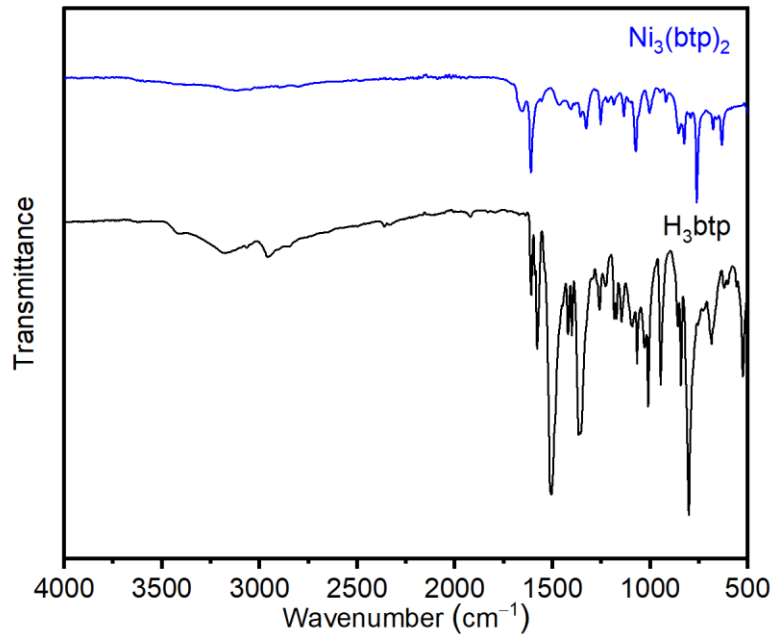

Figure S57. ATR IR spectrum of $Ni_3(btp)_2$ prepared under ionothermal conditions.

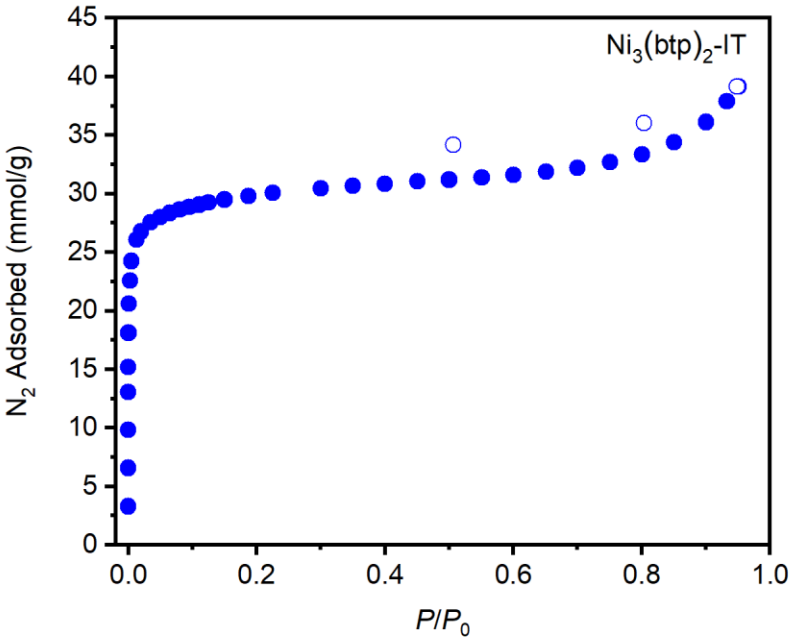

Figure S58. 77 K N_2 adsorption (closed circles) and desorption (open circles) isotherms of $Ni_3(btp)_2$ prepared under ionothermal conditions. Fitting these data yielded a Brunauer–Emmett–Teller (BET) surface area of 2603 ± 8 m^2/g (Lit: 1650 m^2/g).[7]

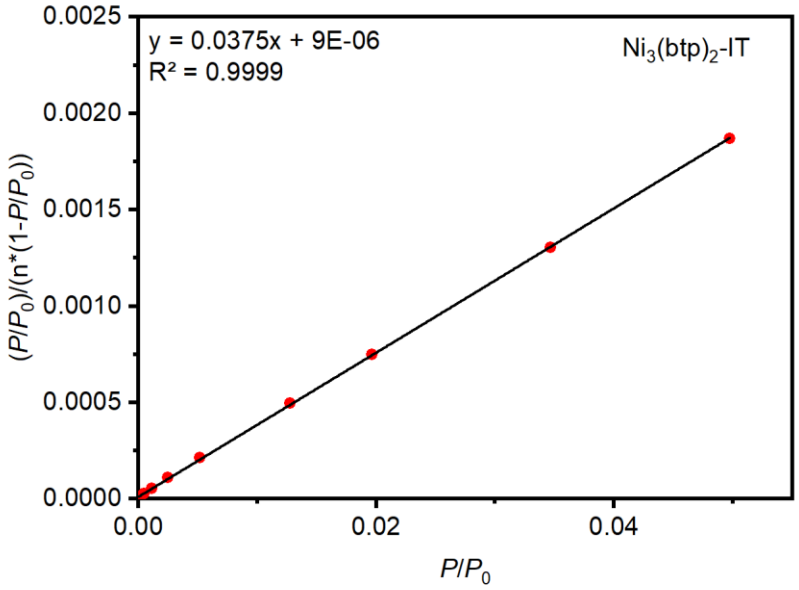

Figure S59. Linearized Brunauer–Emmett–Teller (BET) plot for the adsorption data of $Ni_3(btp)_2$ prepared under ionothermal conditions.

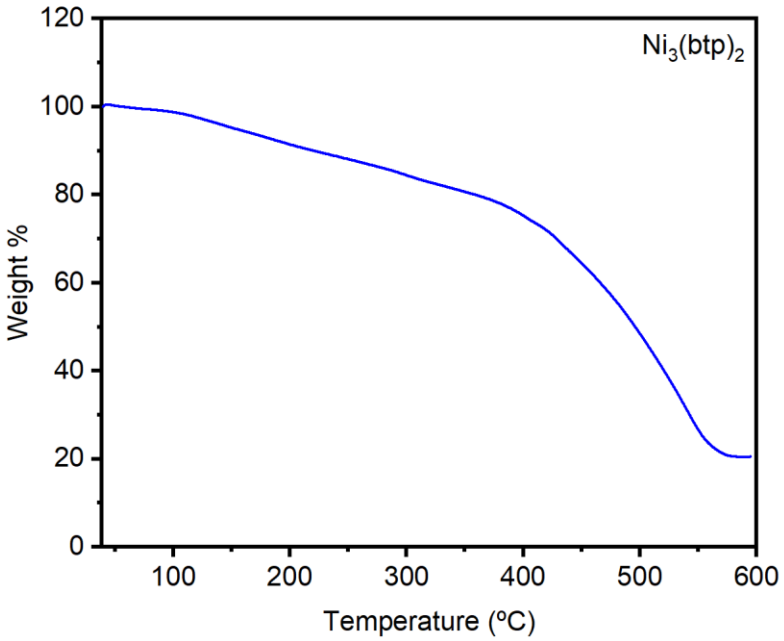

Figure S60. TGA decomposition profile of $Ni_3(btp)_2$ prepared under ionothermal conditions.

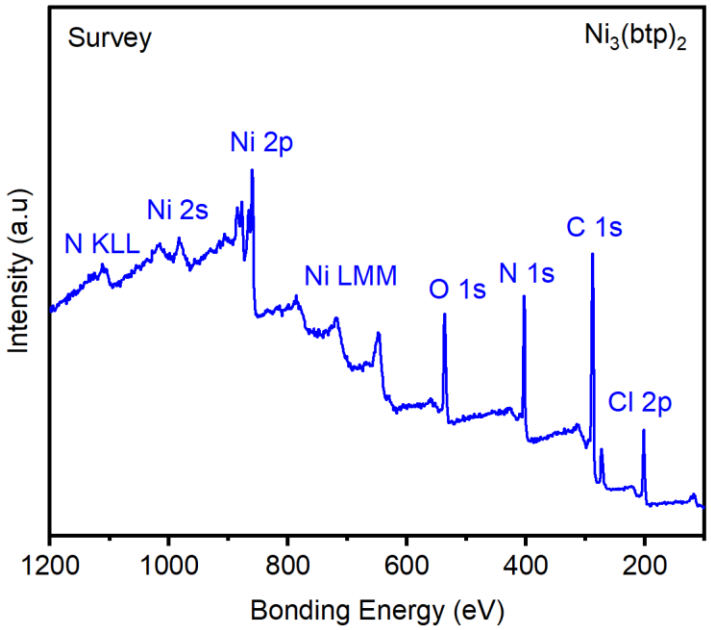

Figure S61. XPS spectral scan of an activated sample of $Ni_3(btp)_2$ prepared under ionothermal conditions. The residual Cl in this sample is likely due to defect sites left over from the $NiCl_2•6H_2O$ precursor. The detected O in this sample is likely due to physisorbed O_2/H_2O.[1]

Table S7. Tabulated survey XPS data for $Ni_3(btp)_2$ prepared under ionothermal conditions.

Element	Peak Label	Position	Area	Atomic %
O	O 1s	532.8	394.26	13.44
C	C 1s	284.8	828.42	28.23
N	N 1s	399.8	464.7	15.83
Ni	Ni 2p	856.8	1274.01	43.16
Total:				100

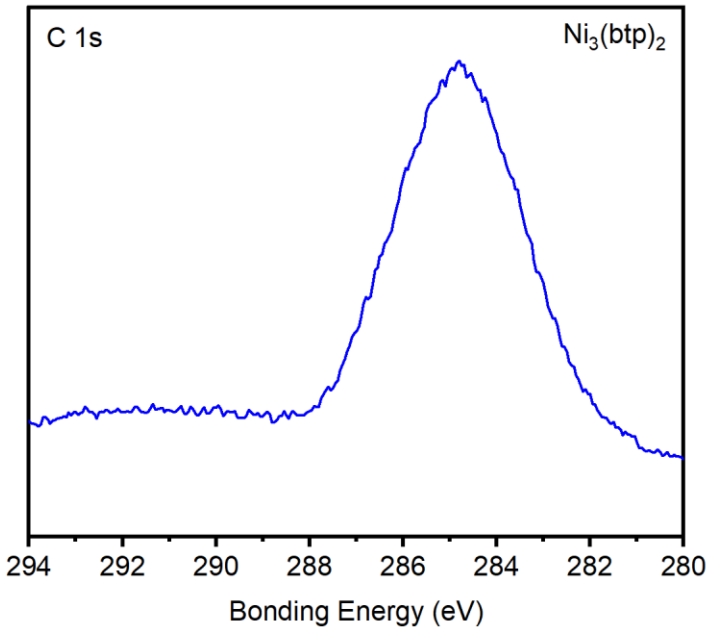

Figure S62. High resolution C 1s XPS spectrum of $Ni_3(btp)_2$ prepared under ionothermal conditions.

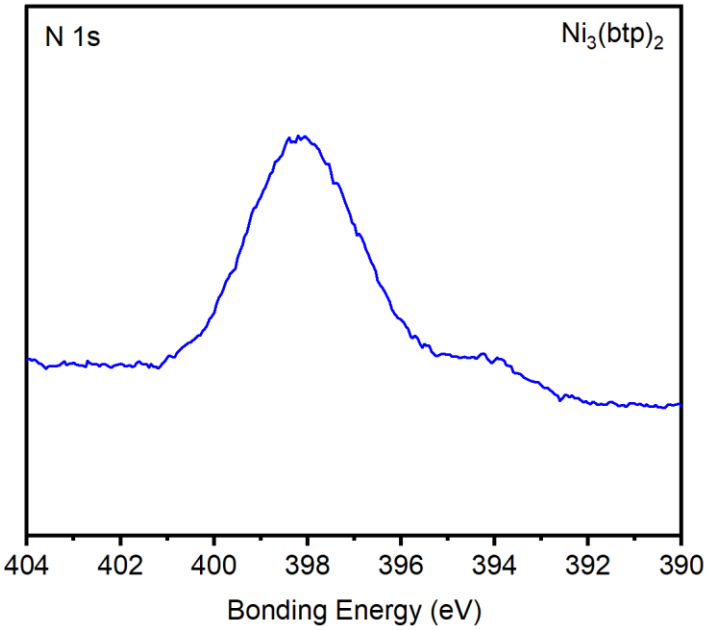

Figure S63. High resolution N 1s XPS spectrum of $Ni_3(btp)_2$ prepared under ionothermal conditions.

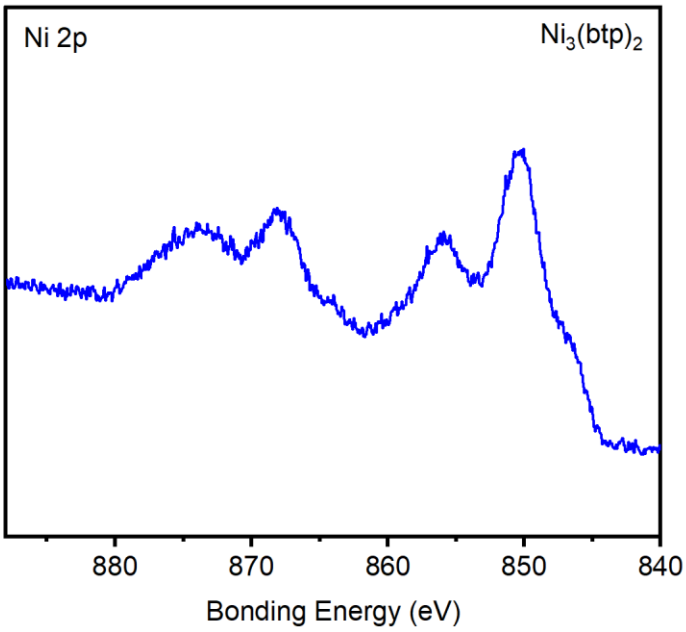

Figure S64. High resolution Ni 2p XPS spectrum of $Ni_3(btp)_2$ prepared under ionothermal conditions.

Table S8. Combustion elemental analysis data for $Ni_3(btp)_2$ prepared under ionothermal conditions.

Element	Theory for $C_{30}H_{18}N_{12}Ni_3$ (wt %)	Found (wt %)
C	49.86	44.22
H	2.51	3.38
N	23.26	20.03

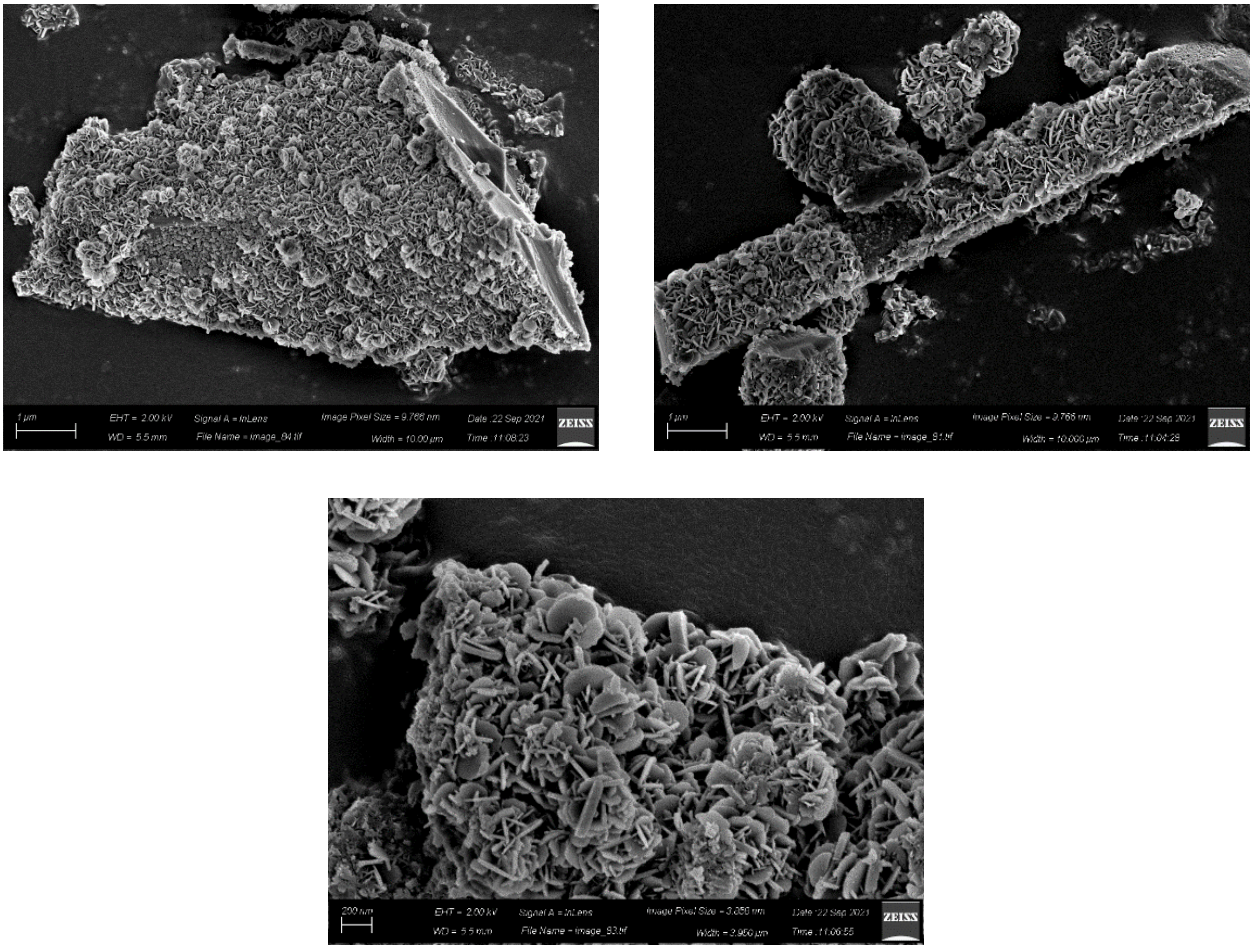

Figure S65. SEM images of $Ni_3(btp)_2$ prepared under ionothermal conditions.

7. Synthesis and characterization of Ni(bdp).

Solvothermal synthesis of Ni(bdp)-ST.

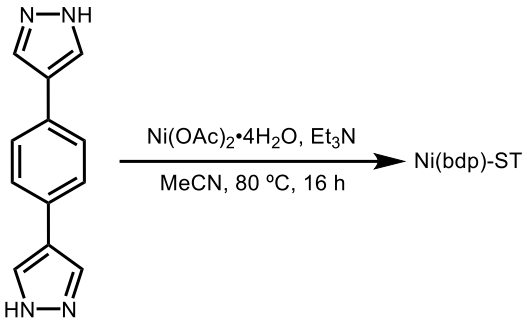

This procedure is adapted from the literature.[8] To a 25 mL round-bottom flask equipped with a reflux condenser, a solution of $Ni(OAc)_2•4H_2O$ (0.111 g, 0.47 mmol, 1.00 equiv.) in acetonitrile (10 mL), H_2bdp (0.100 g, 0.47 mmol, 1.00 equiv.) was added in one portion. The blue mixture was heated to 60 ºC. After 2 min, triethylamine (1.5 mL) was added, at which time the solution turned pink. The reaction was then allowed to stir at 80 ºC for 16 h. The heterogeneous mixture was filtered, and the dark orange solid was returned to the Pyrex jar along with fresh acetonitrile (50 mL). The jar was placed in an oven that had been heated to 65 °C. After 24 h, the acetonitrile was decanted and replaced with fresh acetonitrile (50 mL). This soaking procedure was repeated for a total of three hot acetonitrile soaks. Next, the soaking procedure was repeated with methanol (100 mL) at 65 °C, replacing the solvent every 24 h. This soaking procedure was repeated for a total of three hot methanol soaks. The heterogeneous mixture was filtered. The solid was then activated under dynamic vacuum (<100 mTorr) at 150 °C for 24 h, yielding activated Ni(bdp) as an orange powder.

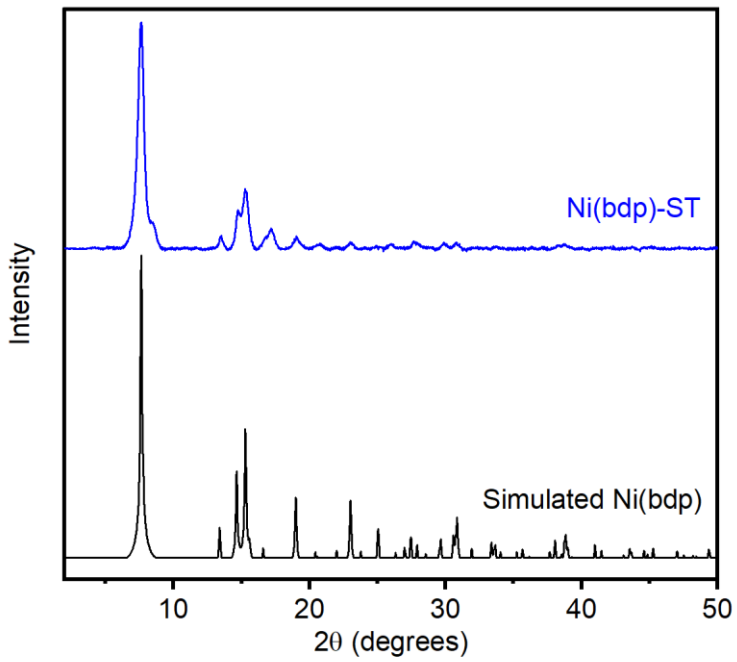

Figure 66. PXRD pattern (λ = 1.5406 Å) of Ni(bdp) prepared under solvothermal conditions. The simulated pattern corresponding to the predicted structure of Ni(bdp) is included for reference.[9] The experimental PXRD pattern was baseline corrected.

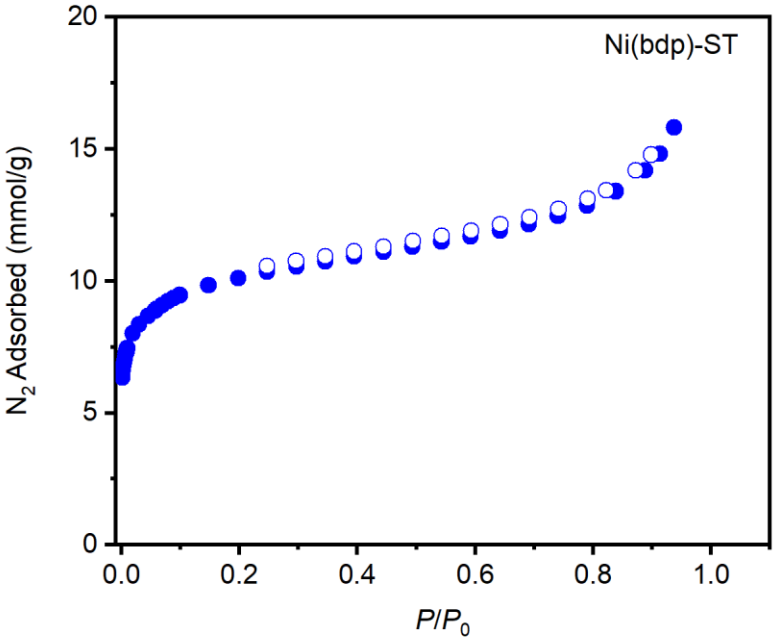

Figure S67. 77 K N_2 adsorption (closed circles) and desorption (open circles) isotherms of Ni(bdp) prepared under solvothermal conditions. Fitting these data yielded a Brunauer–Emmett–Teller (BET) surface area of 754 ± 13 m^2/g (Lit: 1066 m^2/g).[9]

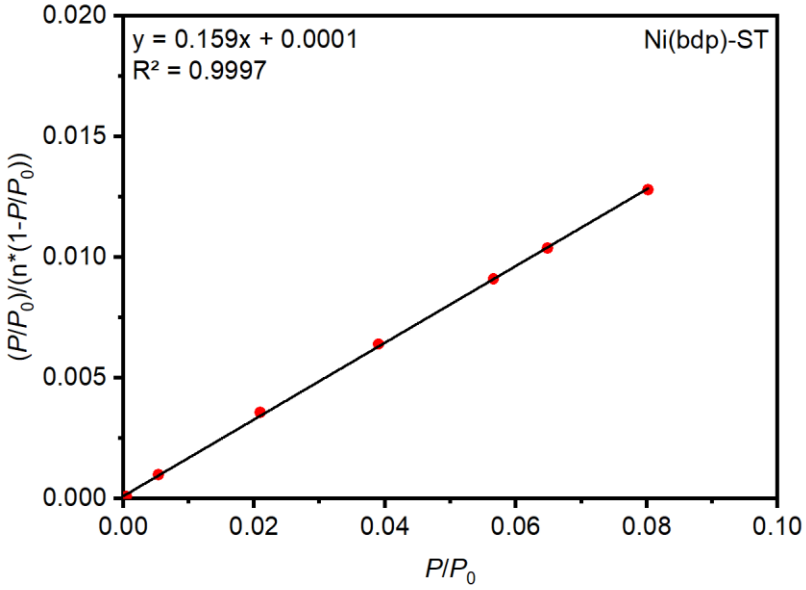

Figure S68. Linearized Brunauer–Emmett–Teller (BET) plot for the adsorption data of Ni(bdp) prepared under solvothermal conditions.

Ionothermal synthesis of Ni(bdp)-IT.

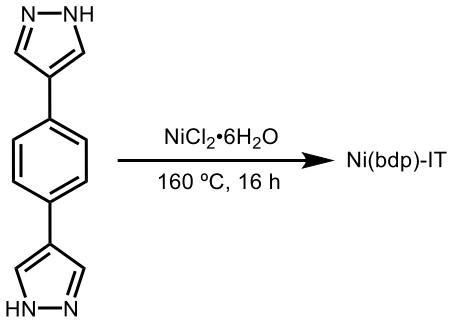

Following General Procedure A, H_2bdp (1.00 g, 4.70 mmol, 1.00 equiv.) and $NiCl_2$•$6H_2O$ (1.13 g, 4.70 mmol, 1.00 equiv.) were combined at 160 °C to yield Ni(bdp)-IT (0.460 g, 27% yield) as an orange solid after activation under vacuum at 150 °C for 24 h.

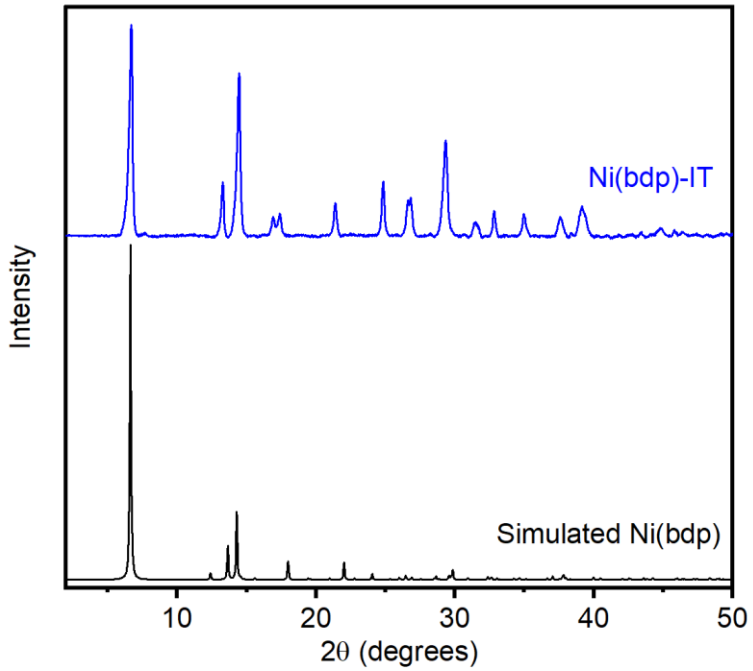

Figure S69. PXRD patterns (λ = 1.5406 Å) of Ni(bdp) prepared under ionothermal conditions. The simulated pattern corresponding to the predicted structure of Ni(bdp) is included for reference.[9] The experimental PXRD pattern was baseline corrected.

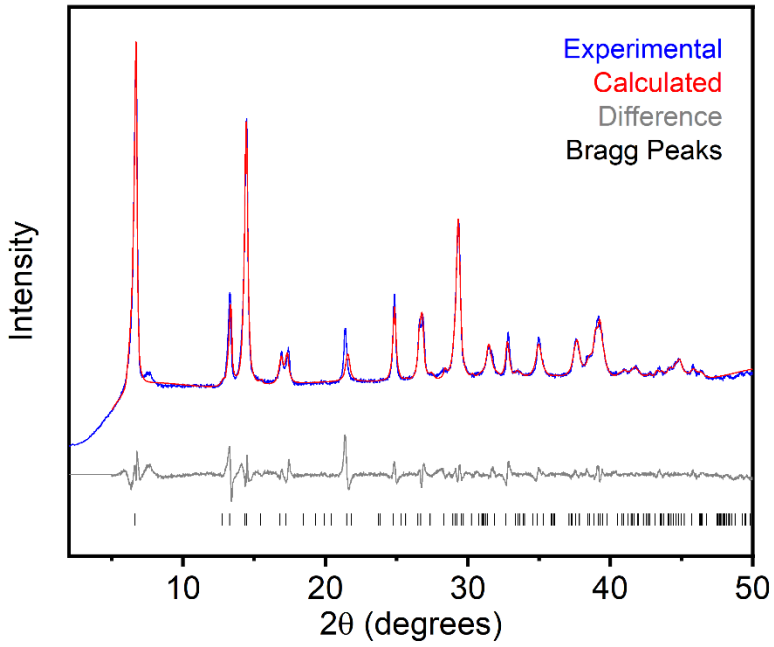

Figure S70. Pawley refinement of PXRD pattern for Ni(bdp) prepared via ionothermal methods and fit to the orthorhombic space group Ima2 (indistinguishable from Imma by this method) with unit cell parameters a = 26.71, b = 6.302, c = 13.89. Figures-of-merit (as defined by Topas): R_{exp} = 1.32, R_{wp} = 4.95, R_p = 3.17, GOF = 3.76.

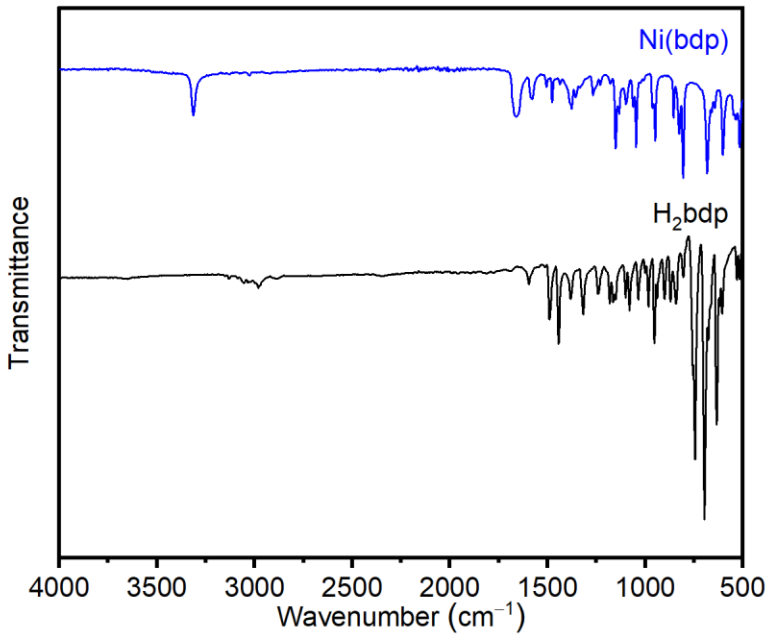

Figure S71. ATR IR spectrum of Ni(bdp) prepared under ionothermal conditions.

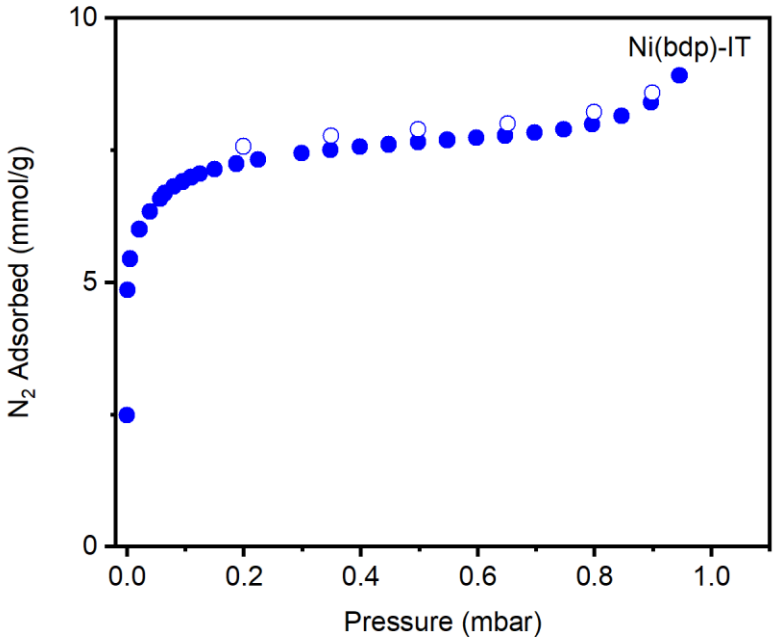

Figure S72. 77 K N_2 adsorption (closed circles) and desorption (open circles) isotherms of Ni(bdp) prepared under ionothermal conditions. Fitting these data yielded a Brunauer–Emmett–Teller (BET) surface area of 626 ± 4 m^2/g (Lit: 1066 m^2/g).[9]

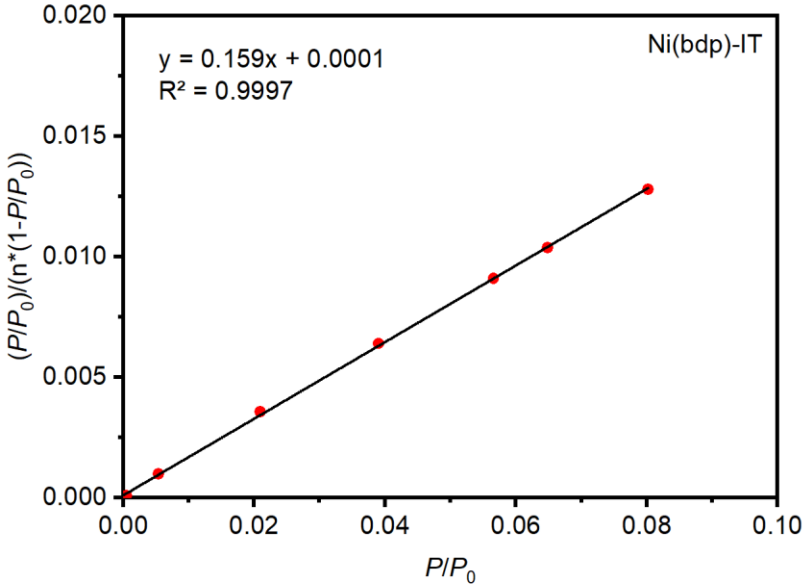

Figure S73. Linearized Brunauer–Emmett–Teller (BET) plot for the adsorption data of Ni(bdp) prepared under ionothermal conditions.

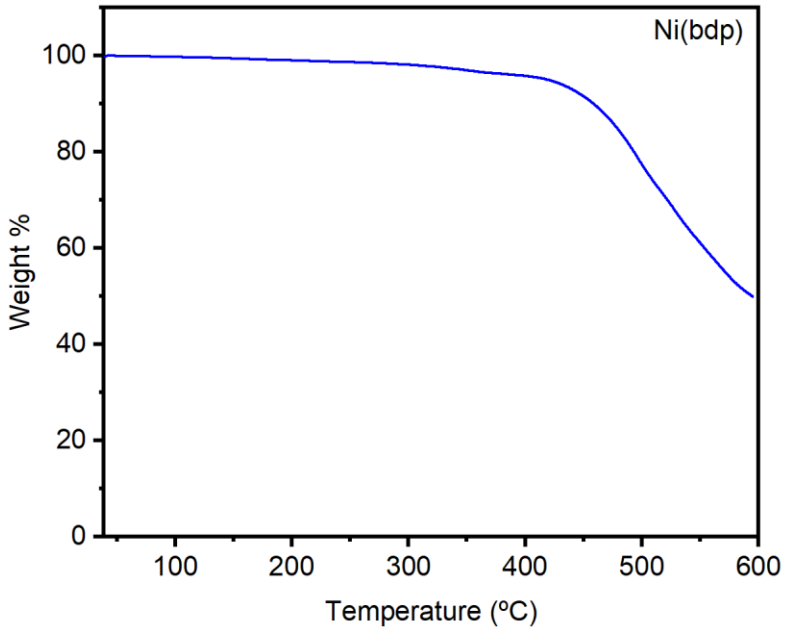

Figure S74. TGA decomposition profile of Ni(bdp) prepared under ionothermal conditions.

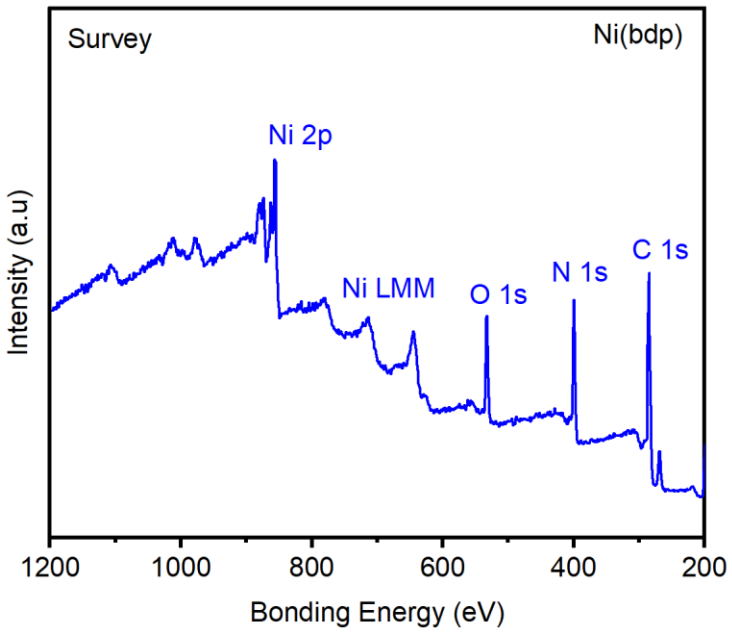

Figure S75. XPS spectral scan of an activated sample of Ni(bdp) prepared under ionothermal conditions. The detected O in this sample is likely due to physisorbed O_2/H_2O.[1]

Table S9. Tabulated survey XPS data for Ni(bdp) prepared under ionothermal conditions.

Element	Peak Label	Position	Area	Atomic %
Ni	Ni 2p	859.95	391.11	16.95
C	C 1s	284.81	1793.81	77.74
N	N 1s	3.18	122.52	5.31
Total:				100

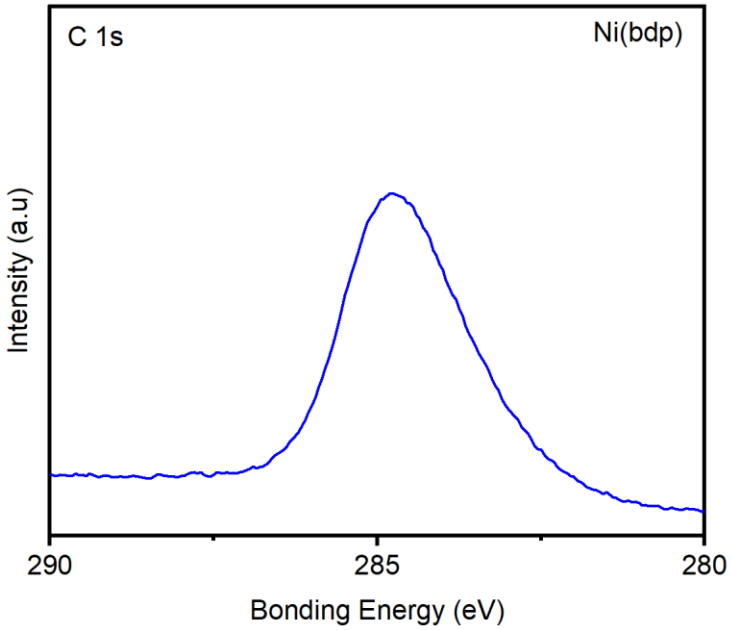

Figure S76. High resolution C 1s XPS spectrum of Ni(bdp) prepared under ionothermal conditions.

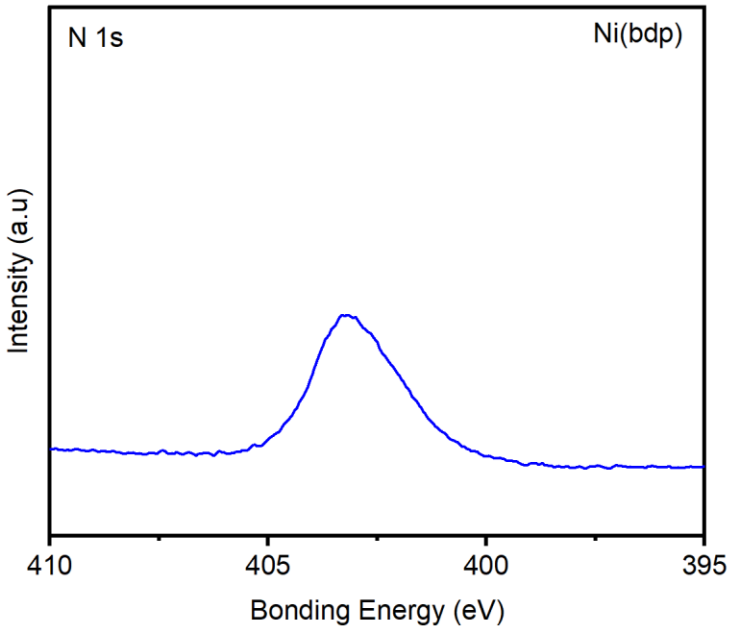

Figure S77. High resolution N 1s XPS spectrum of Ni(bdp) prepared under ionothermal conditions.

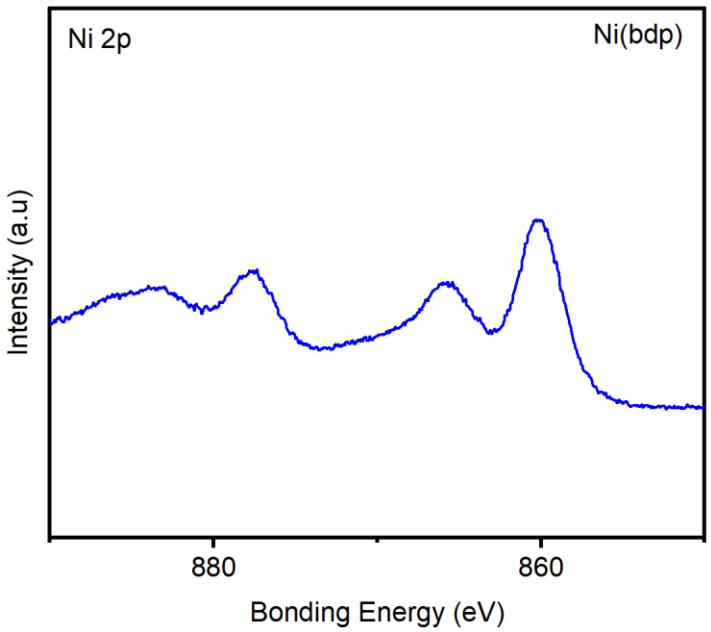

Figure S78. High resolution Ni 2p XPS spectrum of Ni(bdp) prepared under ionothermal conditions.

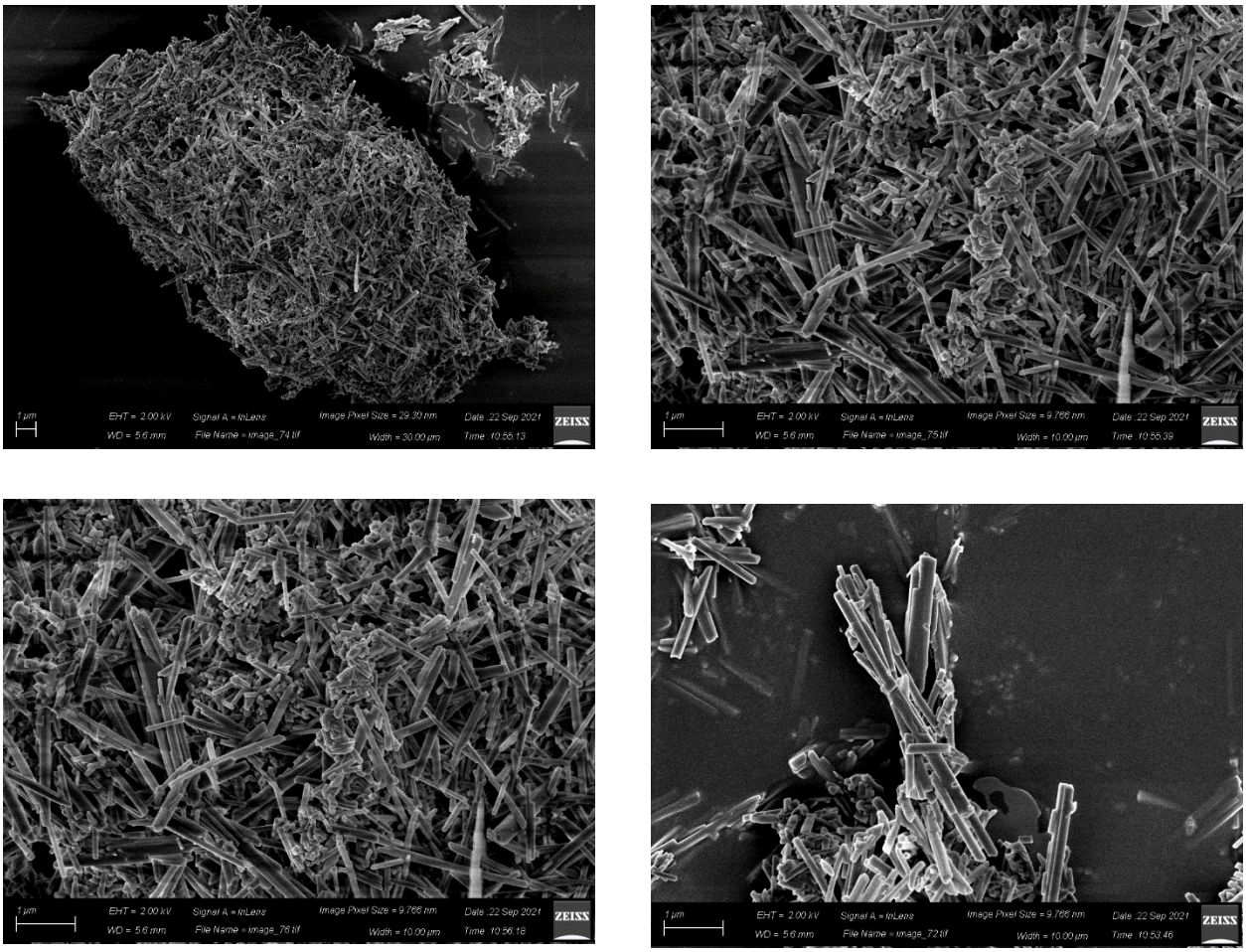

Figure S79. SEM images of Ni(bdp) prepared under ionothermal conditions.

8. Synthesis and characterization of Co_2(dobdc).

Solvothermal synthesis of Co_2(dobdc)-ST.

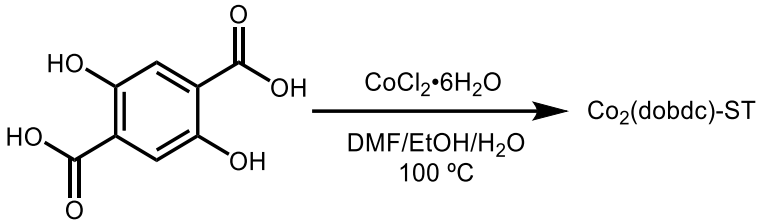

This procedure is adapted from the literature.[10] 2,5-dihydroxyterephthalic acid (H_4dobdc, 0.33 g, 1.66 mmol, 1.00 equiv.) and $CoCl_2$•$6H_2O$ (.868 g, 3.66 mmol, 2.20 equiv.) were added to 1:1:1 DMF-ethanol-DI water (200 mL) in a round bottom flask. After ultrasonication to dissolve the solids, the solution was transferred to a Pyrex jar and heated to 100 °C in an oven. The reaction mixture was allowed to stand at 100 °C for 24 h. The heterogeneous mixture was filtered, and the solid was returned to the Pyrex jar along with fresh DMF (250 mL). The jar was placed in an oven that had been heated to 120 °C. After 24 h, the DMF was decanted and replaced with fresh DMF (250 mL). This soaking procedure was repeated for a total of three hot DMF soaks. Next, the soaking procedure was repeated with methanol (100 mL) at 65 °C, replacing the solvent every 24 h. This soaking procedure was repeated for a total of three hot methanol soaks. The heterogeneous mixture was filtered. The solid was then activated under dynamic vacuum (<100 mTorr) at 180 °C for 24 h, yielding activated Co_2(dobdc) as a brown powder.

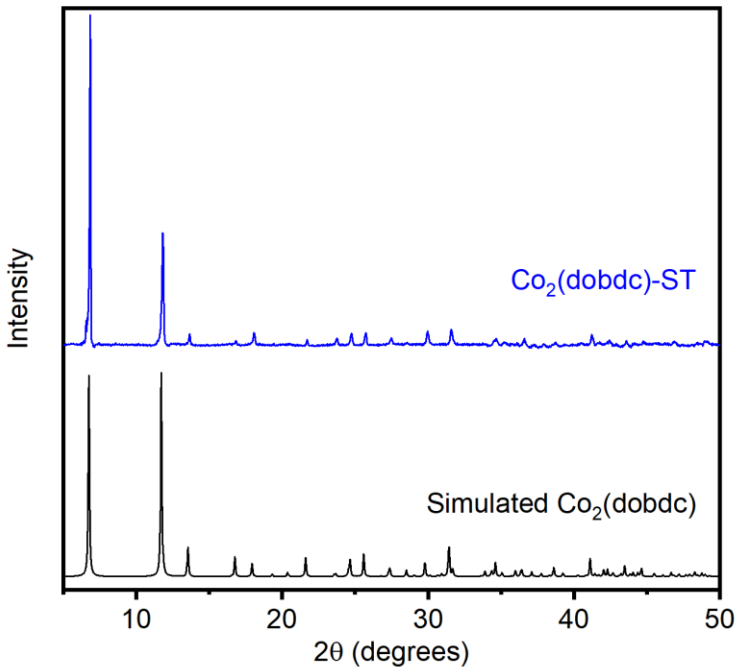

Figure S80. PXRD pattern (λ = 1.5406 Å) of Co_2(dobdc) prepared under solvothermal conditions. The simulated pattern corresponding to the single-crystal X-ray diffraction structure of Co_2(dobdc) is included for reference.[11] The experimental PXRD pattern was baseline corrected.

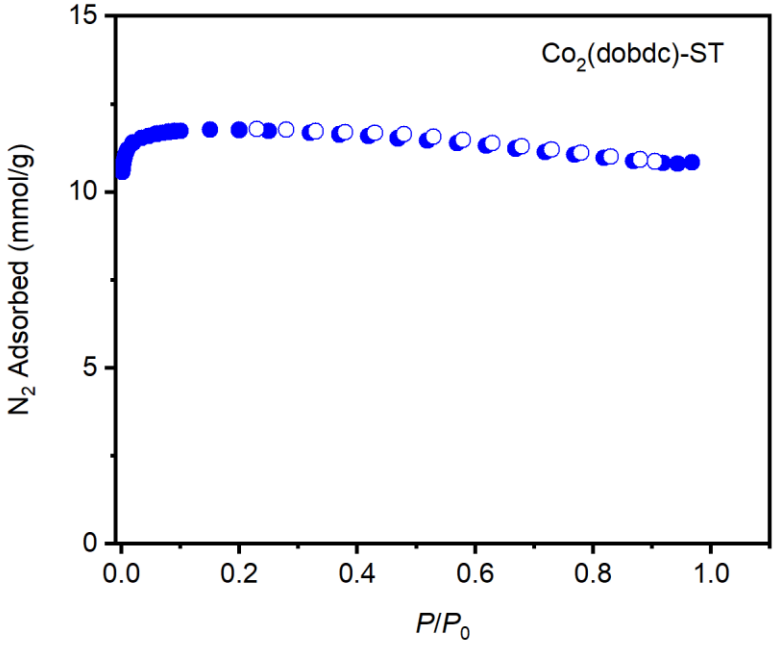

Figure S81. 77 K N_2 adsorption (closed circles) and desorption (open circles) isotherms of Co_2(dobdc) prepared under solvothermal conditions. Fitting these data yielded a Brunauer–Emmett–Teller (BET) surface area of 1135 ± 6 m^2/g (Lit: 1382 m^2/g). [11]

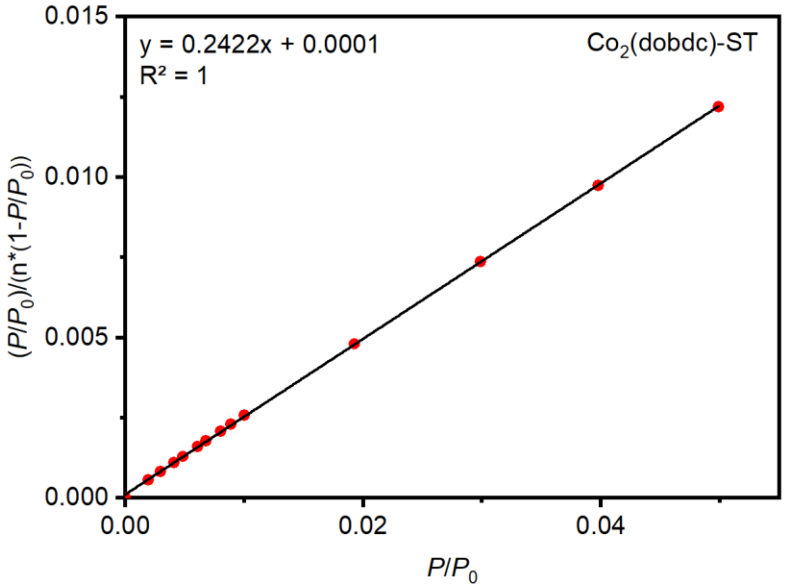

Figure S82. Linearized Brunauer–Emmett–Teller (BET) plot for the adsorption data of Co_2(dobdc) prepared under solvothermal conditions.

Ionothermal Synthesis of Co_2(dobdc)-IT.

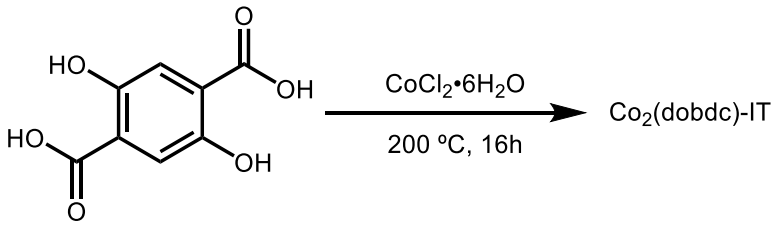

Following a modified General Procedure A, 2,5-dihydroxyterepthalic acid (1.00 g, 5.0 mmol, 1.00 equiv.) and $CoCl_2$•$6H_2O$ (2.97 g, 12.5 mmol, 2.50 equiv.) were combined at 200 °C. A black material was obtained, which was added to six 20 mL centrifuge tubes filled with DMF (10 mL). After centrifugation at 4000 rpm for 15 min, the black liquid was decanted, leaving a brown solid. The brown powder was washed following the steps outlined in General Procedure A to yield Co_2(dobdc) (0.78 g, 34% yield) as a brown powder after activation under dynamic vacuum (<100 mTorr) at 180 °C for 24 h. Synthesis attempts at lower reaction temperatures yielded a combination of unreacted reagents and amorphous materials.

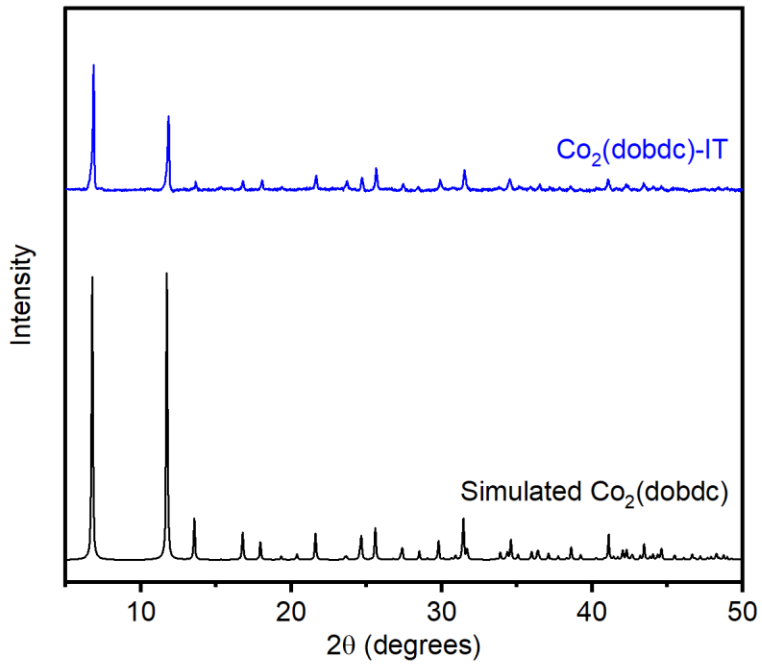

Figure S83. PXRD pattern (λ = 1.5406 Å) of Co_2(dobdc) prepared under ionothermal conditions. The simulated pattern corresponding to the single-crystal X-ray diffraction structure of Co_2(dobdc) is included for reference.[11] The experimental PXRD pattern was baseline corrected.

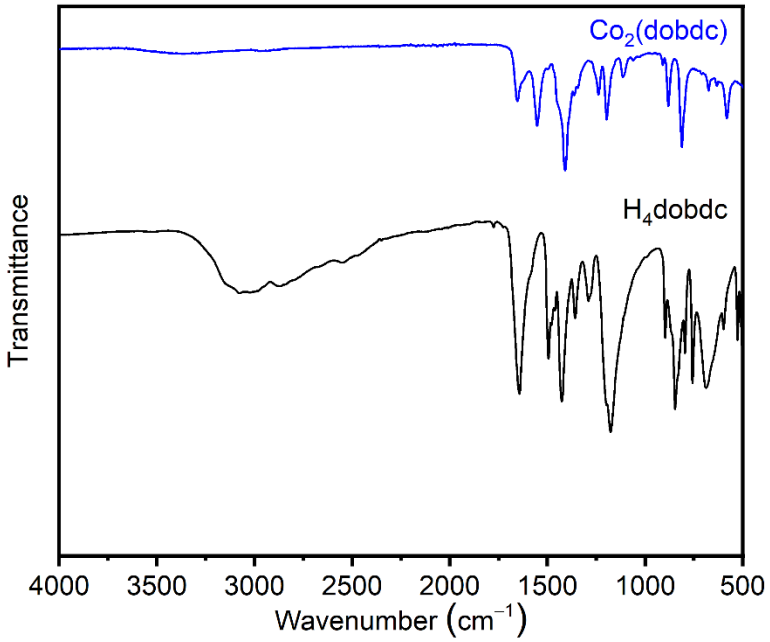

Figure S84. ATIR IR spectrum of Co_2(dobdc) prepared under ionothermal conditions.

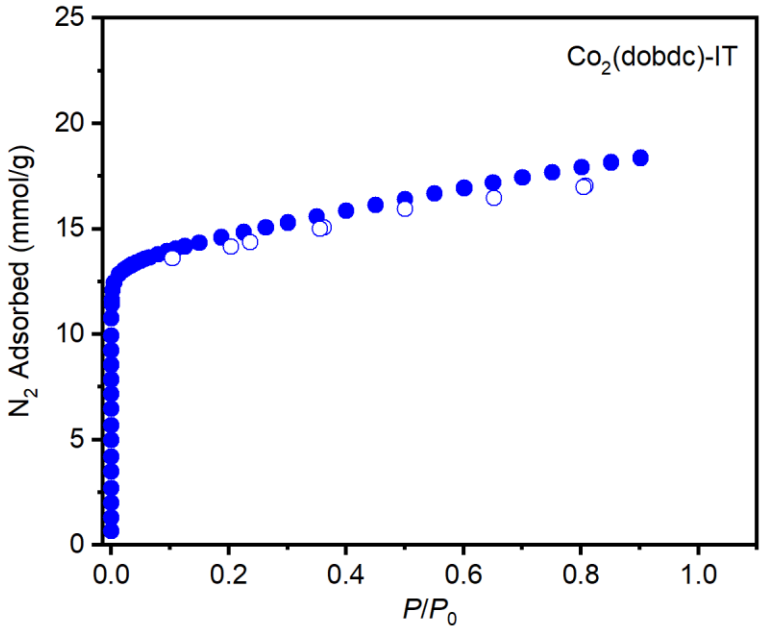

Figure S85. 77 K N_2 adsorption (closed circles) and desorption (open circles) isotherms of Co_2(dobdc) prepared under ionothermal conditions. Fitting these data yielded a Brunauer–Emmett–Teller (BET) surface area of 1042 ± 2 m^2/g.

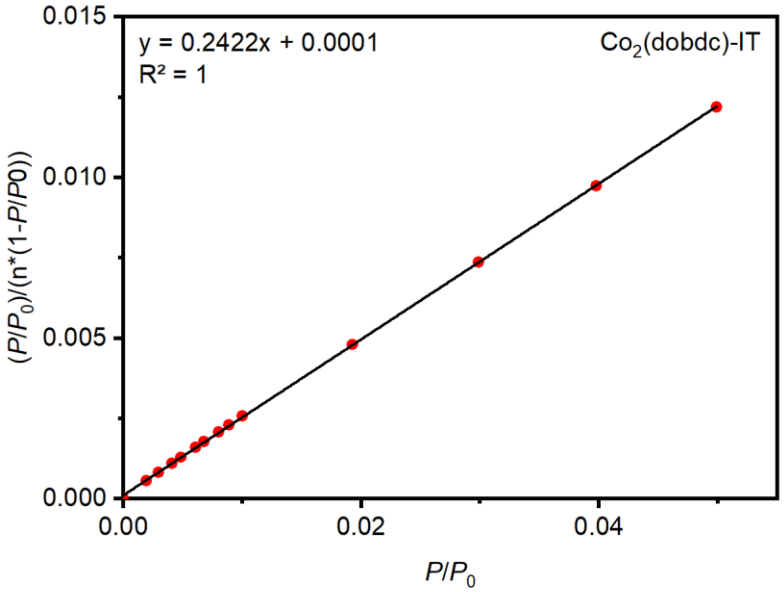

Figure S86. Linearized Brunauer–Emmett–Teller (BET) plot for the adsorption data of Co_2(dobdc) prepared under ionothermal conditions.

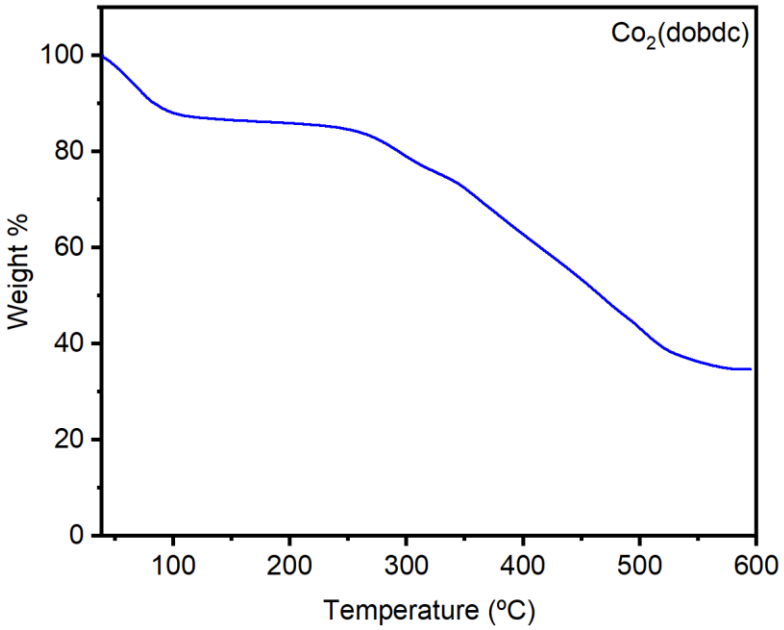

Figure S87. TGA decomposition profile of Co_2(dobdc) prepared under ionothermal conditions.

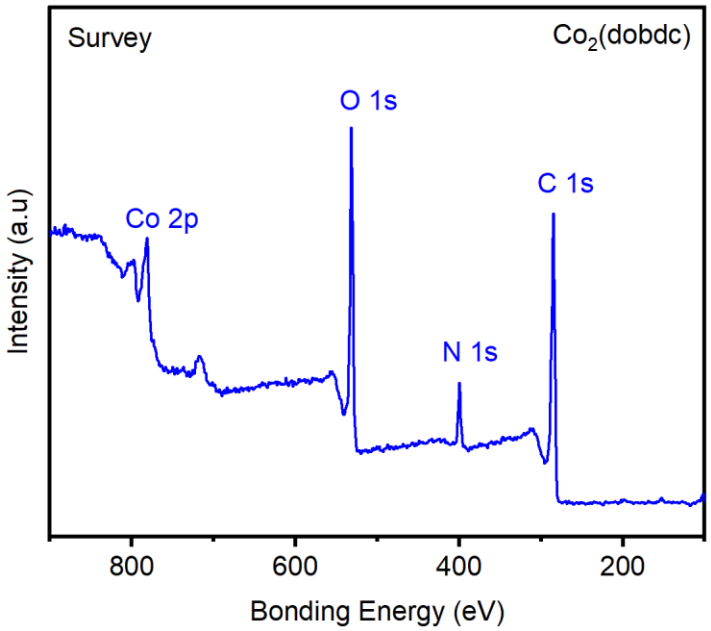

Figure S88. XPS spectral scans of Co_2(dobdc) prepared under ionothermal conditions. The detected N in this sample is likely due to physisorbed N_2.[1]

Table S10. Tabulated survey XPS data for Co_2(dobdc) prepared under ionothermal conditions.

Element	Peak Label	Position	Area	Atomic %
Co	Co 2p	781.8	1935.07	48.76
O	O 1s	531.8	1263.76	31.84
C	C 1s	284.8	1309.67	33.00
Total:				100

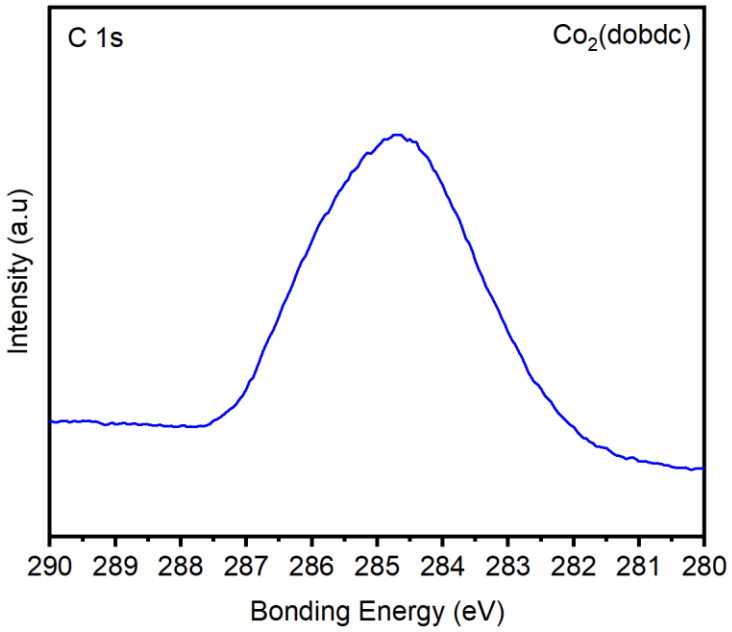

Figure S89. High resolution C 1s XPS spectrum of Co_2(dobdc) prepared under ionothermal conditions.

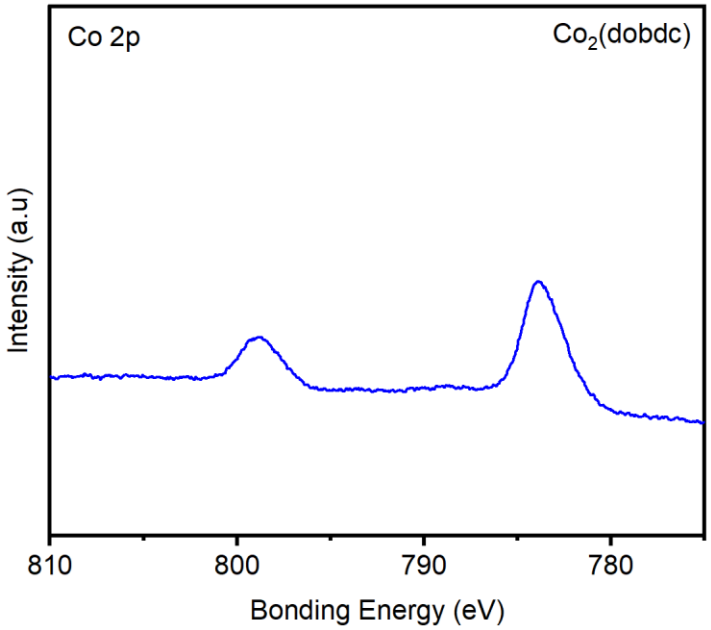

Figure S90. High resolution Co 2p XPS spectrum of Co_2(dobdc) prepared under ionothermal conditions.

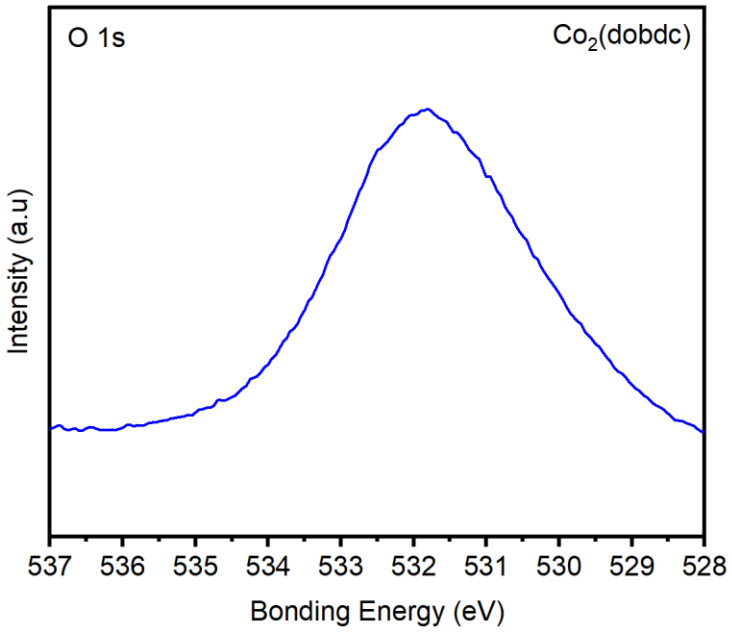

Figure S91. High resolution O 1s XPS spectrum of Co_2(dobdc) prepared under ionothermal conditions.

Table S11. Combustion elemental analysis data for Co_2(dobdc) prepared under ionothermal conditions.

Element	Theory for $C_8H_2Co_2O_6$ (wt %)	Found (wt %)
C	30.80	27.22
H	0.65	1.81

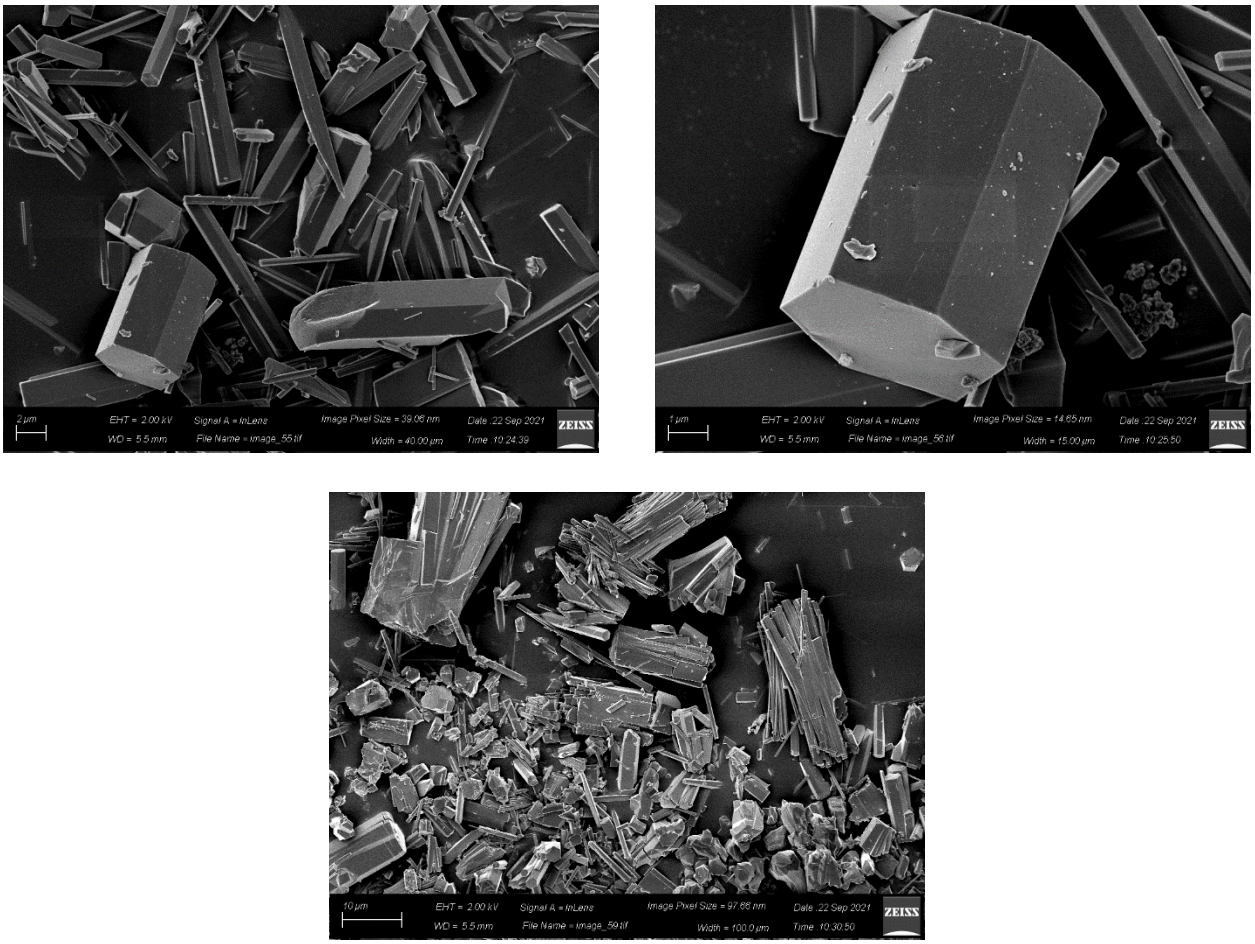

Figure S92. SEM images of Co_2(dobdc) prepared under ionothermal conditions.

9. Synthesis and characterization of Fe_2X_2(dobdc) (X = Cl, OH).

Ionothermal synthesis of Fe_2X_2(dobdc) (X = Cl, OH).

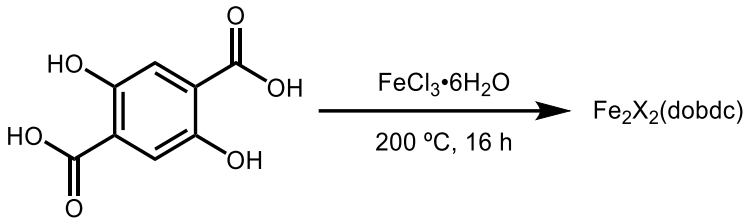

Following General Procedure A, 2,5-dihydroxyterepthalic acid (0.10 g, 0.50 mmol, 1.00 equiv.) and $FeCl_3$•$6H_2O$ (0.272 g, 1.00 mmol, 2.00 equiv.) were combined at 200 °C to yield Fe_2X_2(dobdc) (X = Cl, OH) (0.058 g, 20% yield) as a black powder after activation under vacuum at 180 °C for 24 h. Synthesis attempts at lower temperatures or with shorter reaction times yielded a combination of unreacted reagents and amorphous materials.

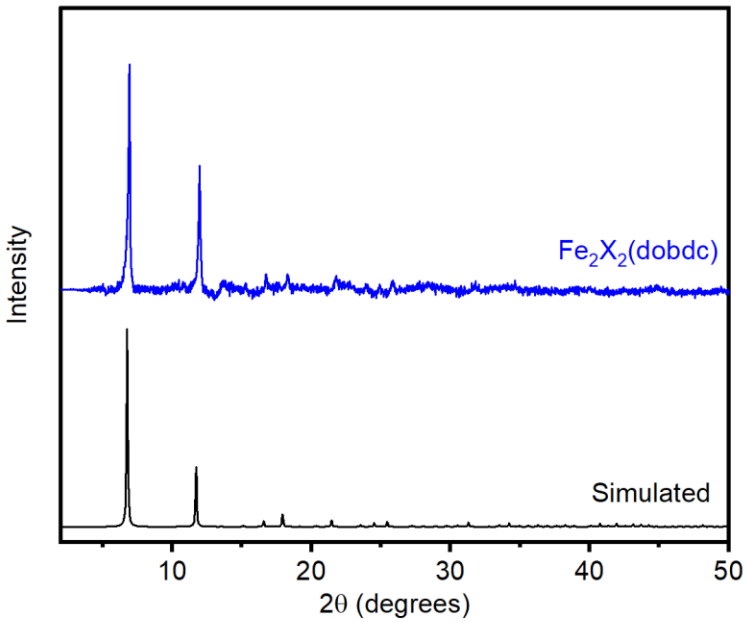

Figure S93. PXRD pattern (λ = 1.5406 Å) Fe_2X_2(dobdc) (X = Cl, OH) prepared under ionothermal conditions. The simulated pattern corresponding to the single-crystal X-ray diffraction structure of Fe_2(dobdc) is included for reference.[12] The experimental PXRD pattern was baseline corrected.

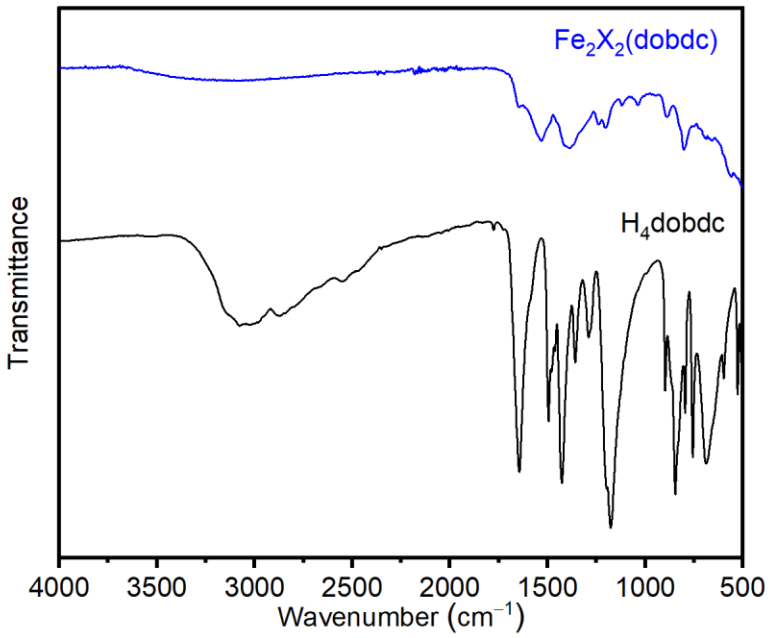

Figure S94. ATR IR spectrum of Fe_2X_2(dobdc) (X = Cl, OH) prepared under ionothermal conditions

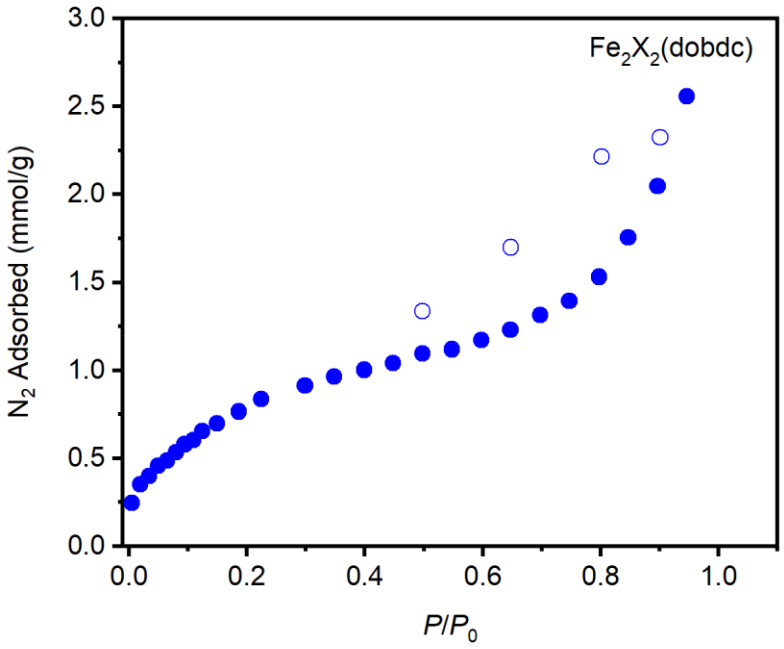

Figure S95. 77 K N_2 adsorption (closed circles) and desorption (open circles) isotherms of Fe_2X_2(dobdc) (X = Cl, OH) prepared under ionothermal conditions. Fitting these data yielded a Brunauer–Emmett–Teller (BET) surface area of 56 ± 3 m^2/g. Activation at lower temperatures did not improve the surface area.

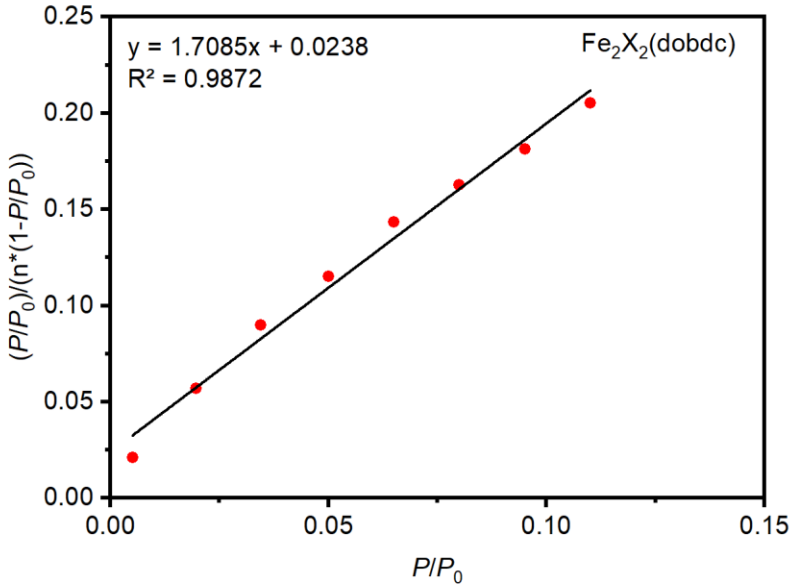

Figure S96. Linearized Brunauer–Emmett–Teller (BET) plot for the adsorption data of Fe_2X_2(dobdc) (X = Cl, OH) prepared under ionothermal conditions.

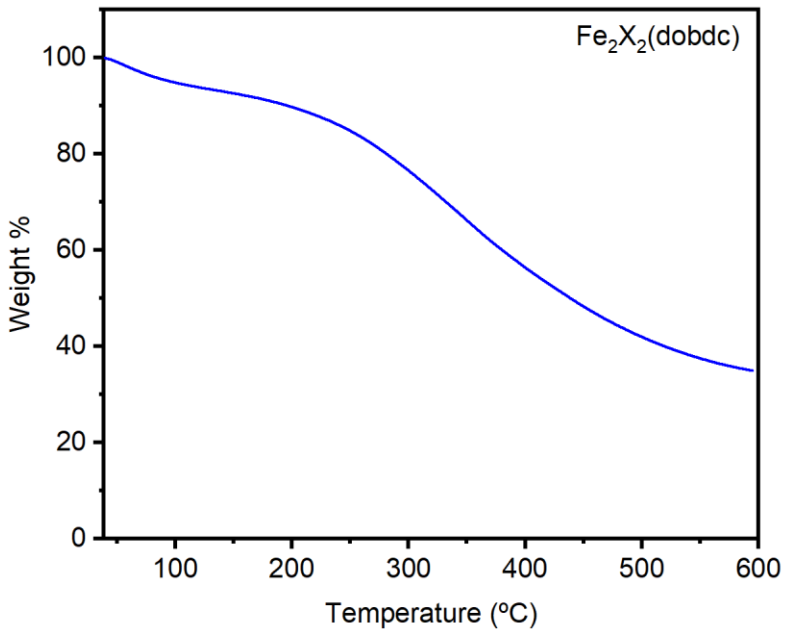

Figure S97. TGA decomposition profile of Fe_2X_2(dobdc) (X = Cl, OH) prepared under ionothermal conditions.

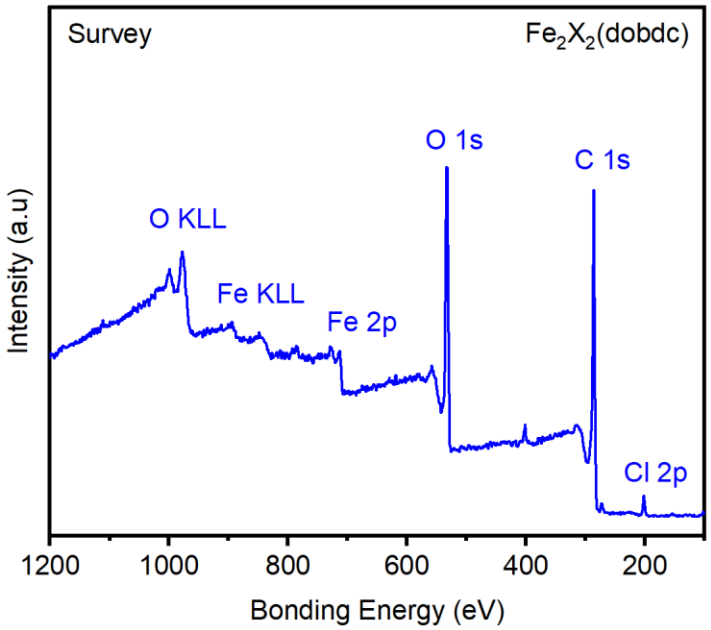

Figure S98. XPS spectral scan of an activated sample of Fe_2X_2(dobdc) (X = Cl, OH). The detected N (~400 eV) in this sample is likely due to physisorbed N_2.[1]

Table S12. Tabulated survey XPS data for Fe_2X_2(dobdc) (X = Cl, OH) prepared under ionothermal conditions.

Element	Peak Label	Position	Area	Atomic %
O	O 1s	530.8	1242.18	22.35
C	C 1s	284.8	1392.26	73.39
Fe	Fe 2p	710.8	628.06	14.52
Cl	Cl 2p	199.8	74.02	1.50
Total:				100

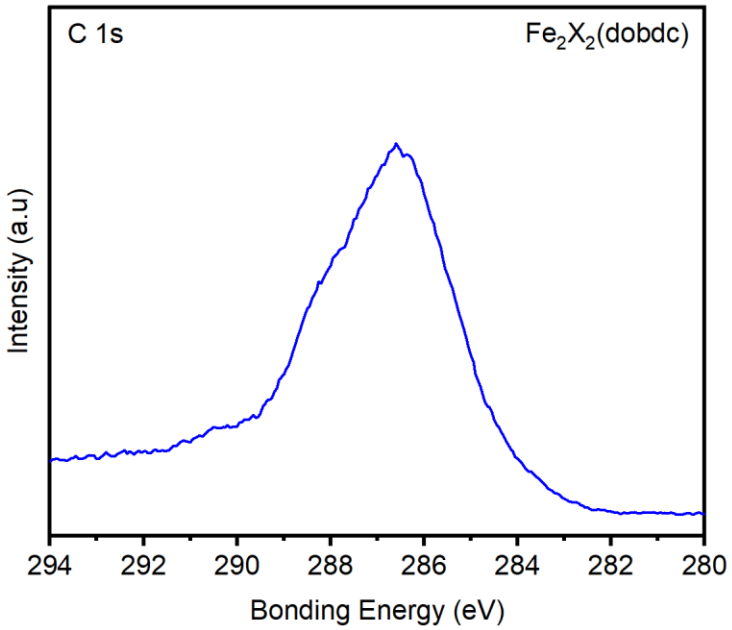

Figure S99. High resolution C 1s XPS spectrum of Fe_2X_2(dobdc) (X = Cl, OH) prepared under ionothermal conditions.

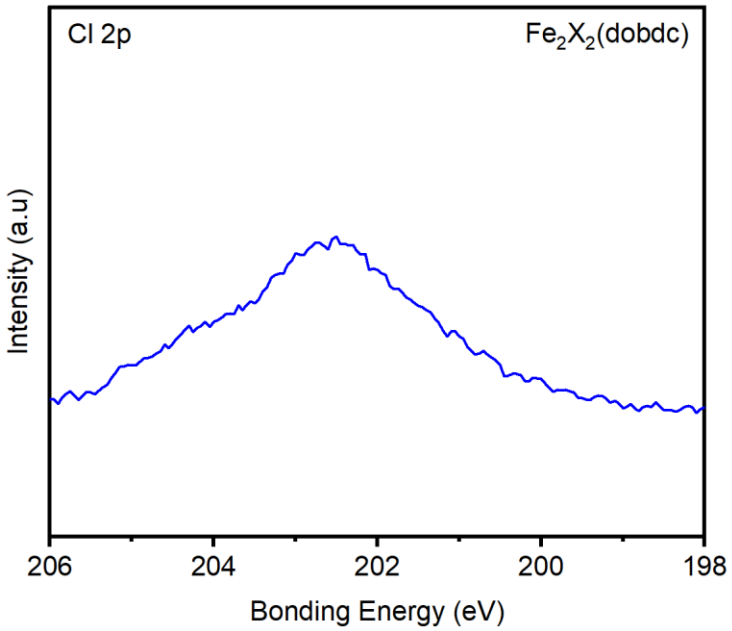

Figure S100. High resolution Cl 2p XPS spectrum of Fe_2X_2(dobdc) (X = Cl, OH) prepared under ionothermal conditions.

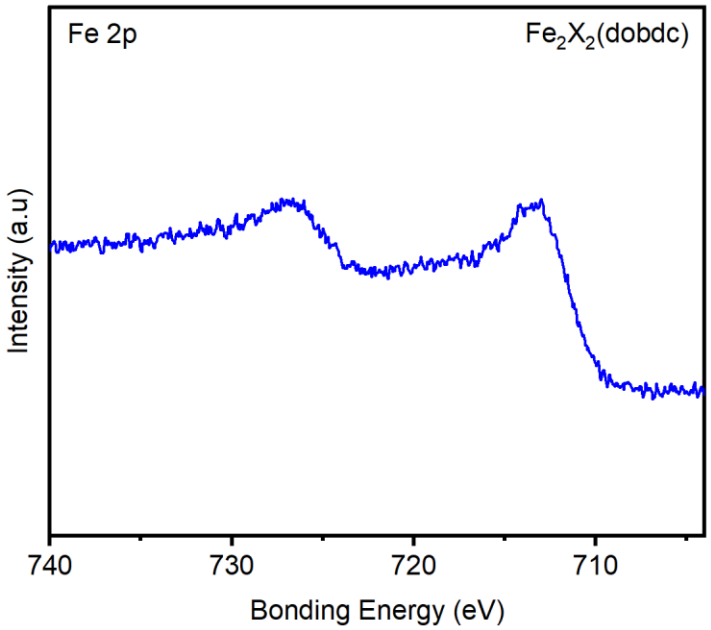

Figure S101. High resolution Fe 2p XPS spectrum of Fe_2X_2(dobdc) (X = Cl, OH) prepared under ionothermal conditions.

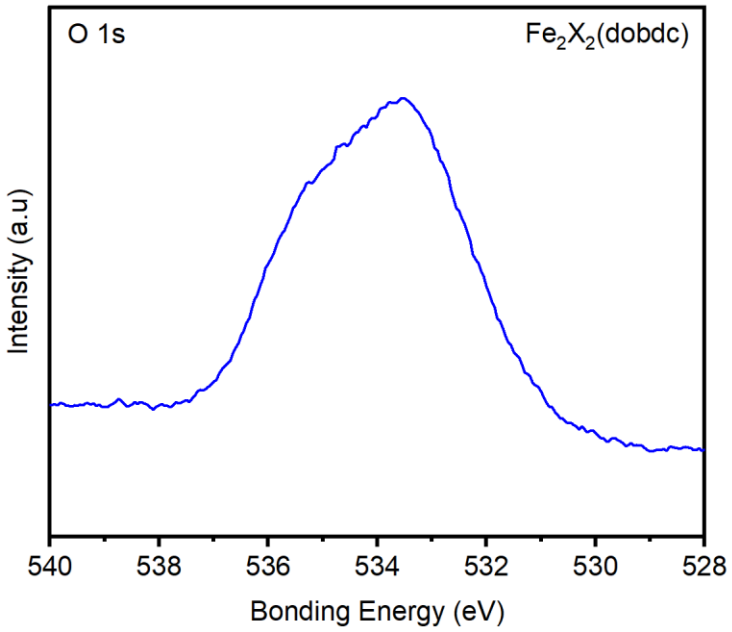

Figure S102. High resolution O 1s XPS spectrum of Fe_2X_2(dobdc) (X = Cl, OH) prepared under ionothermal conditions.

Table S13. Combustion elemental analysis data for Fe_2X_2(dobdc) (X = Cl, OH) prepared under ionothermal conditions.

Element	Theory for Fe_2Cl_2(dobdc) $C_8H_2Cl_2Fe_2O_6$ (wt %)	Theory for $Fe_2(OH)_2$(dobdc) $C_8H_4Fe_2O_8$ (wt %)	Found (wt %)
C	25.51	28.28	29.96
H	0.54	1.19	2.09
Cl	18.82	0	3.16

The lower than expected %Cl for this sample is consistent with the EDS data (Figure S105) and indicates partial exchange of Cl^- for OH^- likely occurs under ambient conditions.

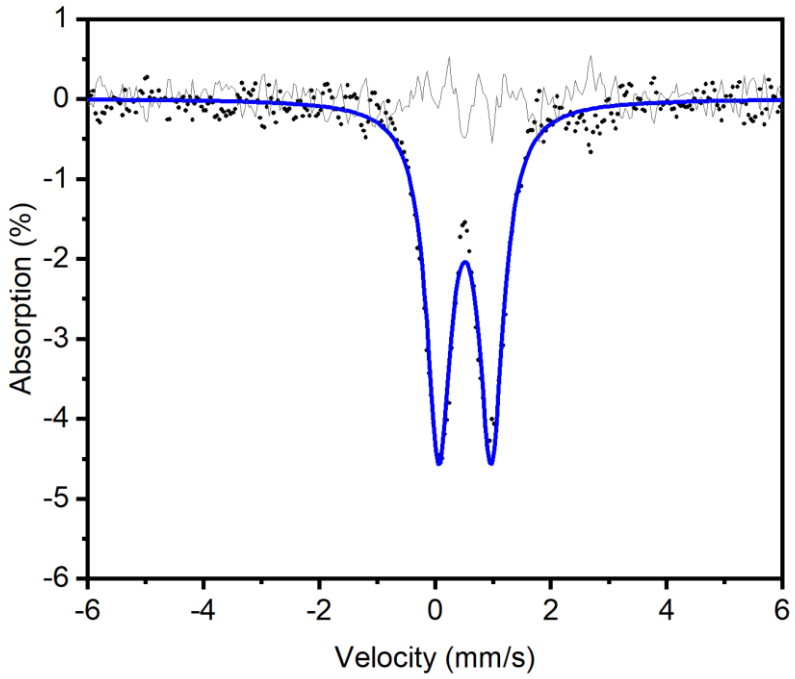

Figure S103. Mössbauer spectrum of Fe_2X_2(dobdc) (X = Cl, OH) prepared under ionothermal conditions collected at 85 K and 0 field. The experimental spectrum is shown as black dots, the simulated spectrum is shown in blue, and the residual is shown in gray.

Table S14. Mössbauer data of Fe_2X_2(dobdc) (X = Cl, OH), showing an isomer shift of 0.51(6) mm/s and quadrupole splitting of 0.90(9) mm/s, which are consistent with S = 5/2 Fe(III).

	Fe_2X_2(dobdc) (X = Cl, OH)
δ **(mm/s)**	0.516 ± 0.001
ΔE_Q **(mm/s)**	0.909 ± 0.002
Γ **(mm/s)**	0.509 ± 0.003
Relative area	1.020 ± 0.004
Reduced χ^2	0.992 ± 0.064

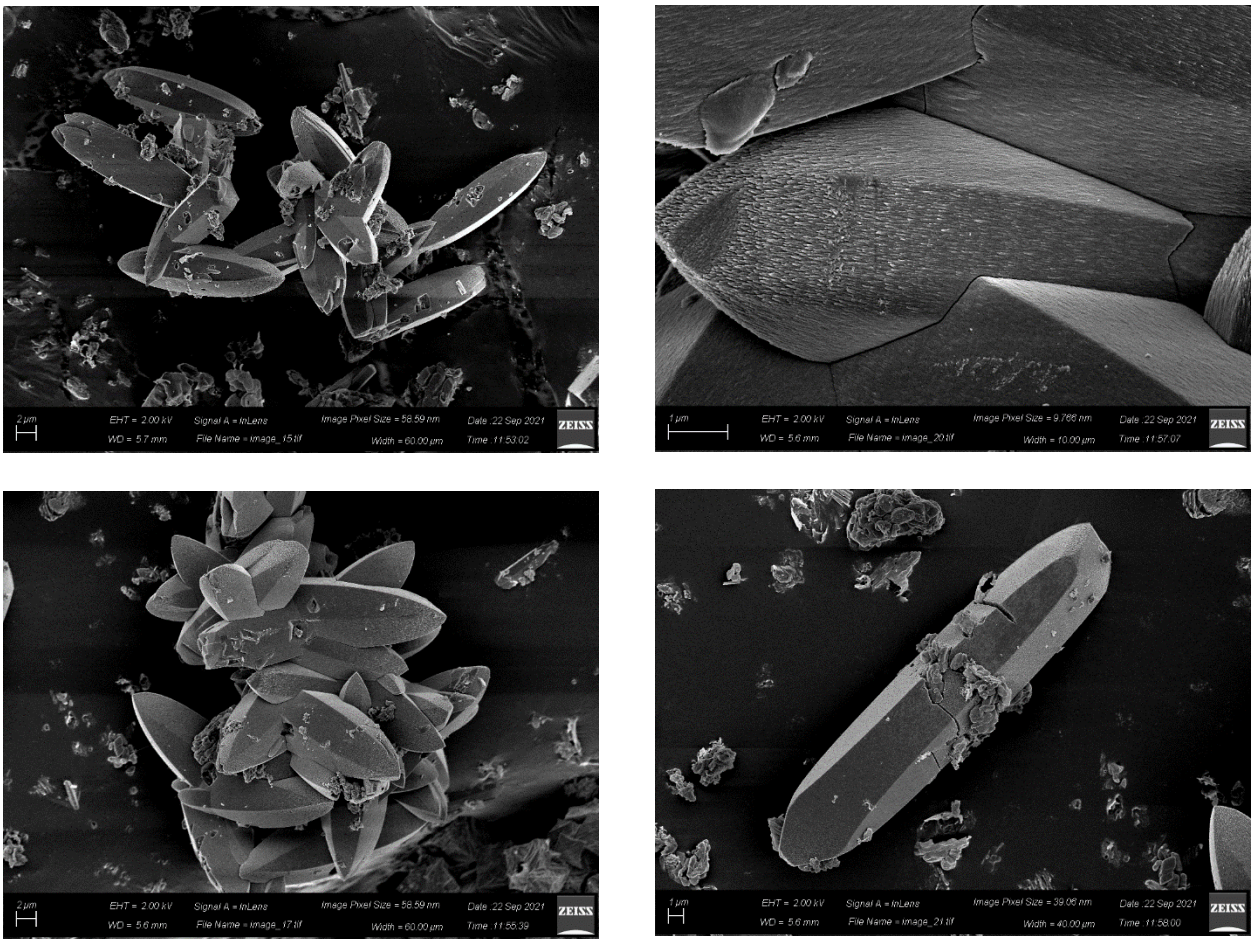

Figure S104. SEM images of Fe_2X_2(dobdc) (X = Cl, OH) prepared under ionothermal conditions.

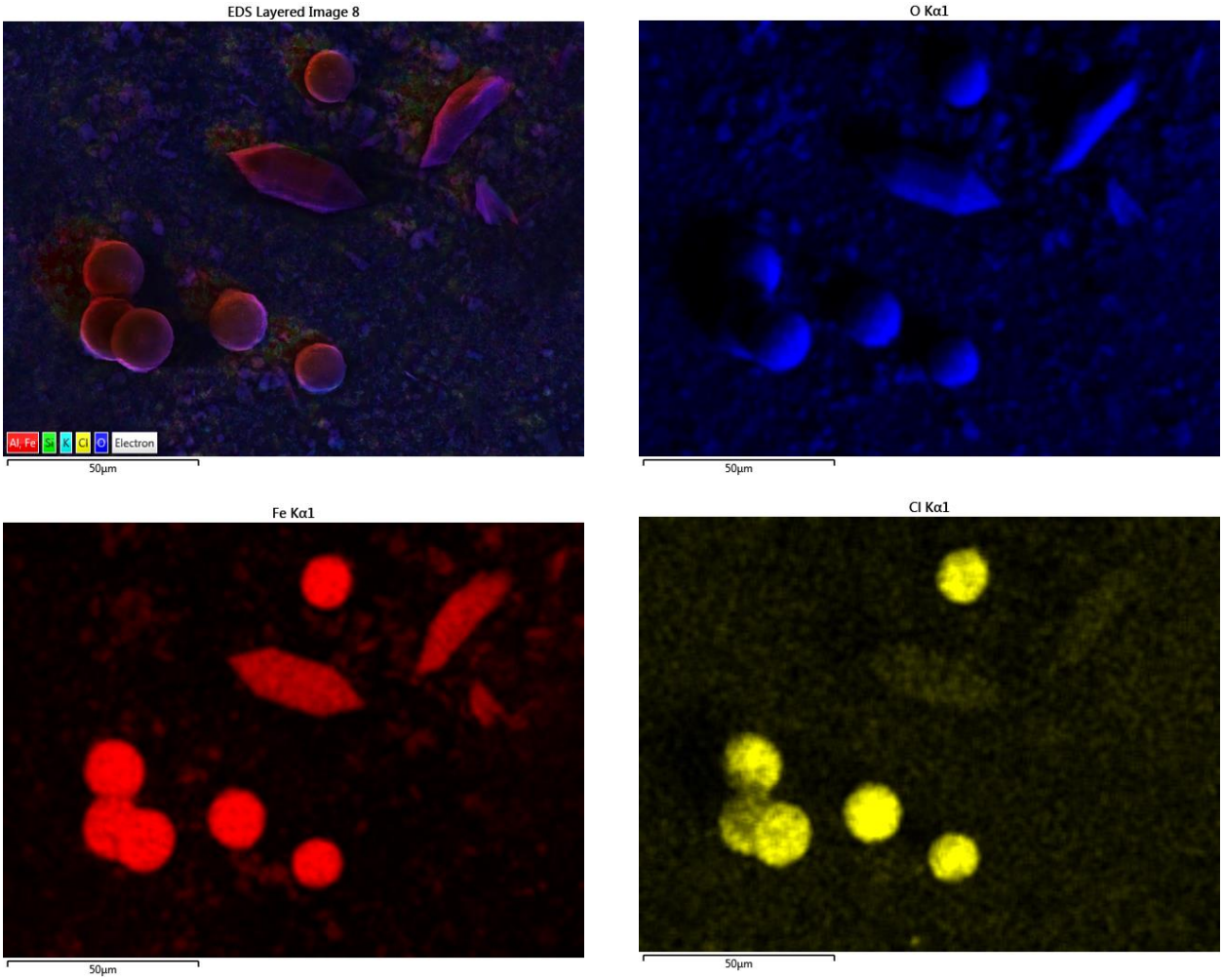

Figure S105. EDS elemental maps of Fe_2X_2(dobdc) (X = Cl, OH) prepared under ionothermal conditions. A relatively uniform distribution of O and Fe is observed. The lack of Cl in certain particles is likely due to partial exchange of surface sites with water to generate Fe(III)−OH sites.

Attempted solvothermal synthesis of Fe_2X_2(dobdc) (X = Cl, OH).

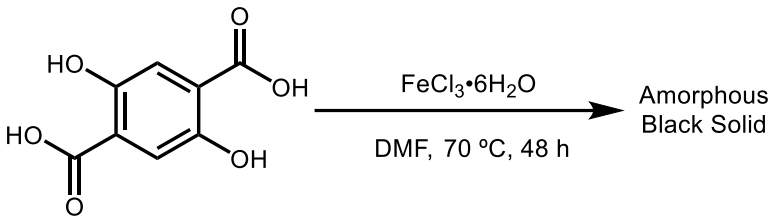

An attempt to synthesize Fe_2X_2(dobdc) (X = Cl, OH) under solvothermal conditions was performed by adapting the procedure for the synthesis of similar M_2(dobdc) MOFs.[10] In a 250 mL Pyrex jar, H_4dobdc (0.10 g, 0.50 mmol, 1.00 equiv.) and $FeCl_3$•$6H_2O$ (0.30 g, 1.11 mmol, 2.20 equiv.) were added to DMF (125 mL). The mixture was allowed to stand at 70 ºC for 48 h. The heterogeneous mixture was filtered, and the solid was returned to the Pyrex jar along with fresh DMF (250 mL). The jar was placed in an oven that had been heated to 120 °C. After 24 h, the DMF was decanted and replaced with fresh DMF (250 mL). This soaking procedure was repeated for a total of three hot DMF soaks. Next, the soaking procedure was repeated with methanol (100 mL) at 65 °C, replacing the solvent every 24 h. This soaking procedure was repeated for a total of three hot methanol soaks. The heterogeneous mixture was filtered. The solid was then activated under dynamic vacuum at 180 °C for 24 h, yielding an amorphous black powder.

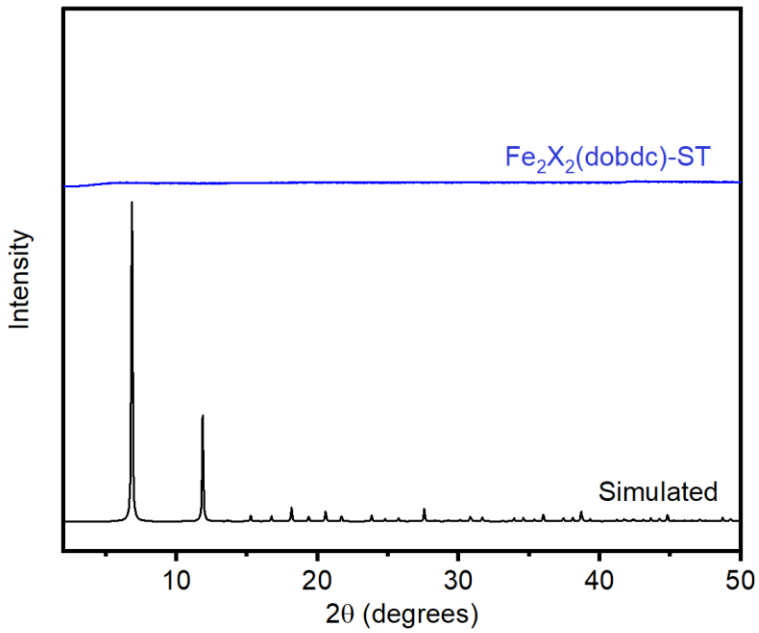

Figure S106. PXRD patterns (λ = 1.5406 Å) of the solid obtained after the attempted synthesis of Fe_2X_2(dobdc) (X = Cl, OH) under solvothermal conditions. The simulated pattern corresponding to the single-crystal X-ray diffraction structure of Fe_2(dobdc) is included for reference.[12] The experimental PXRD pattern was baseline corrected.

10. Synthesis and characterization of Ni_2(*m*-dobdc).

Solvothermal synthesis of Ni_2(*m*-dobdc)-ST.

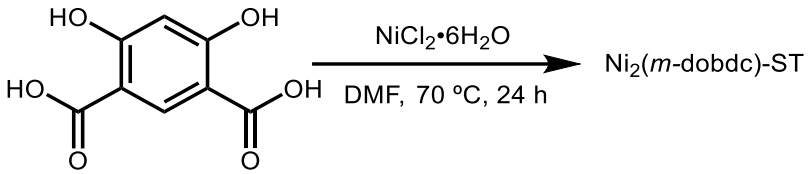

This procedure is adapted from the literature.[13] In a 250 mL round bottom flask, H_4*m*-dobdc (0.33 g, 2.02 mmol, 1.00 equiv.) and $NiCl_2$•$6H_2O$ (1.19 g, 5.05 mmol, 2.20 equiv.) were added to DMF (125 mL) and stirred at 70 ºC for 48 h. The heterogeneous mixture was filtered, and the solid was transferred to a Pyrex jar along with fresh DMF (250 mL). The jar was placed in an oven that had been heated to 120 °C. After 24 h, the DMF was decanted and replaced with fresh DMF (250 mL). This soaking procedure was repeated for a total of three hot DMF soaks. Next, the soaking procedure was repeated with methanol (100 mL) at 65 °C, replacing the solvent every 24 h. This soaking procedure was repeated for a total of three hot methanol soaks. The heterogeneous mixture was filtered. The solid was then activated under dynamic vacuum (<100 mTorr) at 180 °C for 24 h, yielding activated Ni_2(*m*-dobdc) as a brown powder.

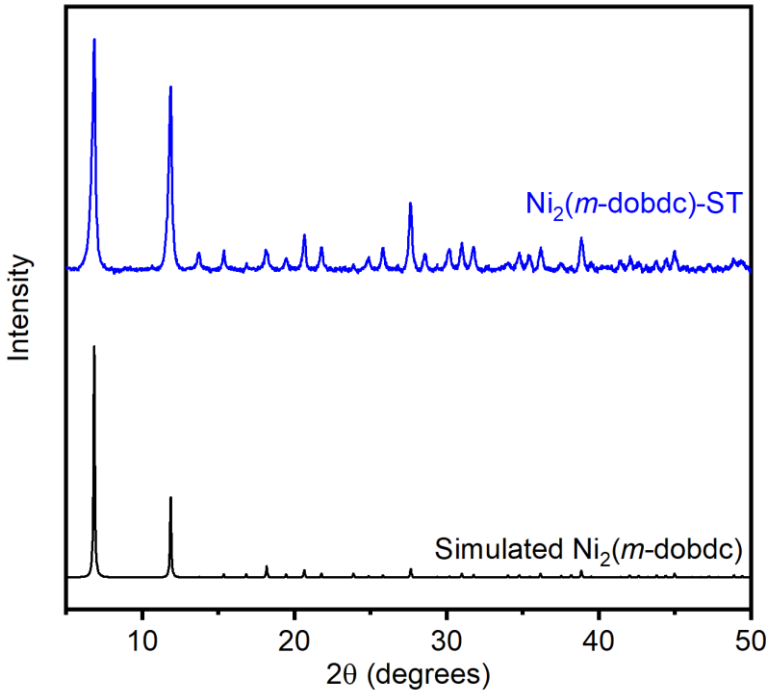

Figure S107. PXRD pattern (λ = 1.5406 Å) of Ni_2(*m*-dobdc) prepared under solvothermal conditions. The simulated pattern corresponding to the powder X-ray diffraction structure of Ni_2(*m*-dobdc) is included for reference.[13] The experimental PXRD pattern was baseline corrected.

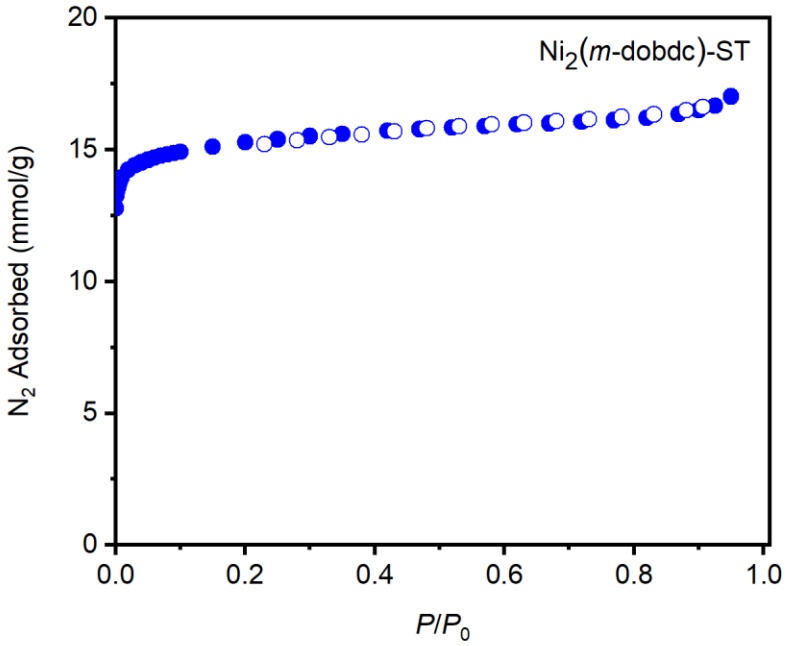

Figure S108. 77 K N_2 adsorption (closed circles) and desorption (open circles) isotherms of Ni_2(*m*-dobdc) prepared under solvothermal conditions. Fitting these data yielded a Brunauer–Emmett–Teller (BET) surface area of 1592 ± 3 m^2/g (Lit: 1321 m^2/g).[13]

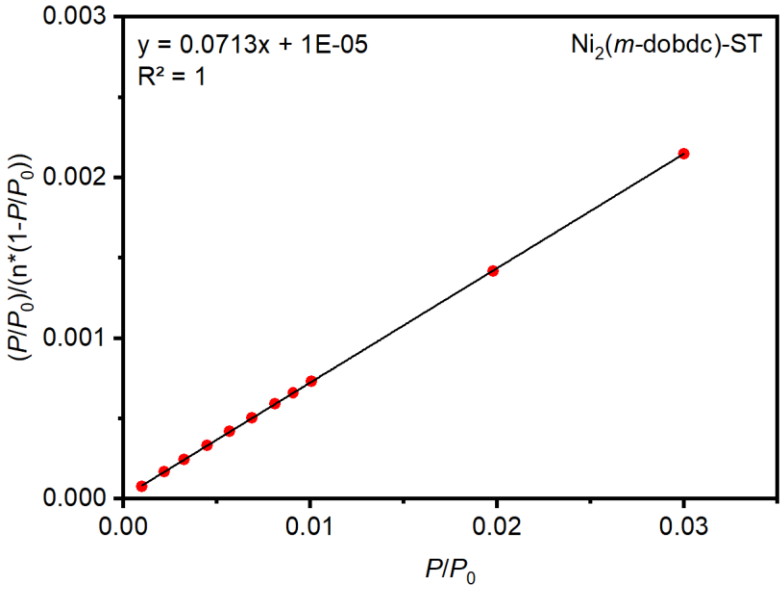

Figure S109. Linearized Brunauer–Emmett–Teller (BET) plot for the adsorption data of Ni_2(*m*-dobdc) prepared under solvothermal conditions.

Ionothermal synthesis of Ni_2(*m*-dobdc)-IT.

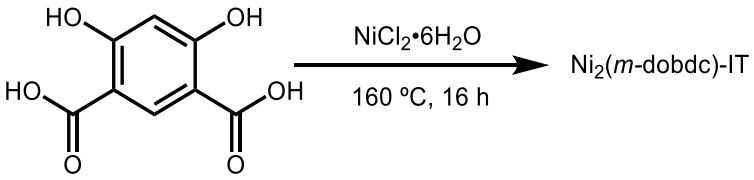

Following General Procedure A, H_4*m*-dobdc (0.100 g, 0.50 mmol, 1.00 equiv.) and $NiCl_2$•$6H_2O$ (0.298 g, 1.26 mmol, 2.50 equiv.) were combined at 160 °C to yield Ni_2(*m*-dobdc) (0.109 g, 44% yield) as a brown powder after activation under dynamic vacuum (<100 mTorr) at 180 °C for 24 h.

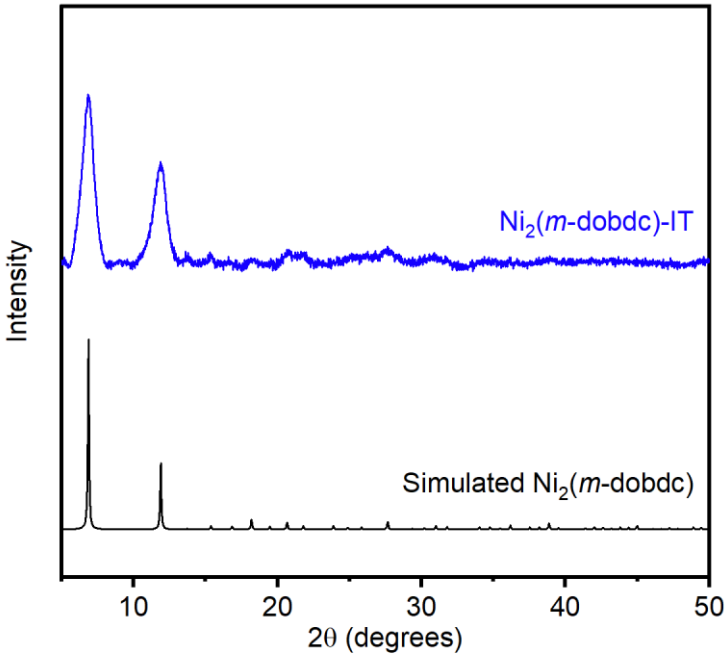

Figure S110. PXRD pattern (λ = 1.5406 Å) of Ni_2(*m*-dobdc) prepared under ionothermal conditions. The simulated pattern corresponding to the powder X-ray diffraction structure of Ni_2(*m*-dobdc) is included for reference.[13] The experimental PXRD pattern was baseline corrected.

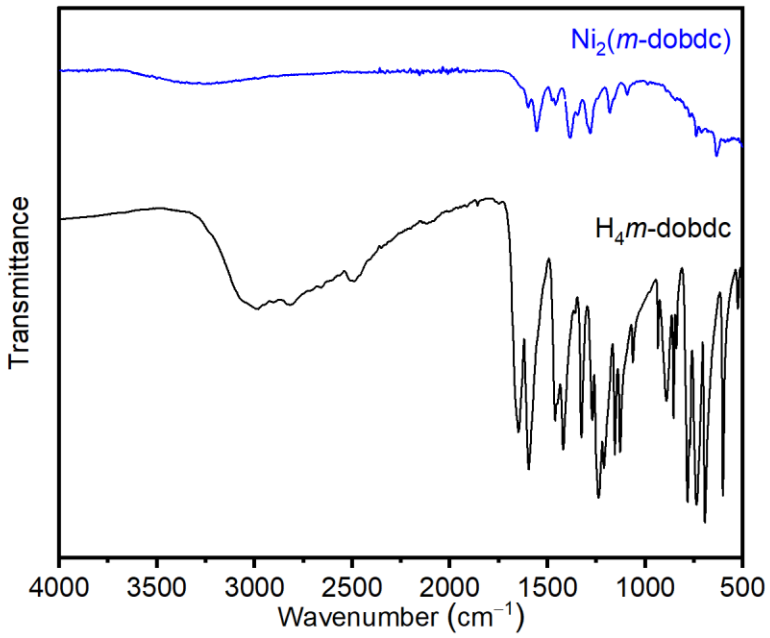

Figure S111. ATR IR spectrum of Ni_2(*m*-dobdc) prepared under ionothermal conditions

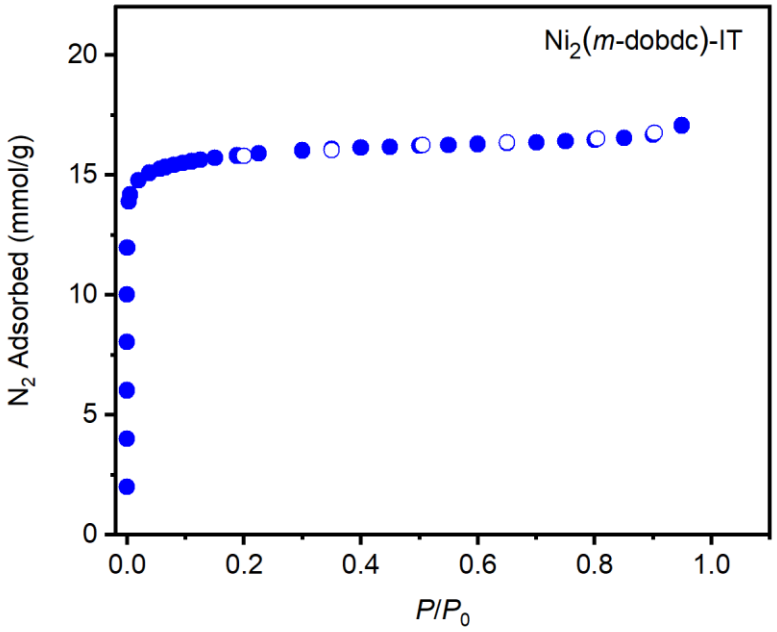

Figure S112. 77 K N_2 adsorption (closed circles) and desorption (open circles) isotherms of Ni_2(*m*-dobdc) prepared under ionothermal conditions. Fitting these data yielded a Brunauer–Emmett–Teller (BET) surface area of 1416 ± 2 m^2/g (Lit: 1321 m^2/g).[13]

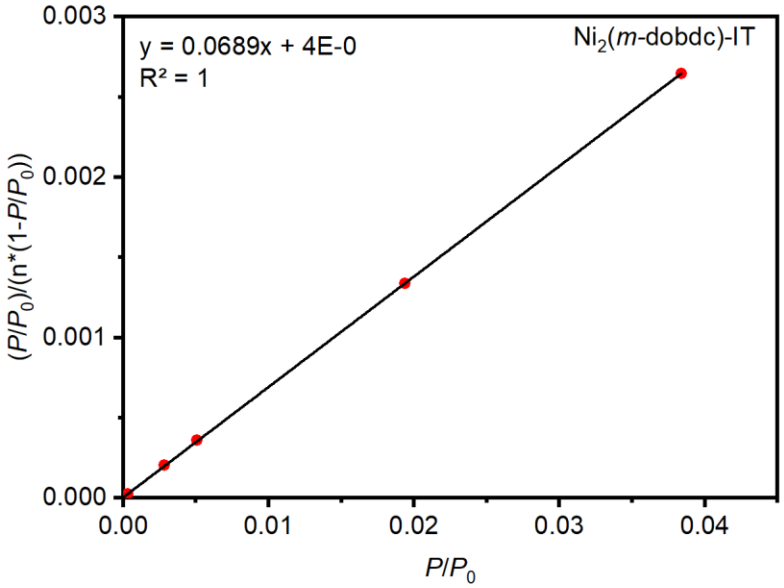

Figure S113. Linearized Brunauer–Emmett–Teller (BET) plot for the adsorption data of Ni_2(*m*-dobdc) prepared under ionothermal conditions.

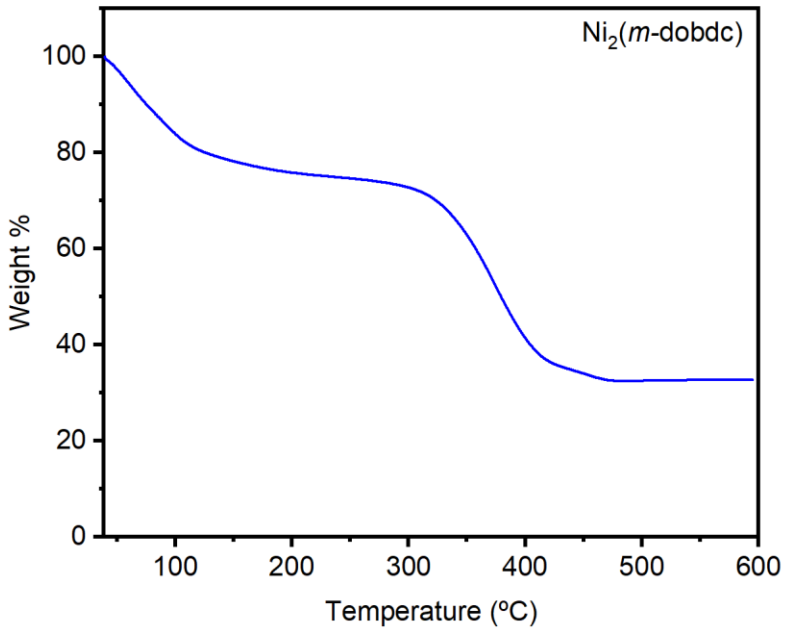

Figure S114. TGA decomposition profile of Ni_2(*m*-dobdc) prepared under ionothermal conditions.

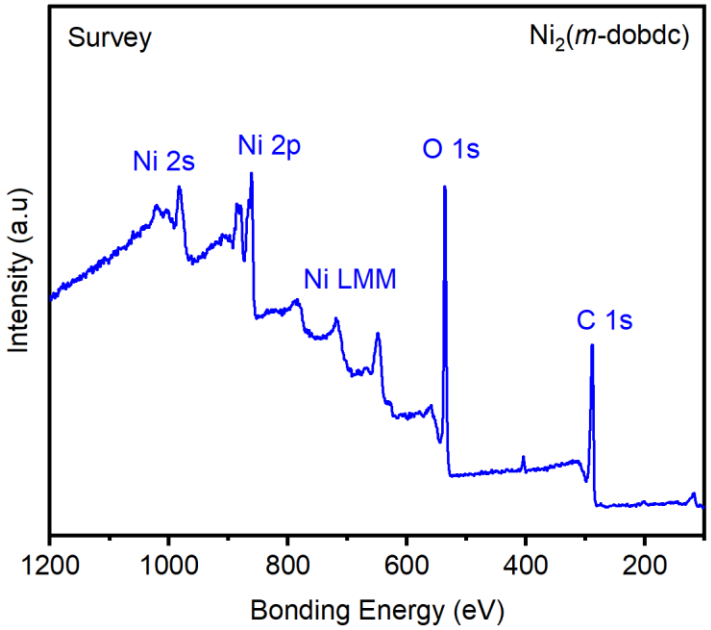

Figure S115. XPS spectral scan of an activated sample of Ni_2(*m*-dobdc). The detected N (~400 eV) in this sample is likely due to physisorbed N_2.[1]

Table S15. Tabulated survey XPS data for Ni_2(*m*-dobdc) prepared under ionothermal conditions.

Element	Peak Label	Position	Area	Atomic %
Ni	Ni 2p	856.8	1710.09	43.56
C	C 1s	284.8	1308.84	33.34
O	O 1s	532.8	906.60	23.09
Total:				100

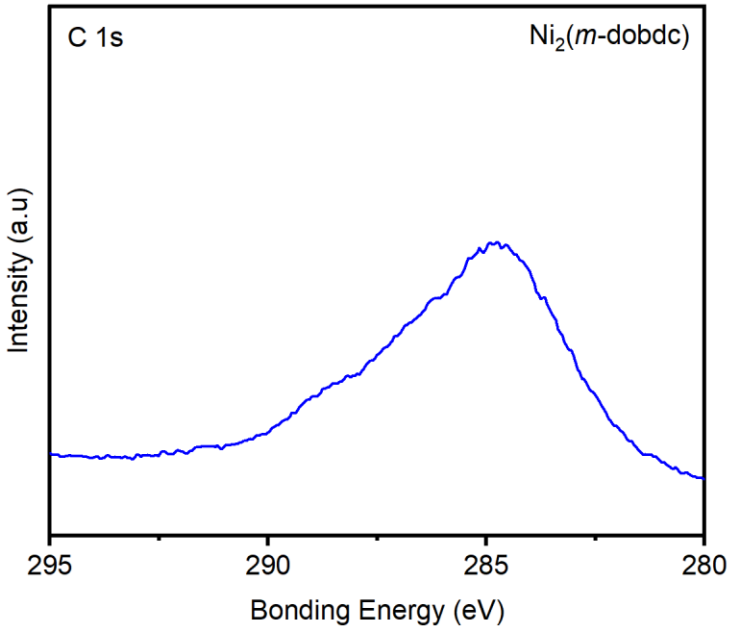

Figure S116. High resolution C 1s XPS spectrum of Ni_2(*m*-dobdc) prepared under ionothermal conditions.

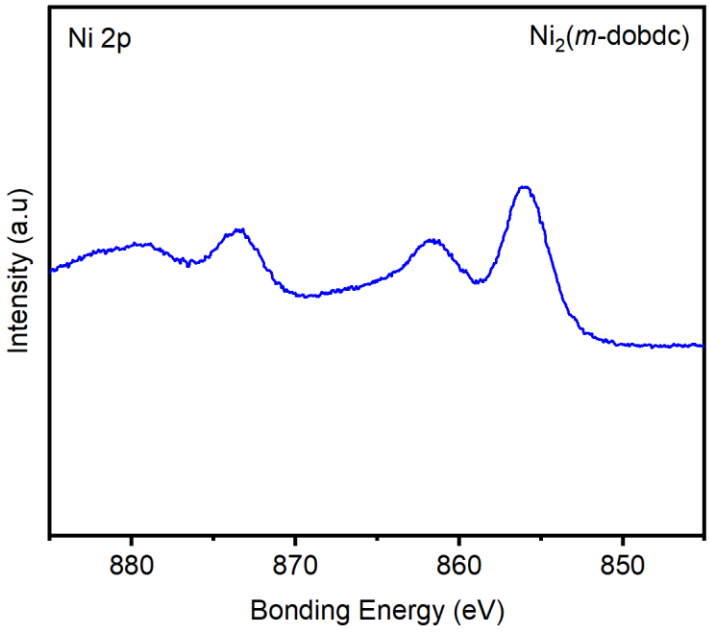

Figure S117. High resolution Ni 2p XPS spectrum of Ni_2(*m*-dobdc) prepared under ionothermal conditions.

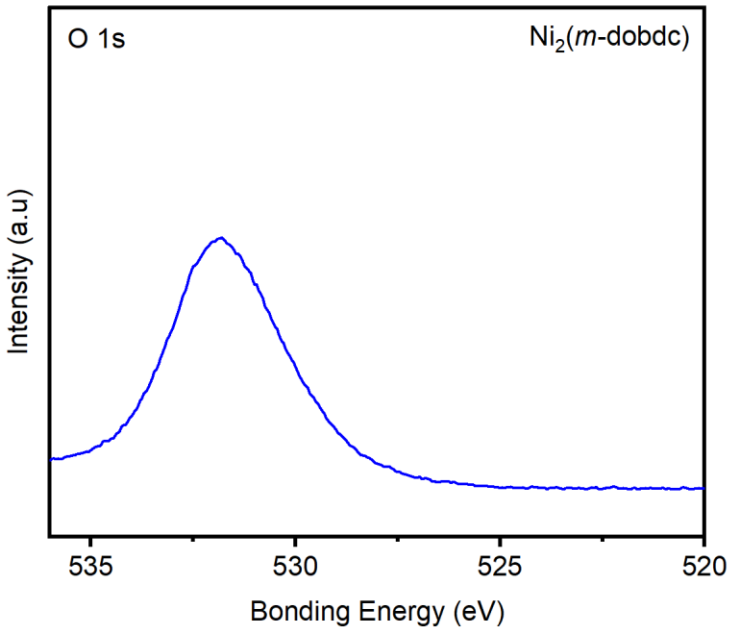

Figure S118. High resolution O 1s XPS spectrum of Ni_2(*m*-dobdc) prepared under ionothermal conditions.

Table S16. Combustion elemental analysis data for Ni_2(*m*-dobdc) prepared under ionothermal conditions.

Element	Theory for $C_8H_2Ni_2O_6$ (wt %)	Found (wt %)
C	30.85	30.12
H	0.65	2.86

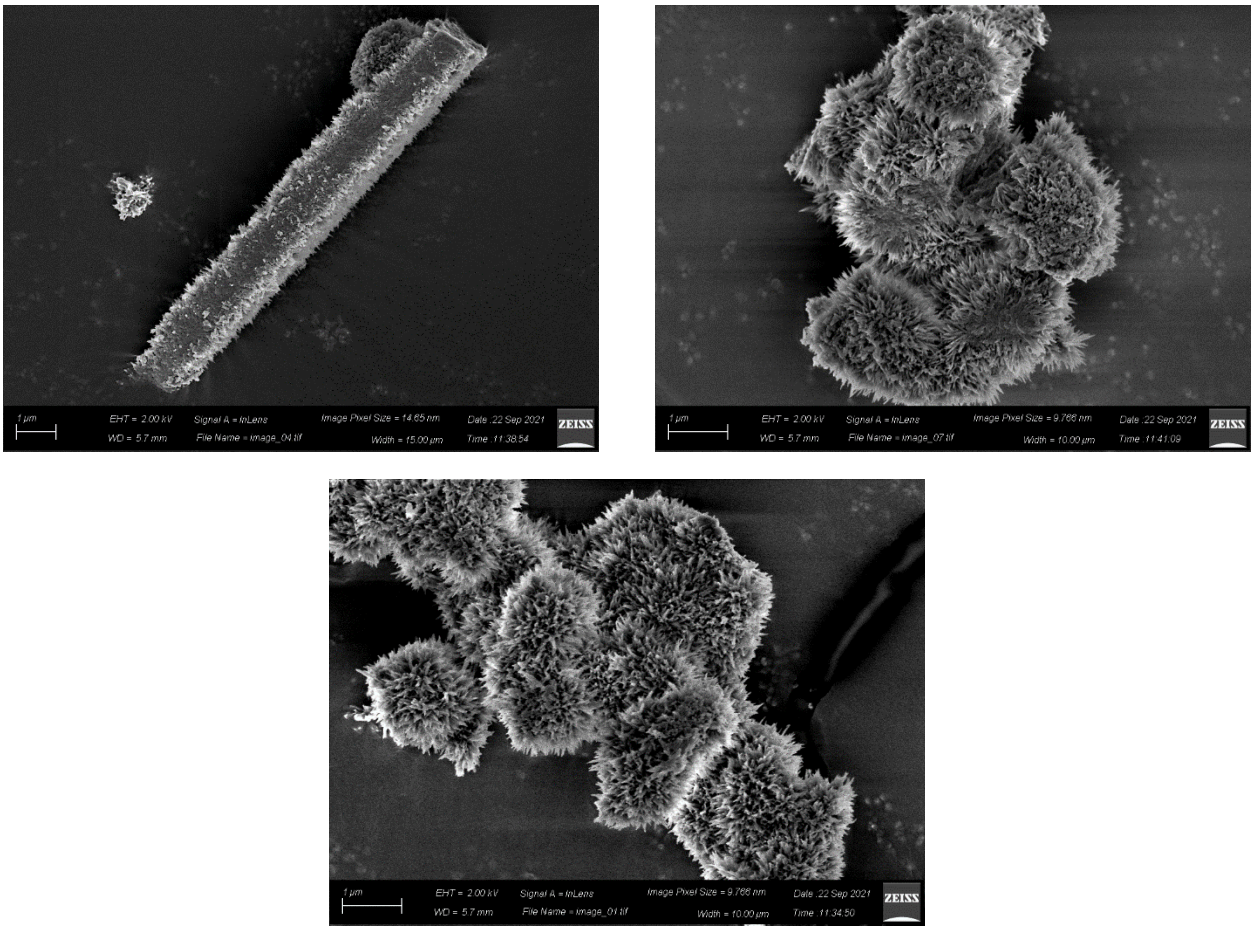

Figure S119. SEM images of Ni_2(*m*-dobdc) prepared under ionothermal conditions.

11. Synthesis and characterization of Fe_2X_2(*m*-dobdc) (X = Cl, OH).

Ionothermal synthesis of Fe_2X_2(*m*-dobdc) (X = Cl, OH).

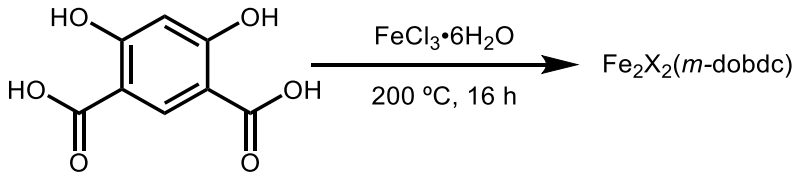

Following General Procedure A, H_4*m*-dobdc (0.100 g, 0.50 mmol, 1.00 equiv.) and $FeCl_3$•$6H_2O$ (0.272 g, 1.00 mmol, 2.00 equiv.) were combined at 200 °C to yield Fe_2X_2(*m*-dobdc) (X = Cl, OH) (0.067 g, 24% yield) as a black powder after activation under dynamic vacuum (<100 mTorr) at 180 °C for 24 h. Synthesis attempts at lower temperatures or with shorter reaction times (4 h) yielded a combination of unreacted reagents and amorphous materials.

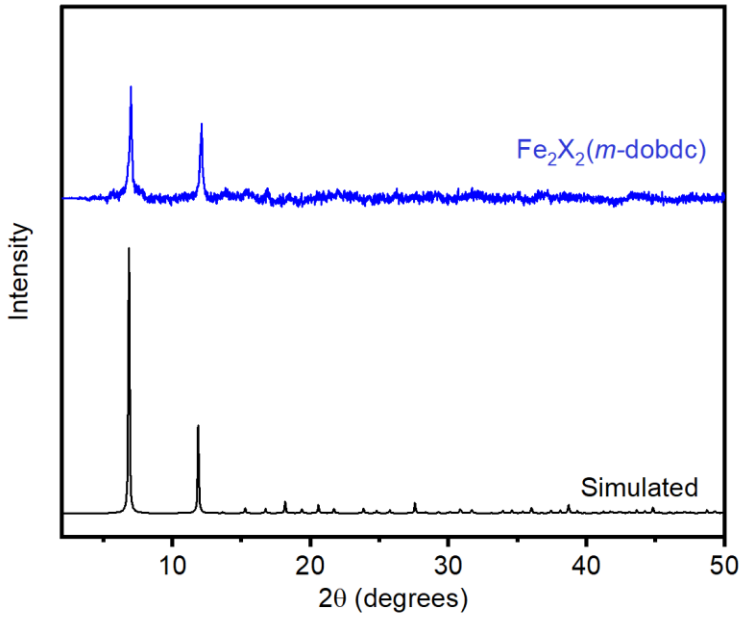

Figure S120. PXRD pattern (λ = 1.5406 Å) of Fe_2X_2(*m*-dobdc) (X = Cl, OH) prepared under ionothermal conditions. The simulated pattern corresponding to the powder X-ray diffraction structure of Ni_2(*m*-dobdc) is included for reference.[13] The experimental PXRD pattern was baseline corrected.

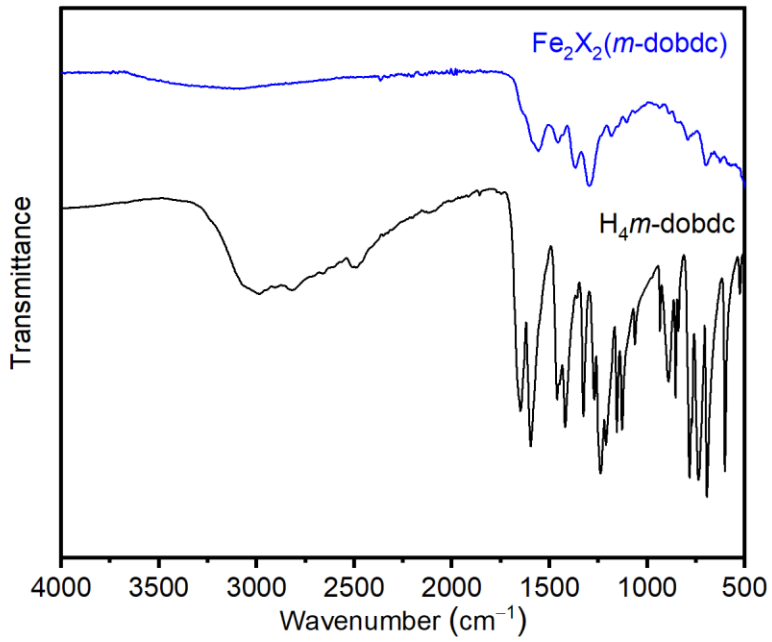

Figure S121. ATR IR spectrum data of Fe_2X_2(*m*-dobdc) (X = Cl, OH) prepared under ionothermal conditions.

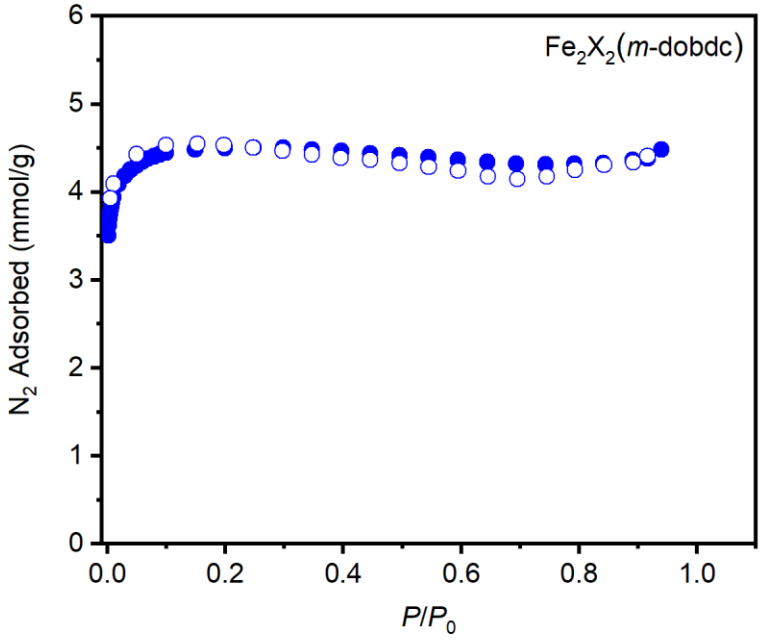

Figure S122. 77 K N_2 adsorption (closed circles) and desorption (open circles) isotherms of Fe_2X_2(*m*-dobdc) (X = Cl, OH) prepared under ionothermal conditions. Fitting these data yielded a Brunauer–Emmett–Teller (BET) surface area of 403 ± 5 m^2/g. Activation at lower temperatures did not improve the surface area.

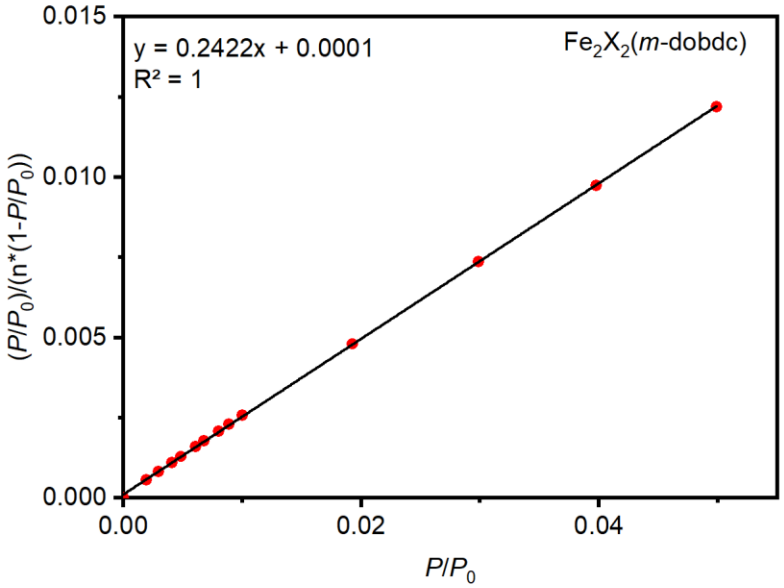

Figure S123. Linearized Brunauer–Emmett–Teller (BET) plot for the adsorption data of Fe_2X_2(*m*-dobdc) (X = Cl, OH).

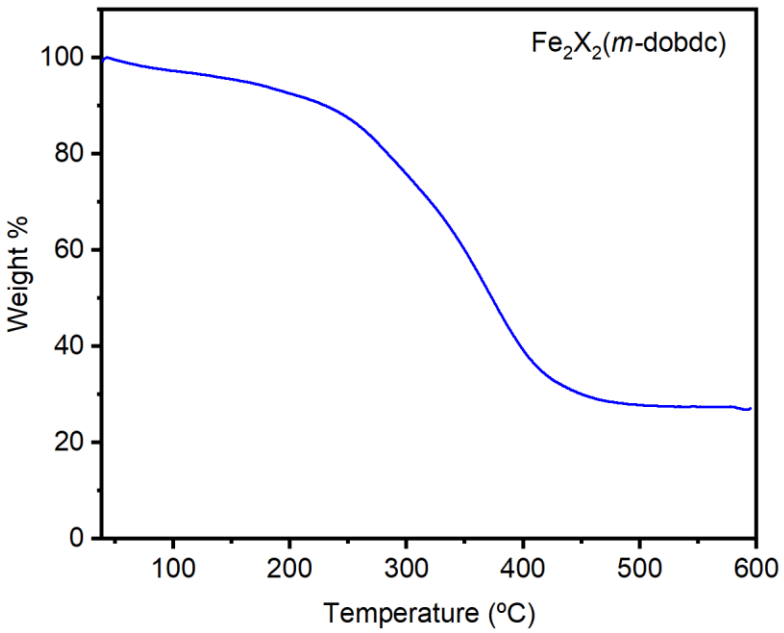

Figure S124. TGA decomposition profile of Fe_2X_2(*m*-dobdc) (X = Cl, OH) prepared under ionothermal conditions.

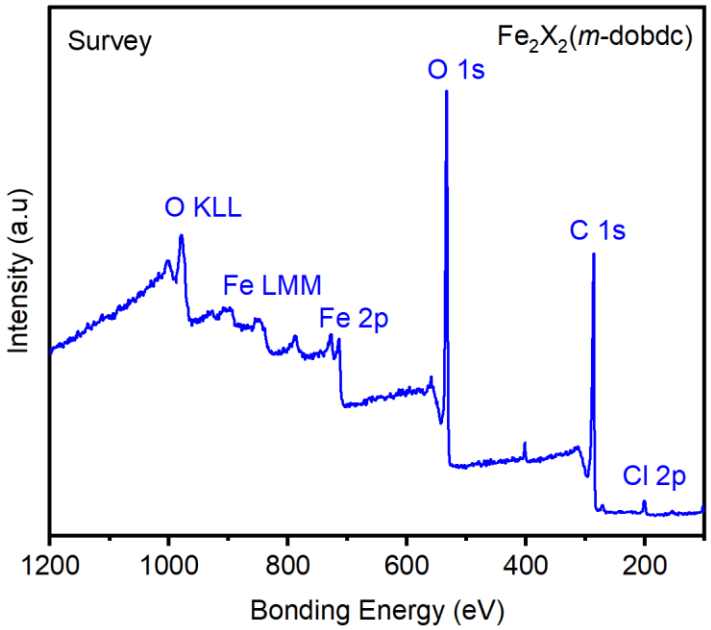

Figure S125. XPS spectral scan of an activated sample of Fe_2X_2(*m*-dobdc) (X = Cl, OH). The detected N (~400 eV) in this sample is likely due to physisorbed N_2.[1]

Table S17. Tabulated survey XPS data for Fe_2X_2(*m*-dobdc) (X = Cl, OH) prepared under ionothermal conditions.

Element	Peak Label	Position	Area	Atomic %
Fe	Fe 2p	711.8	802.90	25.20
Cl	Cl 2p	198.8	62.99	1.98
O	O 1s	531.8	1268.20	39.80
C	C 1s	284.8	1051.86	33.02
Total:				100

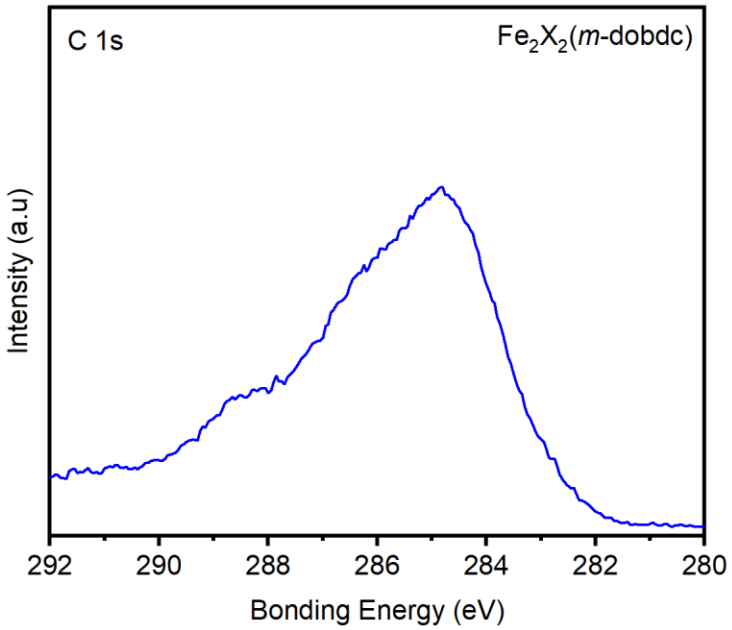

Figure S126. High resolution C 1s XPS spectrum of Fe_2X_2(*m*-dobdc) (X = Cl, OH) prepared under ionothermal conditions.

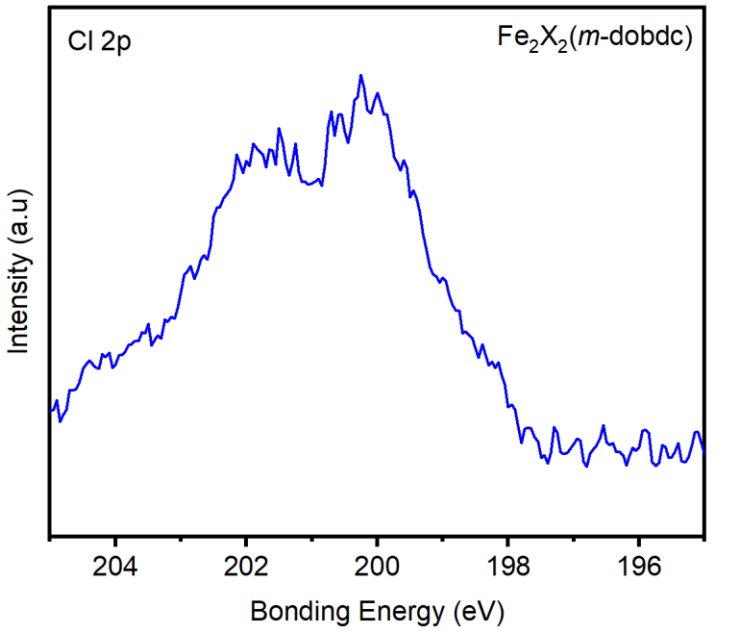

Figure S127. High resolution Cl 2p XPS spectrum of Fe_2X_2(*m*-dobdc) (X = Cl, OH) prepared under ionothermal conditions.

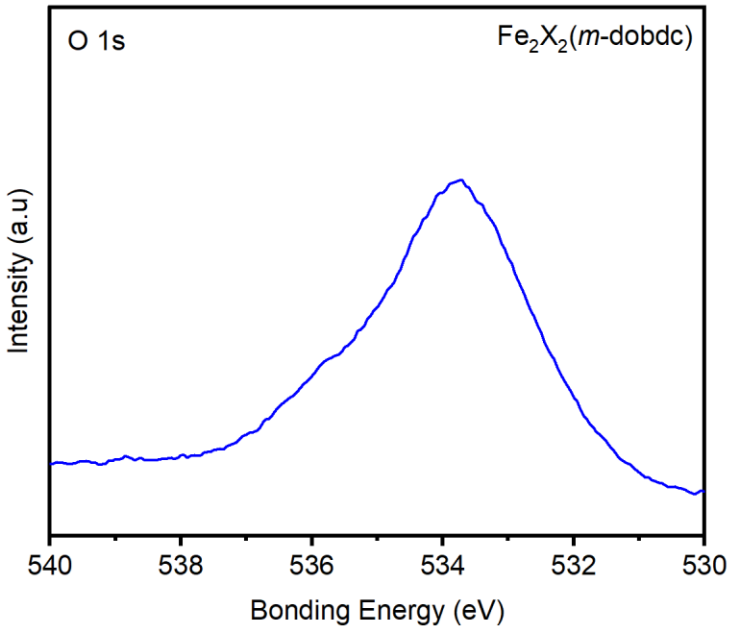

Figure S128. High resolution O 1s XPS spectrum of Fe_2X_2(*m*-dobdc) (X = Cl, OH) prepared under ionothermal conditions.

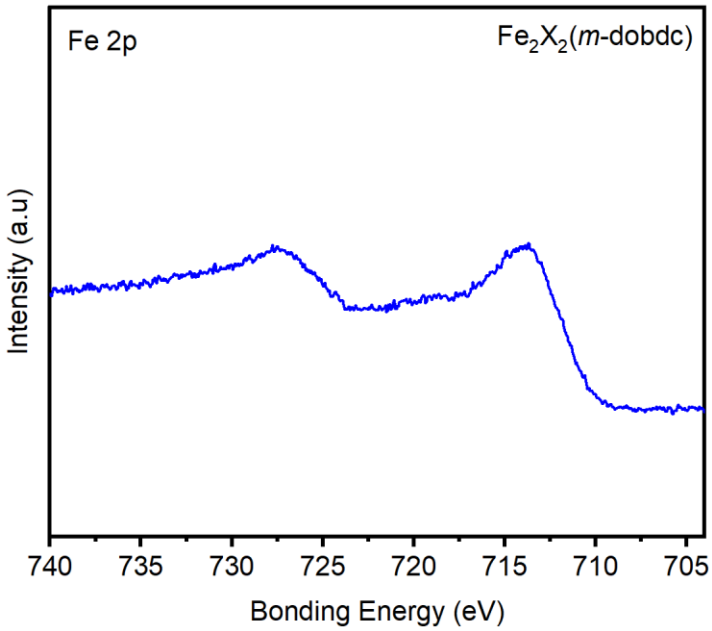

Figure S129. High resolution Fe 2p XPS spectrum of Fe_2X_2(*m*-dobdc) (X = Cl, OH) prepared under ionothermal conditions.

Table S18. Combustion elemental analysis data for Fe_2X_2(*m*-dobdc) (X = Cl, OH) prepared under ionothermal conditions.

Element	Theory Fe_2Cl_2(*m*-dobdc) $C_8H_2Cl_2Fe_2O_6$ (wt %)	Theory $Fe_2(OH)_2$(*m*-dobdc) $C_8H_4Fe_2O_8$ (wt %)	Found (wt %)
C	25.51	28.28	54.65
H	0.54	1.19	3.30
Cl	18.82	0	1.46

The lower than expected %Cl for this sample is consistent with the EDS data (Figure S132) and indicates partial exchange of Cl^- for OH^- likely occurs under ambient conditions. The higher than expected %C for this sample is likely due to partial graphitization.

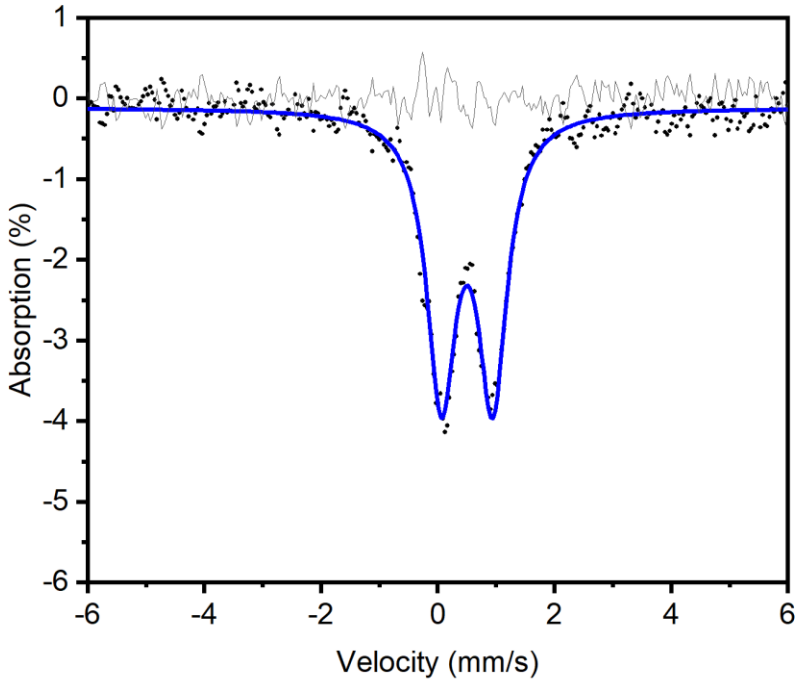

Figure S130. Mössbauer spectrum of Fe_2X_2(*m*-dobdc) (X = Cl, OH) collected at 85 K and 0 field. The experimental spectrum is shown as black dots, the simulated spectrum is shown in blue, and the residual is shown in gray.

Table S19. Mössbauer data of Fe_2X_2(*m*-dobdc) (X = Cl, OH), showing an isomer shift of 0.50(1) mm/s and quadrupole splitting of 0.88(0) mm/s, consistent with S=5/2 Fe(III).

	Fe_2X_2(*m*-dobdc) (X = Cl, OH)
δ (mm/s)	0.501 ± 0.002
ΔE_Q (mm/s)	0.880 ± 0.003
Γ (mm/s)	0.597 ± 0.004
Relative area	0.736 ± 0.003
Reduced χ^2	0.999 ± 0.061

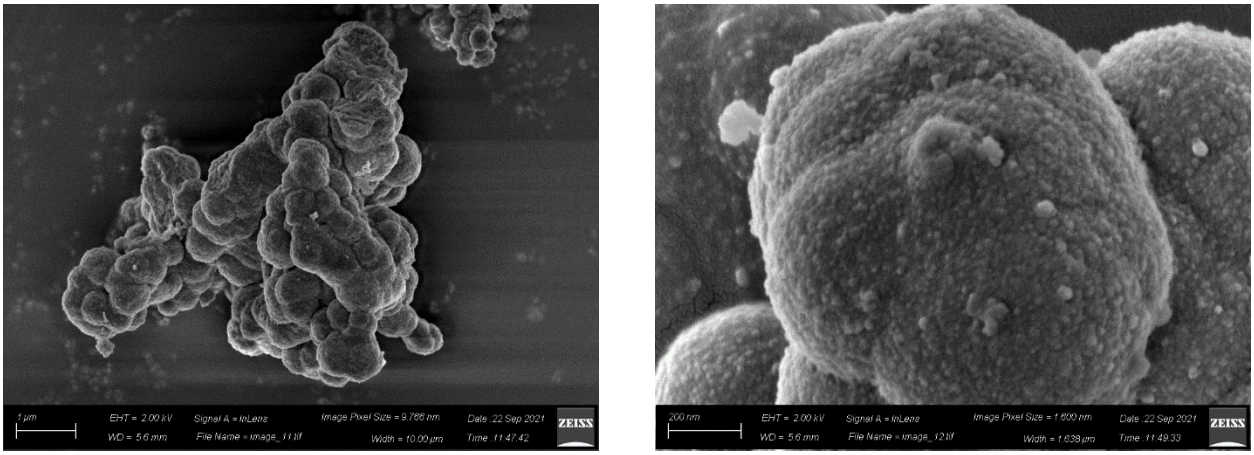

Figure S131. SEM images of Fe_2X_2(*m*-dobdc) (X = Cl, OH) prepared under ionothermal conditions.

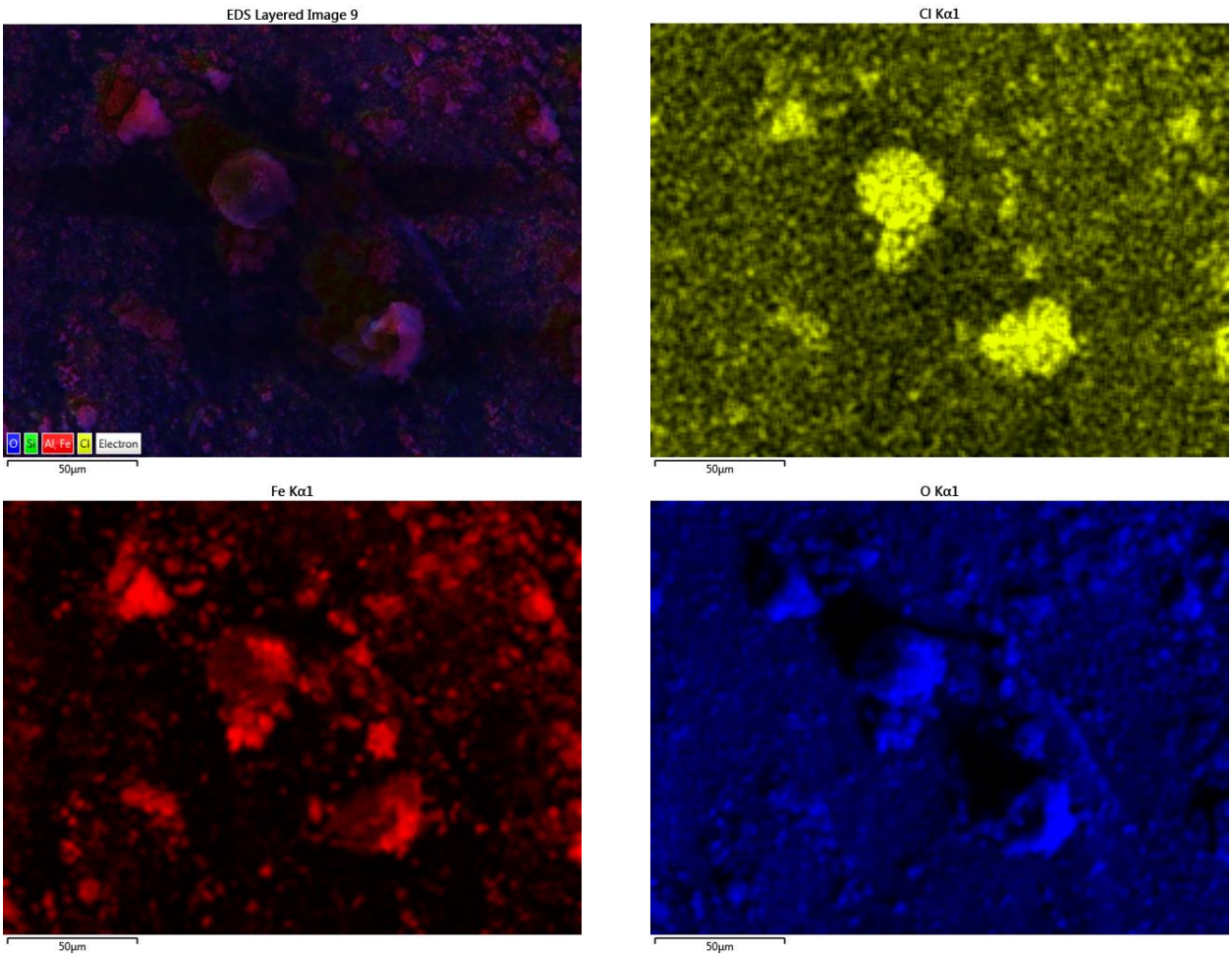

Figure S132. EDS elemental maps of Fe_2X_2(*m*-dobdc) (X = Cl, OH) prepared under ionothermal conditions.

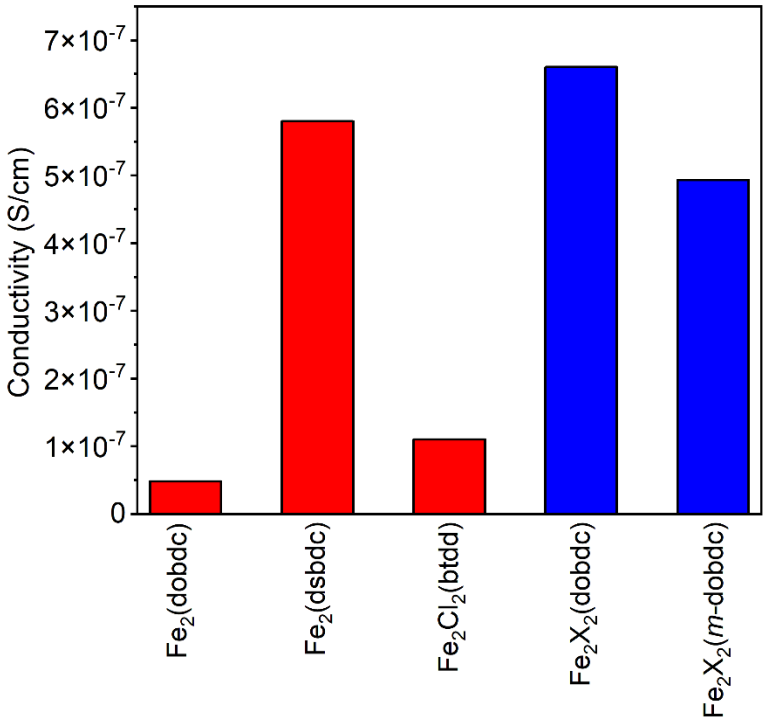

Figure 133. Pressed-pellet conductivities of known Fe(II) materials (red)[14] compared to novel Fe(III) MOFs synthesized under ionothermal conditions (blue).

Table 20. Pressed-pellet conductivities of known Fe(II) materials compared to novel Fe(III) MOFs synthesized under ionothermal conditions.

MOF	Conductivity (S/cm)	Reference
Fe_2(dobdc)	4.80×10^{-8}	14
Fe_2(dsbdc)	5.80×10^{-7}	14
Fe_2Cl_2(btdd)	1.10×10^{-7}	14
Fe_2X_2(dobdc) (X = Cl, OH)	6.60×10^{-7}	This work
Fe_2X_2(*m*-dobdc) (X = Cl, OH)	4.93×10^{-7}	This work

Attempted solvothermal synthesis of Fe_2X_2(*m*-dobdc) (X = Cl, OH).

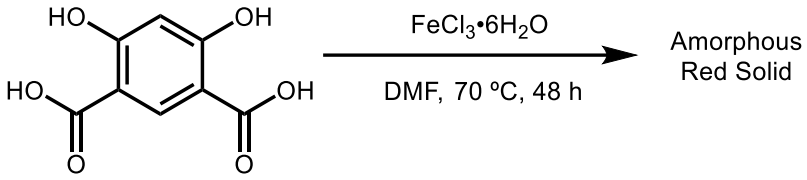

An attempt to synthesize Fe_2X_2(*m*-dobdc) (X = Cl, OH) under solvothermal conditions was performed by adapting the procedure for the synthesis of similar M_2(dobdc) MOFs.[10] In a 250 mL jar, H_4*m*-dobdc (0.100 g, 0.41 mmol, 1.00 equiv.) and $FeCl_3$•$6H_2O$ (0.16 g, 0.82 mmol, 2.20 equiv.) were added to DMF (125 mL). The jar was transferred to an oven that had been pre-heated to 70 °C and allowed to stand at 70 °C for 48 h. The heterogeneous mixture was filtered, and the solid was returned to the Pyrex jar along with fresh DMF (250 mL). The jar was placed in an oven that had been heated to 120 °C. After 24 h, the DMF was decanted and replaced with fresh DMF (250 mL). This soaking procedure was repeated for a total of three hot DMF soaks. Next, the soaking procedure was repeated with methanol (100 mL) at 65 °C, replacing the solvent every 24 h. This soaking procedure was repeated for a total of three hot methanol soaks. The heterogeneous mixture was filtered. The solid was then activated under dynamic vacuum (<100 mTorr) at 150 °C for 24 h, yielding an amorphous red powder.

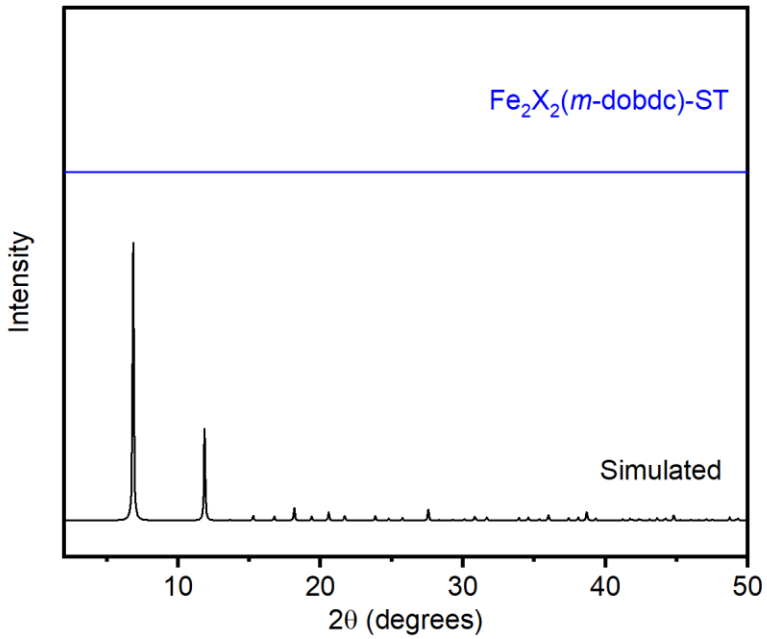

Figure S134. PXRD pattern (λ = 1.5406 Å) of the solids obtained from an attempted synthesis of Fe_2X_2(*m*-dobdc) (X = Cl, OH) under solvothermal conditions. The simulated pattern corresponding to the powder X-ray diffraction structure of Ni_2(*m*-dobdc) is included for reference.[14]

12. Synthesis of Fe_2(dobdc).

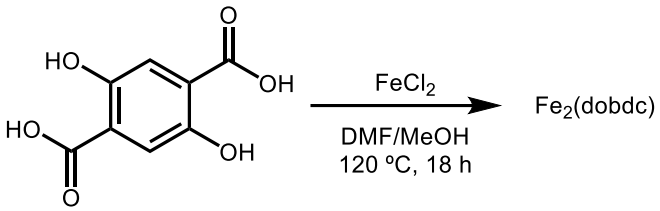

In a N_2-filled glovebox, a 350 mL screw-cap high pressure reaction vessel equipped with a stir bar was charged with $FeCl_2$ (550 mg, 4.50 mmol, 2.50 eq.), 2,5-dihydroxyterephthalic acid (355 mg, 1.80 mmol, 1.00 eq.), fresh, anhydrous, and oxygen-free *N*,*N*-dimethylformamide (150 mL), and oxygen-free, dry methanol (18 mL). The reaction vessel was sealed, and the reaction mixture was allowed to stir slowly at 120 °C for 18 h, resulting in precipitation of an orange-red powder from solution. The reaction mixture was cooled to room temperature. The vessel was transferred to a N_2-filled glovebox. In the N_2-filled glovebox, the solution was decanted from the orange-red solid, and fresh oxygen-free, dry *N*,*N*-dimethylformamide (150 mL) was added to the reaction vessel. The reaction vessel was sealed, removed from the glovebox, and placed in an oil bath that had been pre-heated to 120 °C. The reaction vessel was allowed to stand at 120 °C for 24 h, at which time the vessel was returned to the N_2-filled glovebox. The above washing process was repeated for a total of four oxygen-free DMF washes. The solution was then decanted from the orange-red solid in a N_2-filled glovebox, and oxygen-free methanol (150 mL) was added to the reaction vessel. The above washing procedure was repeated for a total of three oxygen-free methanol washes. During the washing procedure, the solid changed in color from orange-red to yellow. The mixture was filtered in a N_2-filled glovebox, and the collected solid was quickly transferred to a Schlenk flask. The material was activated by heating under high vacuum (<100 mTorr) at 180 °C for 24 h. In a N_2-filled glovebox, the yellow solid was transferred to a glass adsorption tube equipped with a Micromeritics *TransSeal*. The tube was removed from the glovebox and the material was activated for an additional 24 h under high vacuum (<10 μbar) at 180 °C. Activated Fe_2(dobdc) was obtained as a yellow solid. A sample was taken for air-free PXRD by packing ~2 mg of material in a capillary sealed with silicone grease in an N_2-filled glovebox.

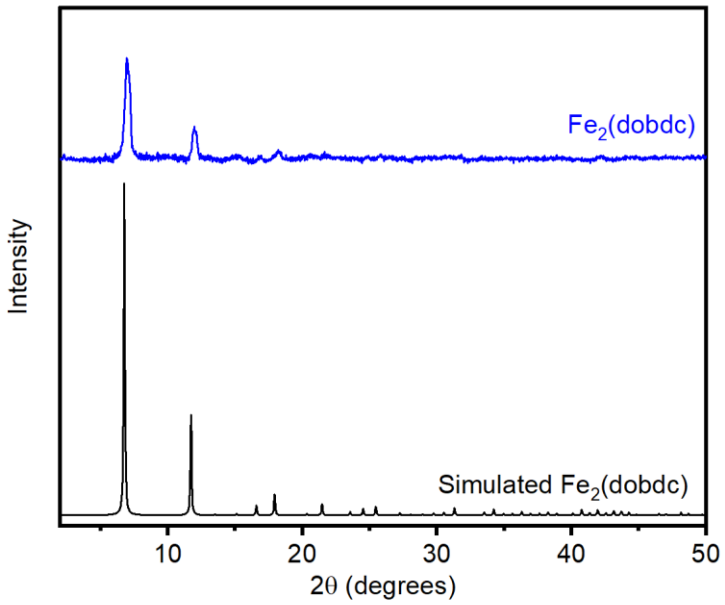

Figure S135. Air-free PXRD pattern (λ = 1.5406 Å) of Fe_2(dobdc) prepared under solvothermal conditions. The simulated pattern corresponding to the single-crystal X-ray diffraction structure of Fe_2(dobdc) is included for reference.[12] The experimental PXRD pattern was baseline corrected.

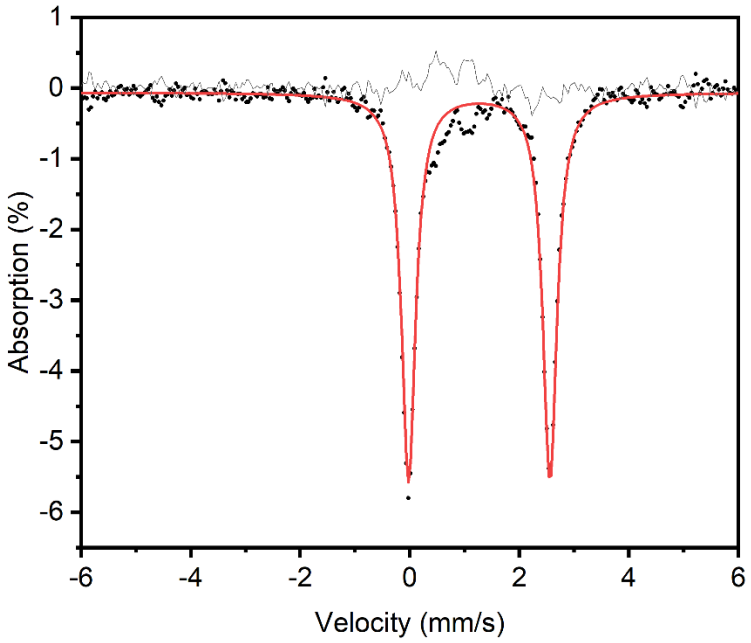

Figure S136. Mössbauer spectrum of Fe_2(dobdc) collected at 85 K and 0 field. The experimental spectrum is shown as black dots, the simulated spectrum is shown in blue, and the residual is shown in gray.

Table S21. Mössbauer data of Fe_2(dobdc), showing an isomer shift of 1.26(6) mm/s and quadrupole splitting of 2.58(2) mm/s, consistent with high-spin Fe(II).

	Fe_2(dobdc)
δ **(mm/s)**	1.266 ± 0.0004
ΔE_Q **(mm/s)**	2.5821 ± 0.0009
Γ **(mm/s)**	0.312 ± 0.001
Relative area	0.813 ± 0.002
Reduced χ^2	0.990 ± 0.065

13. Synthesis of Fe_2(*m*-dobdc).

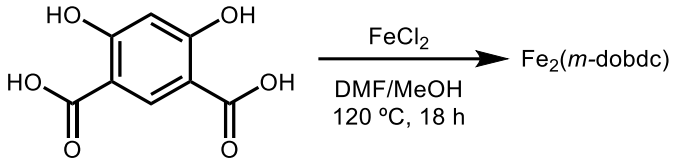

In a N_2-filled glovebox, anhydrous $FeCl_2$ (0.380 g, 3.00 mmol, 2.50 equiv.) and H_4*m*-dobdc (0.240 g, 1.20 mmol, 1.00 equiv.) were added to a solution of oxygen-free, dry MeOH (12 mL) in fresh, anhydrous, and oxygen-free DMF (68 mL). The grey solution was distributed evenly among eight 20 mL scintillation vials, which were then sealed with black electrical tape and placed into a heating block at 120 °C. The vials were allowed to stand at 120 °C for 18 h in a N_2-filled glovebox. The vials were allowed to cool to room temperature, and the heterogeneous solutions were filtered together in a N_2-filled glovebox. The resulting brown solid was transferred into one 20 mL scintillation vial with 20 mL of fresh DMF. The vial was heated at 70 °C for 24 h using a heat block. The vial was allowed to cool to room temperature. The DMF was decanted and replaced with fresh, oxygen-free DMF. This washing procedure was repeated for a total of three oxygen-free DMF soaks. The DMF was decanted and replaced with 20 mL of oxygen-free methanol, and the vial was heated to 70 °C for 24 h using a heat block. The vial was allowed to cool to room temperature. The methanol was decanted and replaced with fresh, oxygen-free MeOH. This washing procedure was repeated for a total of three oxygen-free DMF soaks. The material was collected via filtration and activated in a Schlenk flask in the glovebox at 180 °C for 24 h. Activated Fe_2(*m*-dobdc) was obtained as a brown solid. A sample was taken for air-free PXRD by packing ~2 mg of material in a capillary sealed with silicone grease in an N_2-filled glovebox.

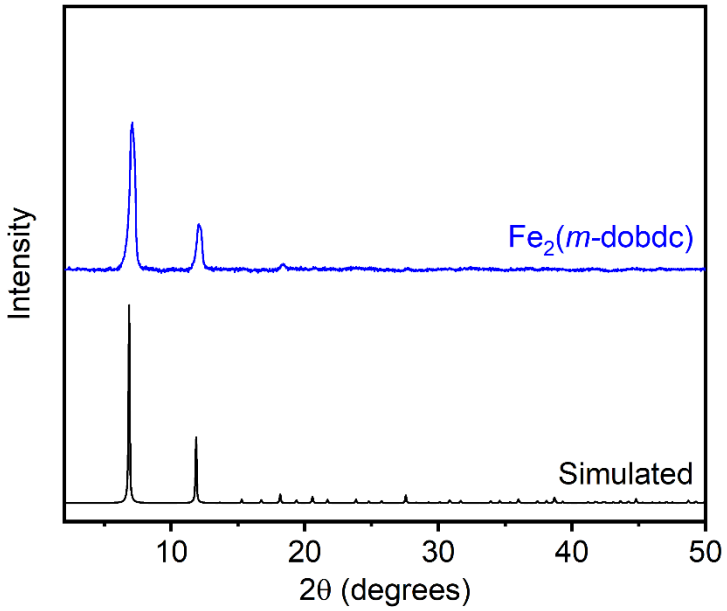

Figure S137. Air-free PXRD pattern (λ = 1.5406 Å) of Fe_2(*m*-dobdc) prepared under solvothermal conditions. The simulated pattern corresponding to the single-crystal X-ray diffraction structure of Ni_2(*m*-dobdc) is included for reference.[13] The experimental PXRD pattern was baseline corrected.

14. Control experiments using Co_2Cl_2(btdd).

Attempted ionothermal MOF synthesis using anhydrous cobalt chloride (Experiment A).

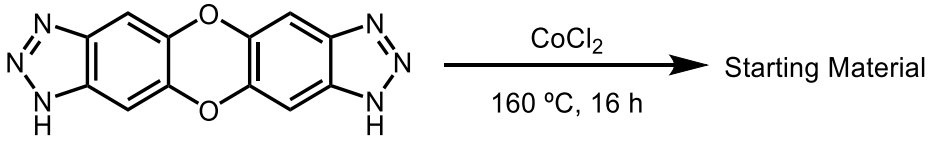

An attempt to synthesize Co_2Cl_2(btdd) under ionothermal conditions using anhydrous $CoCl_2$ (melting point = 735 °C) was performed. H_2btdd (0.100 g, 0.375 mmol, 1.00 equiv.) and $CoCl_2$ (0.097 g, 0.750 mmol, 2.00 equiv.) were combined in a Teflon autoclave in a N_2-filled glovebox. The autoclave was removed from the glovebox and placed in an oven that had been pre-heated to 160 ºC. The autoclave was allowed to stand at this temperature for 16 h. After cooling, a visible mixture of the two starting materials was observed (Figure S138). After washing with 20 mL of methanol and filtering to remove soluble material, a brown powder (0.100 g) was collected. Analysis by PXRD revealed a material with peaks correlating to H_2btdd, with no MOF present (Figure S141). This experiment confirms that water is necessary for MOF formation under ionothermal conditions.

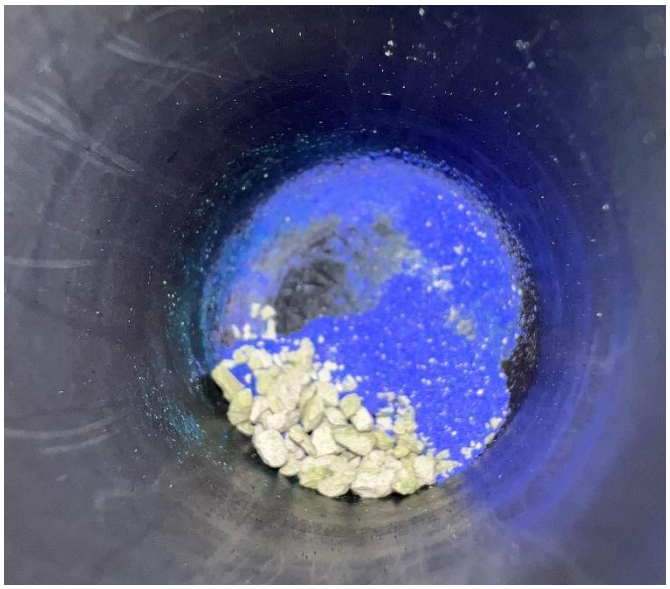

Figure S138. An image taken of the inside of the autoclave after removing the anhydrous control experiment (Experiment A) from the oven.

Attempted ionothermal MOF synthesis using lower reaction temperature (Experiment B).

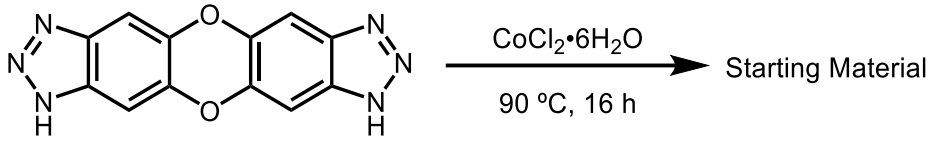

An attempt to synthesize Co_2Cl_2(btdd) under ionothermal conditions at a temperature near the melting point of $CoCl_2$•$6H_2O$ was performed. H_2btdd (0.100 g, 0.375 mmol, 1.00 equiv.) and $CoCl_2$•$6H_2O$ (0.178 g, 0.750 mmol, 2.00 equiv.) were combined in a Teflon autoclave and placed in an oven that had been pre-heated to 90 ºC. The autoclave was allowed to stand at this temperature for 16 h. After cooling, a brown solid was collected (Figure S137) and washed with 20 mL of methanol to remove any soluble material. The resulting brown powder (0.060 g) demonstrated low crystallinity by PXRD, bearing no peaks that correspond to MOF nor either starting material (Figure S139). This experiment confirms that heating well above the melting point of the metal hydrate salt is required for MOF formation.

Figure S139. An image taken of the inside of the autoclave after removing the low-temperature control experiment (Experiment B) from the oven.

Synthesis of Co_2Cl_2(btdd) without post-synthetic DMF washes (Experiment C).

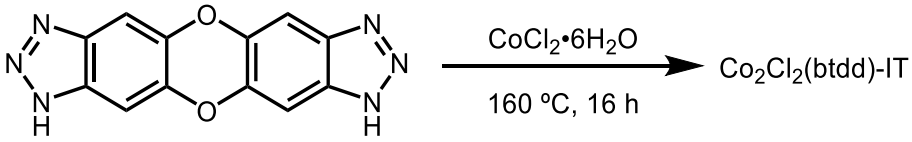

A demonstration of MOF formation without any DMF washes was performed. Following a modified version of General Procedure A, H_2btdd (0.100 g, 0.375 mmol, 1.00 equiv.) and $CoCl_2$•$6H_2O$ (0.178 g, 0.750 mmol, 2.00 equiv.) were combined in a Teflon autoclave and placed in an oven that had been pre-heated to 160 ºC. The autoclave was allowed to stand at this temperature for 16 h. After cooling, a blue-green solid was collected (Figure S140) and washed with 20 mL of methanol to remove any soluble material. The resulting blue-green solid (0.200 g) was confirmed by PXRD to consist largely of Co_2Cl_2(btdd) (Figure S141).

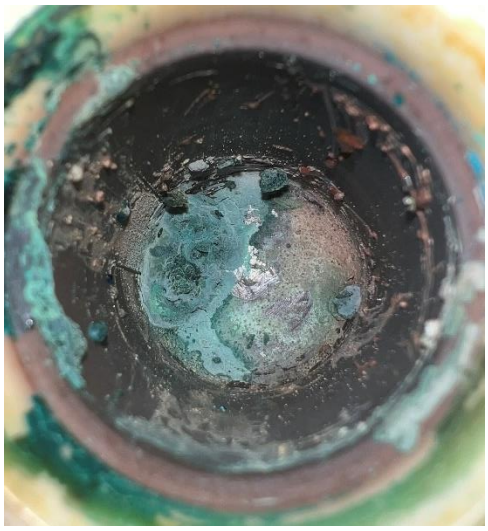

Figure S140. An image taken of the inside of the autoclave after removing the Co_2Cl_2(btdd) ionothermal synthesis control experiment (Experiment C) from the oven.

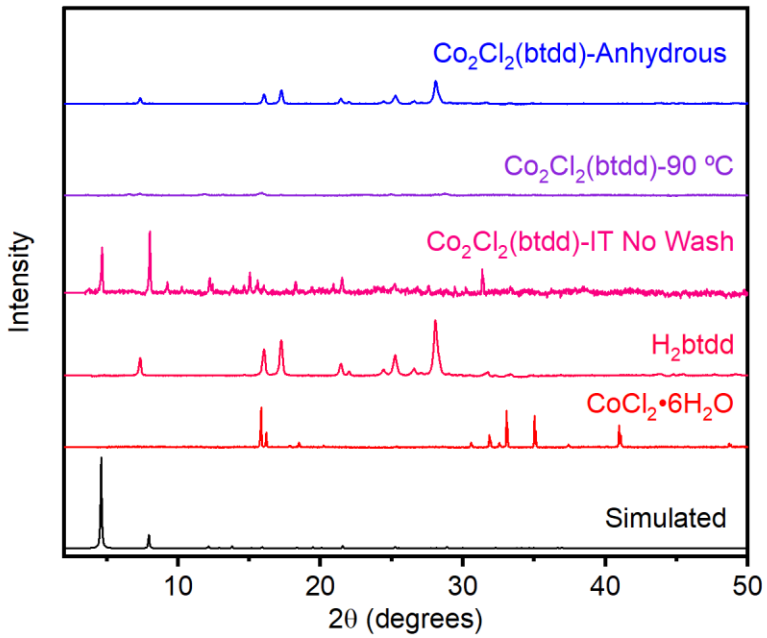

Figure S141. PXRD pattern (λ = 1.5406 Å) of the material collected from the anhydrous salt control experiment (Experiment A), the material collected from the low temperature control experiment (Experiment B), and the Co_2Cl_2(btdd) prepared under ionothermal conditions without DMF washes (Experiment C). The patterns of the starting materials, H_2btdd and $CoCl_2$•$6H_2O$ are included as a reference. The simulated pattern corresponding to the single-crystal X-ray diffraction structure of Mn_2Cl_2(btdd) is also included for reference.[6] The experimental PXRD patterns were baseline corrected.

15. Reproducibility experiments using Co_2Cl_2(btdd).

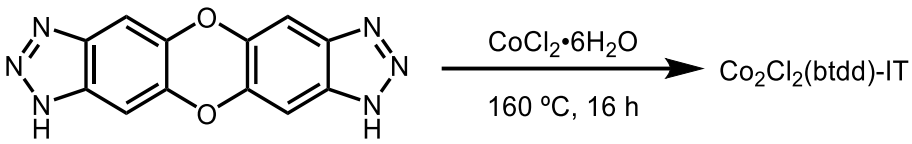

Following General Procedure A, H_2btdd (1.00 g, 3.75 mmol, 1.00 equiv.) and $CoCl_2$•$6H_2O$ (1.78 g, 7.50 mmol, 2.00 equiv.) were combined to yield a second sample of Co_2Cl_2(btdd) (1.13 g, 66% yield) as a dark green solid after activation under dynamic vacuum (<100 mTorr) at 150 °C for 24 h.

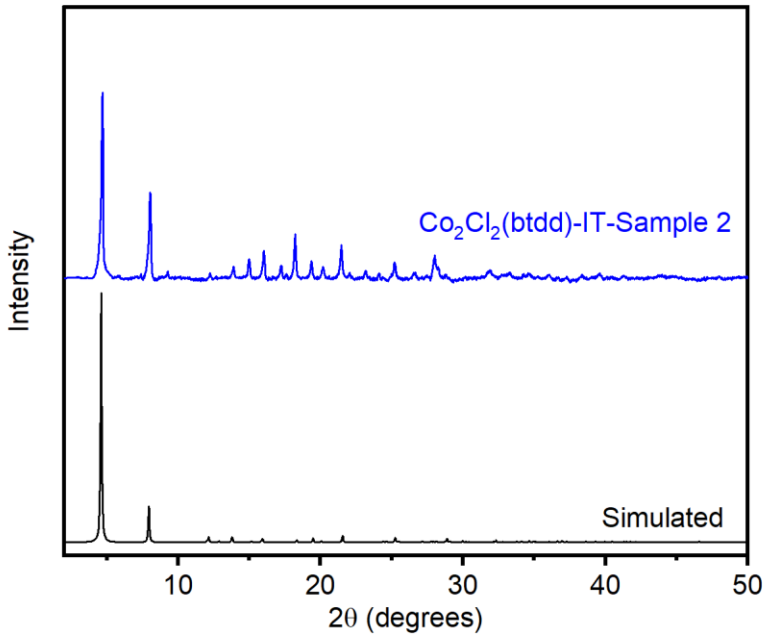

Figure S142. PXRD pattern (λ = 1.5406 Å) of Co_2Cl_2(btdd) prepared under ionothermal conditions. The simulated pattern corresponding to the single-crystal X-ray diffraction structure of Mn_2Cl_2(btdd) is included for reference.[6] The experimental PXRD pattern was baseline corrected.

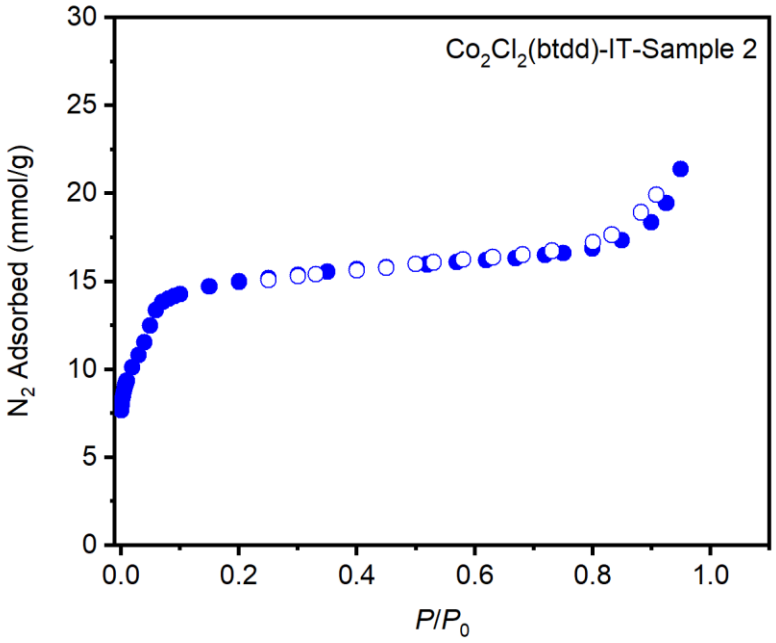

Figure S143. 77 K N_2 adsorption (closed circles) and desorption (open circles) isotherms of a second sample of Co_2Cl_2(btdd) prepared under ionothermal conditions. Fitting these data yielded a Brunauer–Emmett–Teller (BET) surface area of 2110 ± 25 m^2/g.

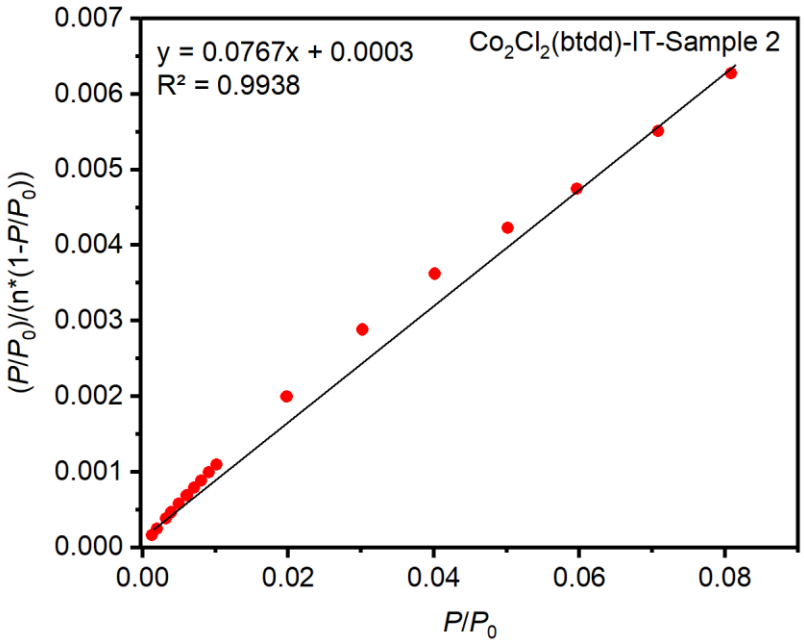

Figure S144. Linearized Brunauer–Emmett–Teller (BET) plot for the adsorption data of a second sample of Co_2Cl_2(btdd) prepared under ionothermal conditions.

16. References.

1. Lefebvre, J.; Galli, F.; Bianchi, C. L.; Patience, G. S.; Boffito, D. C., Experimental methods in chemical engineering: X-ray photoelectron spectroscopy-XPS. *Can. J. Chem. Eng.* **2019,** *97* (10), 2588–2593.
2. Rieth, A. J.; Wright, A. M.; Skorupskii, G.; Mancuso, J. L.; Hendon, C. H.; Dincă, M., Record-Setting Sorbents for Reversible Water Uptake by Systematic Anion Exchanges in Metal–Organic Frameworks. *J. Am. Chem. Soc.* **2019,** *141* (35), 13858–13866.
3. Denysenko, D.; Grzywa, M.; Tonigold, M.; Streppel, B.; Krkljus, I.; Hirscher, M.; Mugnaioli, E.; Kolb, U.; Hanss, J.; Volkmer, D., Elucidating Gating Effects for Hydrogen Sorption in MFU-4-Type Triazolate-Based Metal–Organic Frameworks Featuring Different Pore Sizes. *Chem. Eur. J.* **2011,** *17* (6), 1837–1848.
4. Wang, Z.; Bilegsaikhan, A.; Jerozal, R. T.; Pitt, T. A.; Milner, P. J., Evaluating the Robustness of Metal–Organic Frameworks for Synthetic Chemistry. *ACS Appl. Mater. Interfaces* **2021,** *13* (15), 17517–17531.
5. Kim, J.; Teo, H. T.; Hong, Y.; Oh, J.; Kim, H.; Chi, C.; Kim, D., Multiexcitonic Triplet Pair Generation in Oligoacene Dendrimers as Amorphous Solid-State Miniatures. *Angew. Chem. Int. Ed.* **2020,** *59* (47), 20956–20964.
6. Rieth, A. J.; Tulchinsky, Y.; Dincă, M., High and Reversible Ammonia Uptake in Mesoporous Azolate Metal–Organic Frameworks with Open Mn, Co, and Ni Sites. *J. Am. Chem. Soc.* **2016,** *138* (30), 9401–9404.
7. Colombo, V.; Galli, S.; Choi, H. J.; Han, G. D.; Maspero, A.; Palmisano, G.; Masciocchi, N.; Long, J. R., High thermal and chemical stability in pyrazolate-bridged metal–organic frameworks with exposed metal sites. *Chem. Sci.* **2011,** *2* (7), 1311–1319.
8. Colombo, V.; Montoro, C.; Maspero, A.; Palmisano, G.; Masciocchi, N.; Galli, S.; Barea, E.; Navarro, J. A. R., Tuning the Adsorption Properties of Isoreticular Pyrazolate-Based Metal–Organic Frameworks through Ligand Modification. *J. Am. Chem. Soc.* **2012,** *134* (30), 12830–12843.
9. Galli, S.; Masciocchi, N.; Colombo, V.; Maspero, A.; Palmisano, G.; López-Garzón, F. J.; Domingo-García, M.; Fernández-Morales, I.; Barea, E.; Navarro, J. A. R., Adsorption of Harmful Organic Vapors by Flexible Hydrophobic Bis-pyrazolate Based MOFs. *Chem. Mater.* **2010,** *22* (5), 1664–1672.
10. Liang, X.; Wang, P.; Li, C.; Yuan, M.; Shi, Q.; Dong, J., The activation of Co-MOF-74 with open metal sites and their corresponding CO/N_2 adsorptive separation performance. *Microporous Mesoporous Mater.* **2021,** *320*, 111109.
11. Kim, H.; Sohail, M.; Yim, K.; Park, Y. C.; Chun, D. H.; Kim, H. J.; Han, S. O.; Moon, J.-H., Effective CO_2 and CO Separation Using [M_2(DOBDC)] (M = Mg, Co, Ni) with Unsaturated Metal Sites and Excavation of Their Adsorption Sites. *ACS Appl. Mater. Interfaces* **2019,** *11* (7), 7014–7021.
12. Queen, W. L.; Bloch, E. D.; Brown, C. M.; Hudson, M. R.; Mason, J. A.; Murray, L. J.; Ramirez-Cuesta, A. J.; Peterson, V. K.; Long, J. R., Hydrogen adsorption in the metal–organic frameworks Fe_2(dobdc) and $Fe_2(O_2)$(dobdc). *Dalton Trans.* **2012,** *41* (14), 4180–4187.
13. Kapelewski, M. T.; Geier, S. J.; Hudson, M. R.; Stück, D.; Mason, J. A.; Nelson, J. N.; Xiao, D. J.; Hulvey, Z.; Gilmour, E.; FitzGerald, S. A.; Head-Gordon, M.; Brown, C. M.; Long, J. R. M_2(*m*-dobdc) (M = Mg, Mn, Fe, Co, Ni) Metal–Organic Frameworks Exhibiting Increased

Charge Density and Enhanced H_2 Binding at the Open Metal Sites. *J. Am. Chem. Soc.* **2014,** *136* (34), 12119-12129.
14. Sun, L.; Hendon, C. H.; Park, S. S.; Tulchinsky, Y.; Wan, R.; Wang, F.; Walsh, A.; Dincă, M. Is iron unique in promoting electrical conductivity in MOFs? *Chem. Sci.* **2017,** *8* (6), 4450–4457.